Analysis of Tau Pathology in Transgenic Mouse and Tissue Culture Models of Alzheimer's Disease and Related Disorders

Dissertation

zur

Erlangung der naturwissenschaftlichen Doktorwürde

(Dr. sc. nat.)

vorgelegt der

Mathematisch-naturwissenschaftlichen Fakultät

der

Universität Zürich

von

Luis Javier Carlos Pennanen

von Dottikon AG

Promotionskomitee

Prof. Dr. Peter Sonderegger (Vorsitz)

PD Dr. Jürgen Götz (Leitung der Dissertation)

Prof. Dr. Hanns Möhler

Zürich 2005

TABLE OF CONTENTS

ATTACHMENT

Pennanen, L., Welzl, H., D'Adamo, P., Nitsch, R.M., and Gotz, J. (2004) Accelerated extinction of conditioned taste aversion in P301L tau transgenic mice. *Neurobiol Dis* **15**: 500-509.

SUMMARY

A. Behavioral analysis of P301L tau transgenic mice

Background: Of all forms of human dementias, Alzheimer's disease (AD) is the most prevalent. It is characterized by extracellular β-amyloid-containing (Aβ) plaques, intracellular neurofibrillary tangles (NFT) composed of hyperphosphorylated tau aggregates, reduced synaptic density and neuronal loss, which leads to a progressive deterioration of memory and other cognitive functions. NFT are also abundant, in the absence of amyloid plaques, in additional neurodegenerative diseases such as frontotemporal dementia with Parkinsonism linked to chromosome 17 (FTDP-17), where mutations have been identified in the tau gene, establishing that tau dysfunction alone can cause neurodegeneration and lead to dementia.

Results: The transgenic mice used in my study overexpress the FTDP-17 associated mutation P301L of tau and form tau aggregates in many brain areas including the hippocampus and the amygdala, both of which are characterized by NFT formation in the human disease state. To detect early signs of tau aggregate-associated changes, I investigated in a first set of experiments behavioral alterations and cognitive deficits in six months old transgenic mice on a mixed background (B6D2F1) using an amygdala-specific test battery. At this age, NFT formation is initiated in the amygdala, a brain area involved in mediating effects of emotion (fear, exploration) on learning and memory and in the validation of primarily negative events. Next, to determine whether tau aggregation, in the absent of NFT formation, is sufficient to cause deficits in hippocampus-dependent behavior, I assessed in a second set of experiments six and eleven months old P301L mice backcrossed onto a C57Bl/6 background in a hippocampus-specific test battery.

I found that P301L mice had anxiety levels not different from wild-types, but their exploratory behavior was significantly increased as evidenced by several tasks. The disinhibition of exploratory behavior was independent of the background of the mice and was even more pronounced during aging, indicating that this effect is due to the presence of the tau transgene. Amygdala-specific tests revealed no impairment in the acquisition of a fear response to tone and context and in the acquisition and consolidation of a conditioned taste aversion (CTA). However, extinction of the CTA memory was significantly accelerated in the P301L mice. Next, I determined the distribution of P301L tau in more detail with special emphasis on brain areas shown to be involved in CTA. The aggregation pattern of tau was consistent with the behavioral outcome: Tau aggregates were present in the basolateral nucleus of the amygdala (BLA), which has been shown to be essential for extinction of CTA memory, whereas

acquisition of a CTA is dependent on an intact central nucleus, where no tau aggregates were found.
Moreover, tau aggregation, in the absence of overt NFT formation, caused deficits in spatial reference memory in the water maze at both ages tested. However, due to a floor effect as evidenced by a poor performance of the aged wild-type control group during the probe trial, a significant difference compared to the wild-type group was only seen at six months of age. No impairment was found in acquisition and reversal learning in the water maze and in spatial working memory as assessed by spontaneous alternation behavior in the Y-maze.

Significance: Together, these data suggest that expression of P301L tau in transgenic mice, not yet accompanied by massive NFT formation, causes selective behavioral deficits that are correlated with the regional distribution of tau aggregates in distinct subnuclei of the amygdala. The correlation of NFT as a disease hallmark with the behavioral outcome is an important measure of the validity of our transgenic mice as an animal model for the tau pathology in AD and related disorders.

B. Role of different phospho-epitopes and cleavage sites in tau filament formation in tissue culture

Background: Despite extensive research, the relationship between Aβ and tau and their relative contribution to the clinical features of AD is still unknown. Recently, our group demonstrated pathological interactions between these two hallmarks. Using P301L mice stereotaxically injected with $A\beta_{42}$ fibrils, enhanced NFT formation was achieved that was tightly correlated with the pathological phosphorylation of tau at the phospho-epitopes Ser-422 and AT100 (Thr-212/Ser-214) (Gotz *et al.*, 2001b). Furthermore, using tau overexpressing human SH-SY5Y neuroblastoma cells exposed for five days to pre-aggregated $A\beta_{42}$, tau-containing filaments formed and a decreased tau solubility was observed, both of which were prevented by mutating the Ser-422 phospho-epitope (Ferrari *et al.*, 2003).

Results: To confirm the previous *in vitro* findings and to map further phospho-epitopes and cleavage sites of tau involved in the Aβ-mediated decrease in tau solubility and tau filament formation, I generated several tau mutant and wild-type (wt) constructs and expressed them in SH-SY5Y neuroblastoma cells.
Adding pre-aggregated $A\beta_{42}$ to differentiated wt-tau overexpressing SH-SY5Y cells led to a more than 15-fold increase in Aβ-mediated tau insolubility compared to PBS-treated cells, whereas mutating distinct phospho-epitopes of tau with a proclaimed role in human disease (the AT8-epitope pSer-202/pThr-205, pThr-231 and pSer-422) prevented the decrease in tau

solubility, indicating an interplay of different epitopes in tau filament formation. In addition, truncation of the carboxy-terminal region of tau at the caspase cleavage-site (position 421) prevented the $A\beta_{42}$-mediated decrease in tau solubility in our tissue culture system. This indicates that truncation is not an initial step in filament formation, but rather a subsequent event.

Significance: I could show that the Aβ-mediated increase in tau insolubility depends on the interplay of distinct phospho-epitopes of tau and not only on phosphorylation of the Ser-422 epitope. This novel tau-overexpressing tissue culture system is a useful tool to study aspects of AD and related disorders. Further adaptation of the *in vitro* model, such as the use of an inducible expression system (which I have also initiated), is likely to provide mechanistic insight into tauopathies and may allow the screening and validation of compounds designed to prevent filament formation.

ZUSAMMENFASSUNG

A. Verhaltensanalyse von P301L Tau transgenen Mäusen

Hintergrund: Die Alzheimerkrankheit (AD) ist die häufigste Demenzerkrankung beim Menschen. Sie ist gekennzeichnet durch extrazelluläre β-Amyloid (Aβ) Plaques, intrazelluläre neurofibrilläre Bündel (NFT), die im Wesentlichen aus dem hyperphosphoryliertem Protein Tau bestehen, und neuronalen Zell- und Synapsenverlust, welcher durch einen kontinuierlichen Verlust des Gedächtnisses und anderer kognitiver Funktionen klinisch begleitet ist. Neurofibrilläre Bündel ohne eine Amyloid-Pathologie lassen sich auch in weiteren neurodegenerativen Demenzerkrankungen finden, zu denen auch die mit Chromosom 17 assoziierte frontotemporale Demenz mit Parkinsonismus (FTDP-17) zählt. Die Identifizierung von Mutationen im Tau-Gen bei FTDP-17 Patienten erbrachte den formellen Beweis, dass auch eine Fehlfunktion von Tau selbst zu Neurodegeneration und Demenz führen kann.

Resultate: Die transgenen Mäuse, welche ich in meinen Studien untersucht habe, überexprimieren die FTDP-17 Taumutation P301L und zeigen filamentöse Ablagerungen des Tau-Proteins in vielen Hirnarealen, darunter im Hippocampus und in der Amygdala (Mandelkern). In diesen beiden Hirnarealen findet man beim Alzheimerpatienten sehr früh eine NFT-Pathologie. Um frühe tauaggregatbedingte Verhaltensänderungen und kognitive Defizite aufzeigen zu können, habe ich sechs Monate alte Mäuse auf einem gemischten genetischen Hintergrund (B6D2F1) in einem ersten Set von Experimenten in einer Amygdala-spezifischen Testbatterie untersucht. In diesem Alter werden die ersten NFT in der Amygdala gebildet, ein Hirnareal, das die Steuerung von Emotionen (Angst, Exploration) reguliert und eine Verhaltensbewertung von vornehmlich negativen Ereignissen vornimmt. Als nächstes habe ich, um zu untersuchen ob Tau Aggregation ohne die Ausbildung von NFT ausreichend ist um Defizite im Hippocampus-abhängigem Verhalten (Gedächtnistests) zu bewirken, in einem zweiten Set von Experimenten sechs und elf Monate alte P301L Mäuse, die wir auf den C57Bl/6 Stamm zurückgekreuzt hatten, in einer Hippocampus-spezifischen Testbatterie untersucht.
Ich konnte in verschiedenen Tests aufzeigen, dass P301L Mäuse eine kaum veränderte Ängstlichkeit verglichen mit Wildtyp-Mäusen besassen, wohl aber ein signifikant verstärktes Explorationsverhalten zeigten. Die Enthemmung des Explorationsverhaltens war unabhängig vom genetischen Hintergrund und verstärkte sich mit dem Alter, was darauf hindeutet, dass dieser Effekt auf das Tautransgen zurückzuführen ist. Amygdala-spezifische Tests zeigten keine Beeinträchtigung in der Angst-Konditionierung gegenüber Ton und Kontext und in der Erfassung und Konsolidierung einer Geschmacksaversion (CTA). Hingegen war die Extinktion dieser konditionierten Geschmacksaversion in den transgenen Mäusen signifikant be-

schleunigt. Anschliessend überprüfte ich die Verteilung von P301L Tau etwas eingehender mit dem Hauptaugenmerk auf Hirnareale, welche bei der CTA eine Rolle spielen. Das Aggregationsmuster von Tau stimmte mit dem Verhalten überein: Tauaggregate waren im basolateralen Nukleus der Amygdala präsent, der eine zentrale Bedeutung in der Extinktion des CTA-Gedächtnisses besitzt, während der Erwerb einer CTA von einem intakten zentralen Nukleus abhängig ist, wo keine Tauaggregate gefunden wurden.
Überdies konnte ich zeigen, dass eine Tau Aggregation ohne augenfällige NFT-Bildung ausreichend war um Defizite im räumlichen Referenzgedächtnis (spatial reference memory) im Wasserlabyrinth bei beiden getesteten Altersstufen hervorzurufen. Aufgrund eines schlechten Leistungsverhaltens der älteren Wildtyp-Kontrollgruppe während des Testdurchgangs konnte ein signifikanter Unterschied zu den Wildtyp Mäusen nur im Alter von sechs Monaten aufgezeigt werden.
Keine Defizite wurden beim Erlernen und beim Umkehrlernen der Plattformposition im Wasserlabyrinth aufgezeigt, ebenso im Y-Labyrinth, wo das räumliche Arbeitsgedächtnis (spatial working memory) über spontanes Alternationsverhalten getestet wurde.

Signifikanz: Zusammengefasst deuten diese Daten daraufhin, dass die Expression von P301L Tau in den transgenen Mäusen zu einem Zeitpunkt, der noch nicht durch eine massive NFT Bildung gekennzeichnet ist, selektive Verhaltensdefizite hervorruft, die mit dem Expressionsmuster von Tau in unterschiedlichen Amygdalakernen übereinstimmen. Der Zusammenhang zwischen NFT als einem Krankheitsmerkmal und dem Verhalten ist ein wichtiger Massstab für die Validierung unserer transgenen Mäuse als Tiermodel für die Taupathologie bei Alzheimer und verwandten Erkrankungen.

B. Funktion verschiedener Phosphoepitope und Spaltungsstellen bei der Bildung von Taufilamenten in Zellkultur

Hintergrund: Trotz umfassender Forschungen ist der genaue Zusammenhang zwischen Aβ und Tau und der jeweilige Beitrag zur Pathologie immer noch unklar. Kürzlich hat unsere Gruppe einen pathophysiologischen Zusammenhang zwischen diesen zwei Proteinen demonstriert. Durch stereotaktische Injektionen von fibrillärem Aβ in die Hirne von P301L Tau transgenen Mäusen konnte eine verstärkte NFT-Bildung aufgezeigt werden, die mit einer Phosphorylierung der Tauepitope Ser-422 und AT100 (Thr-212/Ser-214) einher ging (Gotz *et al.*, 2001b). Desweiteren konnte durch eine fünftägige Inkubation Tau überexprimierende humaner SH-SY5Y Neuroblastomzellen mit Aβ-Fibrillen die Bildung von Taufilamenten und eine verminderte Löslichkeit von Tau erzielt werden. Diese wurde durch die Mutation des Ser-422 Epitopes verhindert (Ferrari *et al.*, 2003).

Resultate: Um die früheren *in vitro* Ergebnisse zu bestätigen und die Rolle von zusätzlichen Phosphorylierungs- und Spaltungsstellen von Tau in der Aβ-bedingten Unlöslichkeit von Tau und der Filamentbildung zu untersuchen, habe ich verschiedene Taumutanten und Wildtypkonstrukte erzeugt und diese in SH-SY5Y Neuroblastomzellen überexprimiert.
Die Zugabe von Aβ-Fibrillen zu differenzierten Wildtyp Tau überexprimierenden SH-SY5Y Zellen führte zu einer mehr als 15-fachen Zunahme in der Aβ-bedingten Unlöslichkeit von Tau verglichen mit PBS behandelten Zellen, wohingegen durch Mutation unterschiedlicher Phosphoepitope von Tau mit einer bekannten Rolle bei der menschlichen Erkrankung (wie das AT8-Epitop pSer-202/pThr-205, pThr-231 und pSer-422) die Abnahme in der Löslichkeit von Tau verhindert wurde, was auf ein Zusammenspiel verschiedener Epitope in der Taufilamentbildung hindeutet. Ähnlich wie bei den Phospho-Mutanten wurde durch das Entfernen des carboxy-terminalen Teils von Tau an der putativen Caspase-3 Schnittstelle (Position 421) die Aβ bedingte Verringerung der Taulöslichkeit in unserem Zellkultursystem verhindert. Dies deutet daraufhin, dass der Spaltungsvorgang kein initialer Schritt in der Filamentbildung darstellt, sondern eher nach Bildung der Filamente erfolgt.

Signifikanz: Ich konnte aufzeigen, dass der Aβ-bedingte Anstieg in der Unlöslichkeit von Tau vom Zusammenwirken mehrerer Phosphoepitope abhängig ist und nicht nur vom Ser-422-Epitop alleine. Unser neues Tau-überexprimierendes Zellkultursystem stellt ein geeignetes Werkzeug dar, um Aspekte von Alzheimer und verwandter Erkrankungen *in vitro* zu untersuchen. Durch weitere Anpassungen dieses Models, zum Beispiel durch Einsatz eines induzierbaren Expressionssystems (das ich ebenfalls gestartet habe), dürfte es möglich sein, bessere Einblicke in die Entstehung von Tauopathien zu gewinnen und therapeutische Ansätze und Präparate zu testen, um die Bildung von Taufilamenten zu verhindern.

1 INTRODUCTION

1.1 Alzheimer's Disease (AD)

Of all forms of dementias, Alzheimer's disease (AD) is the most prevalent one. This disease was first described by the German physician Alois Alzheimer almost 100 years ago (Alzheimer, 1907). In the last decades, the numbers of AD patients have risen, as the relative numbers of old people in the population have increased. Approximately 8 % of the people over 65 years are affected by AD. This number rises to about 30 % in people older than 85 years (Hebert *et al.*, 2003).

AD is characterized by a well-defined neuropathological profile which includes extracellular β-amyloid-containing plaques, intracellular neurofibrillary tangles (NFT) of hyperphosphorylated tau protein, reduced synaptic density and neuronal loss in selected brain areas. The most severe neuropathological changes occur in the hippocampal formation, the association cortices and subcortical structures, including the amygdala and the nucleus basalis of Meynert (Arnold *et al.*, 1991). AD is described by cognitive and memory deterioration, progressive impairment of activities of daily living, and a variety of neuropsychiatric symptoms and behavioral disturbances (deterioration of language, visuospatial deficits, motor and sensory abnormalities and gait disturbances) (Cummings, 2004). As the disease advances, patients become incontinent, bedridden and unable to feed themselves. The disease course ranges from 2 to 15 years from the onset of symptoms until death, which occurs typically from pneumonia, upper respiratory infections or nutritional disorders.

1.2 Histopathology

1.2.1 β-amyloid plaques and Aβ processing

The major proteinaceous component of the extracellular plaques is a 40-42 amino acid polypeptide termed Aβ ($A\beta_{40}$ and $A\beta_{42}$), which is derived by proteolysis from the larger amyloid precursor protein APP (Glenner and Wong, 1984; Masters *et al.*, 1985) (Fig. 1.1). APP undergoes several endoproteolytic cleavage events. One of these events results from the activity of the membrane-associated α-secretase, which cleaves APP within the Aβ domain (Esch *et al.*, 1990). This pathway is non-amyloidogenic, as this cleavage precludes the formation of Aβ. Alternatively, cleavage may occur in the endosomal-lysosomal pathway, first by the β-secretase and then by the γ-secretase which together generates the Aβ-peptide. The latter involves an unusual form of proteolysis in which the protein is cleaved within the transmem-

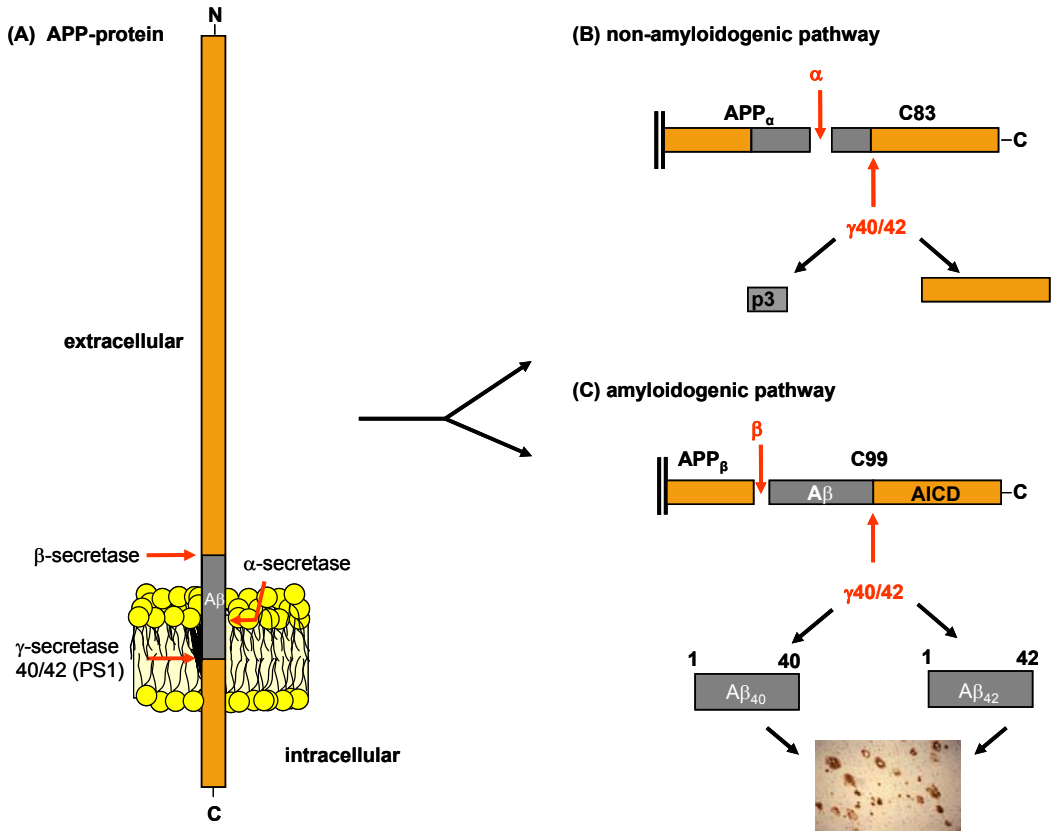

Fig. 1.1 Schematic overview of APP processing. (A) APP is a type I integral membrane protein with a large extra- and a short intracellular domain. (B) Cleavage by α-secretase within the Aß domain leads to secretion of the soluble APPα and prevents the formation of Aß-fragments (non-amyloidogenic pathway). The C-terminal stub C83 is processed further by γ-secretase releasing the p3 peptide. (C) Cleavage of APP in the endosomal-lysosomal pathway by ß-secretase enables the secretion of APPß. Processing of C99 by γ-secretase leads to the release of the Aß-peptides.

brane domain. Further, the cleavage-site of the γ-secretase is critical as it dictates the length of the peptide, with $A\beta_{40}$ being the most common species (around 90%), but $A\beta_{42}$ the more fibrillogenic and neurotoxic species (Sisodia and St George-Hyslop, 2002). β-secretase activity has been attributed to a single protein, BACE, whereas γ-secretase activity was shown to depend on the presence of a total of four components: presenilin (PS), nicastrin, APH-1 and PEN-2 (Edbauer *et al.*, 2003; Vassar *et al.*, 1999).

The precise physiological role of APP is still unknown, however, an involvement in the developing nervous system is likely. Furthermore, the transmembrane structure of APP indicates a role as either a receptor or a mediator of extracellular signalling (Kerr and Small, 2005), whereas the cytoplasmic domain may act as a transcription factor regulating gene expression (Cao and Sudhof, 2001).

Likewise, the mechanism of Aβ toxicity is unclear, but it may involve aberrant microglial activation (Roher *et al.*, 1996), induction of apoptosis (Loo *et al.*, 1993), increased ER and oxidative stress (Barnham *et al.*, 2004; Behl *et al.*, 1994; Nakagawa *et al.*, 2000), activation of ion channels and disruption of intracellular calcium homeostasis (Mattson *et al.*, 1992), leading to synaptic dysfunction.

1.2.2 Tau and NFTs

The second histopathological hallmark of AD are the neurofibrillary lesions that are found in cell bodies and apical dendrites as NFT, in distal dendrites as neuropil threads, and in the abnormal neurites that are associated with some β-amyloid plaques (neuritic plaques). Their major proteinaceous components are abnormal filaments which are termed either straight (SF) or paired helical filaments (PHF) (Crowther and Wischik, 1985; Wischik *et al.*, 1985). The core protein of these filaments is the microtubule-associated protein tau (Goedert *et al.*, 1988) that is widely expressed in the mammalian nervous system, but other non-neuronal cells, like astrocytes and oligodendrocytes, also express tau although at lower levels. The major function of tau is to regulate the stability and assembly of microtubules, and thus plays an important role in axonal transport and organization of the actin cytoskeleton. Additional functions have been assigned to tau in signal transduction and anchoring of phosphatases and kinases (Anderton *et al.*, 2000; De *et al.*, 2000; Ebneth *et al.*, 1998; Flanagan *et al.*, 1997; Jenkins and Johnson, 1998; Lee and Rook, 1992; Maas *et al.*, 2000; Morishima-Kawashima and Kosik, 1996; Reszka *et al.*, 1995; Sontag *et al.*, 1999).

In the adult human brain, six tau isoforms are produced by alternative mRNA splicing of exons 2, 3, and 10 from a single gene located on chromosome 17q21 (Goedert *et al.*, 1988; Goedert *et al.*, 1989) (Fig 1.2). They differ by the presence or absence of one or two short inserts in the amino-terminal half (exon 2 and 3), and have either three or four microtubule-binding repeat motifs in the carboxy-terminal half (3R and 4R). At the protein level, the isoforms ranging from 352 to 441 amino acids, with apparent molecular weights between 45 to 65 kDa on a SDS-PAGE. All six brain tau isoforms are found in neurofibrillary lesions of AD patients (Goedert *et al.*, 1992). Tau mRNA splicing is developmentally regulated and in the fetal brain only the shortest 3R-tau isoform is expressed (Goedert *et al.*, 1989). In addition, tau from fetal brain is phosphorylated at more sites than tau from adult brain, implying regulation during brain maturation. In general, tau is a phosphoprotein already under physiological conditions. The sequence of the protein is rich in serines and threonines followed by prolines (so-called SP/TP sites), and in tyrosines (Chen *et al.*, 2004a). In the course of the disease, tau becomes hyperphosphorylated, which means that the protein is phosphorylated to a higher degree at physiological sites, and at additional “pathological” sites (Augustinack *et al.*, 2002; Buee *et al.*, 2000). Phosphorylation tends to dissociate tau from microtubules. Since this increases the soluble pool of tau it might be an important first step in the assembly of tau filaments (Buee *et al.*, 2000; Chen *et al.*, 2004a; Goedert *et al.*, 1995; Gotz, 2001; Gotz *et al.*, 2004b; Lee *et al.*, 2001; Lichtenberg *et al.*, 1988; Schweers *et al.*, 1994). Hyperphosphorylated tau also displays a reduced electrophoretic mobility due to its increased phosphorylation state and has a lower range of pI values, indicating a more negatively charged, acidic character than normal tau (Hanger *et al.*, 1991; Ksiezak-Reding *et al.*, 1990).

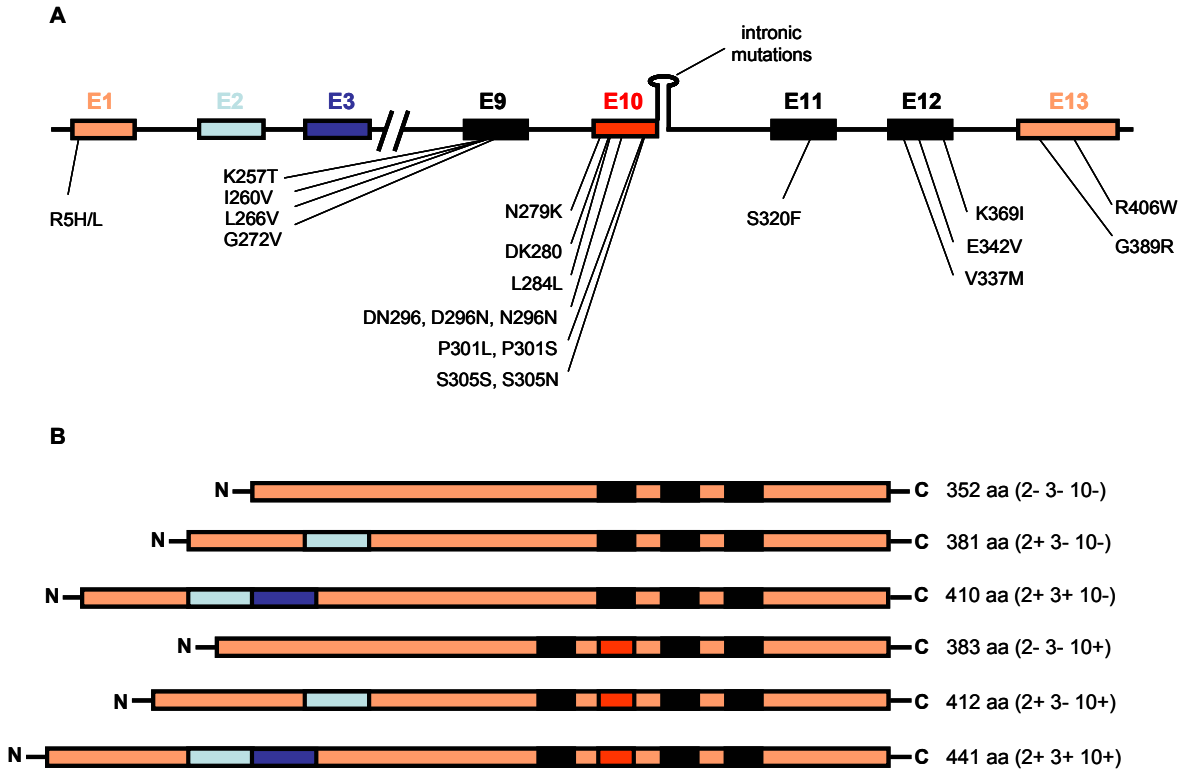

Fig. 1.2 Mutations in the tau gene and alternative splicing. (A) In FTDP-17, the majority of the exonic mutations are clustered around the microtubule-binding domain (exons 9-12). The intronic mutations are indicated by the predicted stem-loop pre-mRNA structure at the junction between exon 10 and the following intron. (B) In the adult human brain six tau isoforms are produced by alternative mRNA splicing of exons 2, 3 and 10. They differ by the presence or absence of one or two short inserts in the N-terminal part, and have either three or four microtubule-binding repeat motifs in the C-terminal half.

Furthermore, to aggregate into filaments, tau undergoes a shift from a natively unfolded or random coiled conformation to a more compact state and is relocalized from axonal to somatodendritic compartments (Mandelkow *et al.*, 1996; Schweers *et al.*, 1994). One of the first alterations, which is found already in pretangle neurons but persists in NFT-containing neurons, is the folding of the amino terminal portion of the tau molecule which binds to the third microtubule-binding domain. This conformation is known as the “Alz50 state”, as it is specifically recognized by the monoclonal antibody Alz50 (Carmel *et al.*, 1996). Another conformational change is revealed by the monoclonal antibody TG3 raised to PHFs from AD brain homogenates recognizing a conformation-dependent phospho-epitope of tau at position Thr-231 (Jicha *et al.*, 1997). Further alterations in the conformation of tau are detected during tangle evolution including various truncation events at both the amino- and carboxy termini (Binder *et al.*, 2005). In addition, posttranslational modifications of tau other than phosphorylation were described as well, which may occur either before of after filament formation (Buee *et al.*, 2000; Chen *et al.*, 2004a).

1.3 AD-causing mutations

The existence of early-onset familial forms of AD (FAD) allowed the identification of causative genes and key proteins, the elucidation of pathogenic mechanisms, and the development of transgenic animal models (see below under 1.5). In FAD, pathogenic mutations have been identified in either the APP gene itself or in the genes encoding presenilin 1 and 2 as a part of the γ-secretase complex (Sherrington *et al.*, 1995; Van Broeckhoven *et al.*, 1992).
The first missense mutation in FAD families was found in the APP gene of a British family in 1991 (V717I, the so-called “London mutation”) (Goate *et al.*, 1991). Since then, more than 20 pathogenic mutations have been identified in the APP gene. Immediately upstream of the Aβ domain, the most famous mutation was discovered in a Swedish FAD family, consisting in a double base pair substitution (K670D/M671L “Swedish mutation”) (Mullan *et al.*, 1992). The Swedish mutation leads to enhanced cleavage through β-secretase and thereby to increased Aβ formation, whereas the London mutation (and other pathogenic mutations at the same position) lead to an increased proportion of $A\beta_{42}$ being produced and secreted.
80% of FAD cases are caused by mutations in PS1 (> than 120) and PS2 (only 8 mutations to date). In FAD, most missense mutations in presenilins lead to an increased production of the more fibrillogenic $A\beta_{42}$ over $A\beta_{40}$ (Sinha and Lieberburg, 1999).
Although FAD-mutations are estimated to account for less than 1% of the total number of AD cases (Delacourte *et al.*, 2002), the histopathological hallmarks are indistinguishable when FAD is compared with sporadic AD (SAD). For these, a complex etiology has been reported that is due to environmental conditions and susceptibility genes. These genetic factors act as predisposing agents and increase the risk of getting the disease. However, of the two dozen genes identified until today, only the apolipoprotein E (ApoE) gene, a regulator of lipid metabolism, has been confirmed unanimously as a risk gene and found to be associated with SAD (Rocchi *et al.*, 2003). Further studies are required to confirm the definite role of other genes in AD.

1.4 Therapeutic strategies and Anti-Aβ vaccination

Currently, there is no cure for AD available. The main efforts in the development of treatment strategies for AD focus on the prevention of Aβ production and aggregation or downstream neurotoxic events. β- and γ-secretases are attractive drug targets of the pharmaceutical industry (Lahiri *et al.*, 2003). However, a major problem in drug development arises from the finding that APP is not the only substrate of these secretases. Other approaches aim to block

the assembly of Aβ using β-sheet breakers (Soto *et al.*, 1998) or lowering zinc levels, as zinc can form complexes with Aβ (Cherny *et al.*, 2001).

Since ApoE has been confirmed as a risk gene in SAD, it is reasonable to assume that lipids such as cholesterol are involved in the pathogenesis of AD. Recent epidemiological and biochemical studies have strengthened this assumption by demonstrating an association between cholesterol and AD (Puglielli *et al.*, 2003). Other available drugs like NMDA-antagonists (memantine) or cholinesterase inhibitors (donepezil) only alleviate the symptoms but are ineffective against cognitive decline over time (Cummings, 2004).

As transgenic animal models provided evidence that both active and passive Aβ immunization can reduce cognitive dysfunction in APP transgenic mouse models without any side effects (Schenk *et al.*, 1999), an immunization trial was initiated in humans. In 2001, a phase IIa clinical trial was started in a multicenter placebo-controlled double-blind design where patients received a pre-aggregated synthetic $A\beta_{42}$ preparation (AN-1792 vaccine) (Schenk, 2002). However, the clinical trial was halted in January 2002 when four patients who had received the vaccine developed signs of subacute meningoencephalitis (Check, 2002; Senior, 2002).

A follow-up study from the Zurich center demonstrated that ~80% of their patients developed specific antibodies against Aβ which did not cross-react with human full-length APP. These antisera stained Aβ plaques on brain slices of APP transgenic mice and post-mortem brain sections from AD patients (Hock et al., 2002). The specific immune reaction against Aβ was still stable after one year. Moreover, this immune reaction showed a significant correlation with slowed cognitive decline (Hock et al., 2003). Together, these results indicate that vaccination against Aβ might be a potential treatment for AD, provided that a safe treatment modality can be introduced. Concurrently, it is important to note that immunization against Aβ does not seem to remove NFT pathology as shown in postmortem studies of three vaccinated patients (Ferrer et al., 2004; Masliah et al., 2005; Nicoll et al., 2003).

1.5 FTDP-17 and other tauopathies

No mutations have been identified in the tau gene in AD until today. In addition to AD, NFT are also found in the presence of either no or only scant amyloid plaques in additional neurodegenerative diseases, collectively termed tauopathies. They include diseases as diverse as Pick's disease (PiD) (Delacourte *et al.*, 1998; Hof *et al.*, 1994), progressive supranuclear palsy (PSP) (Bergeron *et al.*, 1997), corticobasal degeneration (CBD) (Bugiani *et al.*, 1999), pallido-ponto-nigral degeneration (Yasuda *et al.*, 1999), subcortical gliosis (Goedert *et al.*, 1999b), and frontotemporal dementia with Parkinsonism linked to chromosome 17 (FTDP-

17). In contrast to AD, where hyperphosphorylated tau forms filaments only in neurons, in PSP and CBD they also form abundantly in glial cells (Bergeron *et al.*, 1997; Chin and Goldman, 1996; Komori, 1999).

In 1998, exonic and intronic mutations were identified in the tau gene in patients with FTDP-17 (Hutton *et al.*, 1998; Poorkaj *et al.*, 1998; Spillantini *et al.*, 1998), establishing that tau dysfunction alone can cause neurodegeneration and lead to dementia. Most mutations identified so far are located in or near the microtubule-binding region in the carboxy-terminal half of the tau protein, suggesting that it is a hot spot of disease-causing mutations (Fig. 1.2). Mutations in exons 9 and 11-13 (such as G272V or R406W) affect all six tau isoforms. By contrast, mutations in exon 10 (such as P301L) only affect 4R tau isoforms. In vitro studies have demonstrated that the majority of the exonic mutations disrupt tau-microtubule interactions, reducing the ability of tau to promote microtubule assembly (D'Souza *et al.*, 1999; Goedert *et al.*, 1999a; Hasegawa *et al.*, 1998; Nacharaju *et al.*, 1999).

The intronic mutations are located close to the splice-donor site of the intron that follows the alternatively spliced exon 10, all destabilizing a potential stem-loop structure which is involved in regulating the alternative splicing of exon 10 (Fig. 1.2). This causes a more frequent usage of the 5' splice site and an increased proportion of tau transcripts that include exon 10, thereby disrupting the normal balance between three-repeat and four-repeat tau isoform expression (4R>3R) (Grover *et al.*, 1999; Hutton *et al.*, 1998; Poorkaj *et al.*, 1998; Spillantini *et al.*, 1998; Varani *et al.*, 1999).

Depending on the brain area affected by neuronal loss, the clinical phenotype in FTDP-17 patients can differ with variable cognitive and behavioral features (Kramer et al., 2003). Often, the clinical feature of FTDP-17 includes initial personality changes, disinhibition, loss of initiative or apathy and psychiatric manifestations, as well as stereotypical behavior (Neary *et al.*, 1998). Neuropsychological changes include short-term memory, attention and concentration (Bird *et al.*, 1999; Mirra *et al.*, 1999; Reed *et al.*, 1997; Sumi *et al.*, 1992; van Swieten *et al.*, 1999).

1.6 Animal models of tauopathies

1.6.1 APP transgenic mouse models

Several APP and PS transgenic mouse models have been generated over the past several years (for review, see (Ashe, 2001; Gotz *et al.*, 2004b)). In the APP single transgenic mice a role for Aβ could be demonstrated in progressive plaque formation, synaptic loss, gliosis and memory deficits which progressed with ageing. Transgenic co-expression of mutant prese-

nilins and mutant APP enhanced the histopathological and behavioral phenotype compared with APP single transgenic mice. These models are suited to test therapeutic strategies aimed at reducing Aβ levels and behavioral impairment associated with Aβ (see also 1.4). However, although these models contributed enormously to a better understanding of the pathogenesis of AD, they have their limitations. They do not show massive nerve cell death, with the exception of some motor neurons, nor do they develop NFT, the second hallmark of AD. To address the role of NFT-formation tau transgenic models has been developed.

1.6.2 Tau transgenic mouse models

The first tau transgenic model was established in 1995 (Table 1.1), by expressing the longest human 4R brain tau isoform, without a pathogenic mutation, under control of the hThy1 promoter for neuronal expression (Gotz *et al.*, 1995). Despite the lack of NFT pathology, these mice modeled aspects of human AD, such as somatodendritic localization and tau hyperphosphorylation and, therefore, represented an early pre-NFT phenotype. The use of stronger promoters to drive transgene expression caused a more pronounced phenotype (Ishihara *et al.*, 1999; Probst *et al.*, 2000; Spittaels *et al.*, 1999). However, despite the decreased solubility of tau as the mice became older, NFT did not form, unless the mice reached a very old age (Ishihara *et al.*, 2001). Taken together, these findings demonstrated that overexpression of human wild-type tau can lead to an axonopathy resulting in nerve cell dysfunction and amyotrophy (Gotz, 2001; Gotz *et al.*, 2004b).

With the identification of mutations in tau, several groups created transgenic models expressing different tau mutations (Table 1.1). NFT formation was achieved both in neurons (Allen *et al.*, 2002; Gotz *et al.*, 2001a; Lewis *et al.*, 2000; Tanemura *et al.*, 2001; Tatebayashi *et al.*, 2002) and in glial cells of transgenic mice (Forman *et al.*, 2005; Gotz *et al.*, 2001c; Higuchi *et al.*, 2002). The P301L mutation was one of the first FTDP-17 mutations which had been identified in human patients (Hutton *et al.*, 1998). This mutation was shown *in vitro* to cause both an accelerated aggregation of tau into filaments and a marked reduction in the ability of tau to promote microtubule assembly (Barghorn *et al.*, 2000; Hasegawa *et al.*, 1998; Nacharaju *et al.*, 1999). The P301L mutation is also quite frequent (Sobrido *et al.*, 2003), and therefore, this made it a fitting choice to be expressed in transgenic mice.

When a human tau isoform lacking the two amino-terminal inserts was expressed together with the P301L mutation under control of the murine PrP promoter, 90% of the mice developed severe motor and behavioral disturbances by 10 months of age (Lewis *et al.*, 2000). Importantly, NFT were identified in brain and spinal cord, and motor neurons were reduced twofold in spinal cord. The same mutation was expressed using the longest human tau iso-

Table 1.1: List of tau transgenic mouse models

mutation	strain name (genetic background)	promoter	tau isoform	Neurological characteristics	Reference
wild-type	ALZ7 (B6D2F1)	hThy1	4R-tau (2N)	Early pre-NFT phenotype: Somatodendritic localization and hyperphosphorylation of tau, but no NFT.	(Gotz *et al.*, 1995)
wild-type	TG23 (C57Bl/6 x CBA-F2)	mHMG-CoAR	3R-tau (0N)	Early pre-NFT phenotype: Somatodendritic localization and hyperphosphorylation of tau, but no NFT.	(Brion *et al.*, 1999)
wild-type	htau44 (B6D2F1)	mPrP	3R-tau (0N)	Accumulation of intraneuronal filamentous inclusions of insoluble, hyperphosphorylated tau, profound astrocytosis and axonal degeneration, but no NFT.	(Ishihara *et al.*, 1999)
wild-type	htau40 (FVB)	mThy1.2	4R-tau (2N)	Axonal degeneration in brain and spinal cord, astrogliosis and ubiquitination in accumulated proteins of dilated axons.	(Spittaels *et al.*, 1999)
wild-type	ALZ17 (B6D2F1)	mThy1.2	4R-tau (2N)	Somatodendritic staining for hyperphosphorylated tau, and prominent axonopathy.	(Probst *et al.*, 2000)
wild-type	Tα1-3RT	Tα1 α-tubulin	3R-tau (0,1,2N)	Age-dependent accumulation of filamentous tau aggregates in oligodendrocytes and, to a lesser extent, astrocytes that was Gallyas and thioflavin-S positive. Neuronal tau abnormalities also occurred.	(Higuchi *et al.*, 2002)
wild-type	GFAP/tau (C57Bl/6 x C3H)	mGFAP	4R-tau (1N)	Age-dependent accumulation of abnormally phosphorylated, ubiquitinated, and filamentous insoluble tau protein in astrocytes that was Gallyas and thioflavin-S positive. Mild blood-brain barrier disruption, induction of low-molecular-weight HSPs and focal neuronal degeneration.	(Forman *et al.*, 2005)
P301L	JNPL3 (Swiss Webster)	mPrP	3R-tau (2N)	NFT identified in brain and spinal cord; motor neurons reduced 2-fold in spinal cord. Progressive motor disturbances by 10 months of age.	(Lewis *et al.*, 2000)
P301L	pR5 (B6D2F1 + C57Bl/6)	mThy1.2	4R-tau (2N)	Numerous abnormal, tau-reactive nerve cell bodies and dendrites; large numbers of pathologically enlarged axons containing NFT- and tau-reactive spheroids. Neuronal lesions similar to FTDP-17.	(Gotz *et al.*, 2001a)
G272V	pR3 (B6D2F1)	mPrP-TA	4R-tau (2N)	Filaments in murine oligodendrocytes, associated with tau phosphorylation at AT8 epitope Ser-202/Thr-205 in vivo. In the spinal cord, fibrillary inclusions identified by thioflavin-S in oligodendrocytes and motor neurons.	(Gotz *et al.*, 2001c)
V337M	Tg214 (B6SYL)	mPDGF	4R-tau (2N)	Neurons of irregular shape in hippocampus were immunoreactive for paired helical filament-associated tau, and showed signs of atrophic cell death.	(Tanemura *et al.*, 2001)
R406W	(B6SYL)	CaMKII	4R-tau (2N)	Accumulation of insoluble tau in aged mice. Congophilic hyperphosphorylated tau inclusions only in forebrain neurons of aged mice.	(Tatebayashi *et al.*, 2002)
P301S	2541 (C57BL/6 × CBA)	mThy1.2	4R-tau (0N)	Massive NFT formation. Perchloric-acid soluble tau phosphorylated at many phospho-epitopes of tau (but not the AT100 epitope Ser-214); sarkosyl-insoluble tau strongly immunoreactive with all antibodies, including AT100.	(Allen *et al.*, 2002)

form which contains both amino-terminal inserts. The mThy1.2 promoter was chosen instead of the PrP promoter, which may account for different expression patterns in these mice (pR5-line) (Gotz *et al.*, 2001a). As above, NFT were identified by Gallyas silver staining and thioflavin-S fluorescent microscopy. In addition, tau filaments were revealed by immuno-electron microscopy of sarcosyl extracts using phospho tau-specific antibodies. Subsequent studies showed an upregulation of glyoxalase I, a critical player in the detoxification of dicarbonyl compounds (Chen *et al.*, 2004b) and a mitochondrial dysfunction (David *et al.*, 2005) in these P301L mice. Due to low expression levels in motor neurons of the spinal cord, no motor phenotype was observed, which would affect behavioral testing.

1.6.3 Additional transgenic animal models for tauopathies

In addition to transgenic mice, a variety of animal models of tauopathies have been used to provide additional insight into the mechanism of tau dysfunction. These models include the nematode Caenorhabditis elegans (Kraemer *et al.*, 2003), the fruit fly Drosophila melanogaster (Jackson *et al.*, 2002; Shulman and Feany, 2003; Wittmann *et al.*, 2001), and the sea lamprey (Hall *et al.*, 2001; Hall *et al.*, 2002). Furthermore, Xenopus oocytes, in which most of the M-phase regulators during mitosis have been discovered, were used to investigate the relationship between tau phosphorylation and mitosis (Delobel *et al.*, 2002). Each of these models offers its unique advantages like powerful genetics (easily genetically manipulations), simple and fast breeding, large screenings for pharmacological compounds and well characterized neurons (Gotz *et al.*, 2004b; Lee *et al.*, 2005). However, these phylogenetically lower species have a brain anatomy much different from humans, making interpretation of the findings and direct comparisons difficult.

1.7 Relationship between Aβ- and tau pathology

The pathogenic relationship of the two major lesions of AD, Aβ-plaques and NFT, and their relative contribution to the clinical features of AD is one of the most crucial and controversial topics in AD research. Patients bearing APP mutations develop both hallmarks, whereas tau mutation carriers only develop NFT, providing evidence that Aβ can induce NFT formation but that the opposite has not been established. These led to the proposition of the amyloid cascade hypothesis (Hardy and Higgins, 1992), which claims that (at least in familial AD) β-amyloid causes or enhances the NFT pathology. Although this concept at first sight seems consistent, it is difficult to combine it with the highly puzzling finding that plaques and NFT are neuroanatomically separated. NFT develop in specific sites of the brain and spread in a

predictable, non-random manner across it. Six stages of disease progression based on the tau pathology have been distinguished (Braak and Braak, 1991, 1995): the transentorhinal stages I-II representing clinically silent cases; the limbic stages III-IV of incipient AD; and the neocortical stages V-VI of fully developed AD. A comparative study of Aβ-associated pathology defined five phases which differ strikingly from the NFT-stages. Further, Aβ-deposition expands anterogradely into regions that receive neuronal projections from regions already exhibiting Aβ (Thal *et al.*, 2002).

Numerous correlation studies failed to demonstrate a clear relationship between the severity of dementia and Aβ deposition in human AD brains whereas correlation between NFT numbers and severity of dementia has been reported (Arriagada *et al.*, 1992; Bierer *et al.*, 1995; Crystal *et al.*, 1988; Nagy *et al.*, 1996). It was shown that total NFT counts in specific brain areas such as the entorhinal and frontal cortex, as well as neuron numbers in the CA1 region of the hippocampus were the best predictors of cognitive deficits in brain aging and AD (Giannakopoulos *et al.*, 2003).

Recently, however, a synergistic interaction between the APP- and the tau-related pathology, despite the different spatiotemporal distribution of plaques and NFT, could be proposed (Delacourte *et al.*, 1999; Delacourte *et al.*, 2002). It was also shown that whenever Aβ aggregates were detected, tau pathology was found, at least in the entorhinal cortex. The opposite was not true because cases were found with advanced tau pathology, with no trace of Aβ aggregates (Delacourte *et al.*, 2002).

1.7.1 Relationship between Aβ and tau pathology addressed in transgenic mice

To test the role of Aβ in tau pathogenesis, our group previously addressed this issue, using the P301L tau transgenic mouse model (pR5-line), by stereotaxically injecting pre-aggregated β-amyloid fibrils into the somatosensory cortex and the hippocampus (CA1) of these mice (Gotz *et al.*, 2001b). This stereotaxic approach caused a fivefold increase in the numbers of NFT in the amygdala of P301L mice, but not in wild-type tau transgenic or control mice. NFT formation was associated with the pathological phosphorylation of tau at the epitopes Thr-212/Ser-214 (AT100) and Ser-422 (pS422). Furthermore, mitochondria from P301L mice displayed an increased vulnerability towards Aβ insult, suggesting a synergistic action of tau and Aβ pathology on the mitochondria (David *et al.*, 2005).

An alternative approach was pursued by intercrossing Aβ-producing APP-mutant mice (Tg2576 mice overexpressing the APP^{SWE} mutation) with P301L tau transgenic mice (JNPL3-line) (breeding approach) (Lewis *et al.*, 2001). Double transgenic mice showed a more than sevenfold increase in NFT numbers in the olfactory bulb, the entorhinal cortex and the amyg-

dala compared to P301L single transgenic mice. In contrast, plaque formation was unaffected by the presence of the tau mutation compared to APP^{SWE} single transgenic mice.
Later on, a triple transgenic mouse model (3×Tg) harboring the APP^{SWE} mutation, the P301L tau (4R0N) mutation and the $PS1_{M146V}$ mutation was generated (Oddo *et al.*, 2003). These mice develop synaptic dysfunction, including LTP deficits, which manifests in an age-related manner, but before plaque and tangle pathology. The authors also claim that extracellular Aβ deposits appear prior to tau pathology, however, a causal relationship can not be established by this approach.
Together, these data established an interaction between APP/Aβ and tau by significantly accelerating the NFT formation in P301L mice. However, the discovery that the injection of Aβ-fibrils was not capable of inducing NFT formation in wild-type tau transgenic mice (which develop no NFT) imply that at least in the mouse model Aβ can not induce NFT formation *de novo.* Together with the findings from human tauopathies which are associated with NFT formation, but lack β-amyloid pathology, these would imply that other factors than Aβ induce NFT formation in the brain, but that Aβ has the ability to significantly accelerate the disease progress.

1.7.2 Relationship between Aβ and tau pathology addressed in the cell culture

Based on the *in vivo* data of the tau transgenic mice, our group established a cellular system using the human SH-SY5Y neuroblastoma cell line (Gotz *et al.*, 2004a). Both four-repeat wild-type and P301L mutant human tau were stably overexpressed in these cells. Addition of extracellular pre-aggregated $Aβ_{42}$-peptides for five days caused the development of numerous AD-like tau filaments (Ferrari *et al.*, 2003). Mutating the Ser-422 phospho-epitope of tau (which was hyperphosphorylated in P301L tau transgenic mice after β-amyloid injections (Gotz *et al.*, 2001b), prevented both the $Aβ_{42}$-mediated decrease in solubility and the generation of tau filaments in tissue culture, suggesting a pivotal role of this Ser-422 epitope in fibrillogenesis. Furthermore, stable reference genes were identified in this tissue culture system using custom-made gene arrays (Hoerndli *et al.*, 2004), enabling the subsequent identification of genes involved in the regulation of molecular and cellular processes of tau aggregation.

1.8 Aims of the study

1.8.1 Behavioral analysis of P301L tau transgenic mice

Transgenic mouse models of human diseases are well suited to provide insight into the underlying biochemical mechanisms and to assist in the development of treatment strategies (see above). In addition to reproducing the histopathological hallmarks of the human disease, correlation of these hallmarks with the behavioral outcome is an important measure of the validity and experimental use of any animal model. Therefore, the first part of my thesis consisted in the analysis of P301L tau transgenic mice (pR5-line) in several behavioral tasks to define the behavioral phenotype of these FTDP-17 tau mutant mice as a model for the tau pathology in AD and related disorders and to correlate the behavioral outcome with the expression pattern of the tau transgene.

In a first study I analyzed the mice in several amygdala-dependent tasks as expression levels of tau were high in the amygdala and as NFT formation was initiated in this brain region (Gotz *et al.*, 2001b; Pennanen *et al.*, 2004). The amygdala is involved in mediating effects of emotion (fear, exploration) on learning and memory and in the validation of primarily negative events.

P301L tau aggregates were also found in the hippocampus, yet, unlike the amygdala, NFT developed in the hippocampus only at high age (>18 months). In a follow-up study, to determine whether tau aggregation is sufficient to cause deficits in hippocampus-dependent behavior, the P301L mice were investigated also in a hippocampus-specific test battery (Pennanen *et al.*, 2005).

1.8.2 Role of different phospho-epitopes and cleavage sites in tau filament formation in tissue culture

To further map phospho-epitopes and cleavage sites of tau involved in filament formation, I generated, in the second part of my thesis, different tau mutant constructs and expressed them in human SH-SY5Y neuroblastoma cells. Upon treatment of differentiated tau-bearing SH-SY5Y cells with aggregated β-amyloid peptides ($A\beta_{42}$) and subsequent sequential extraction using buffers with increasing ionic strengths, the β-amyloid-induced decrease in tau solubility was determined.

To further validate and improve the *in vitro* model, an inducible expression system, the Tet-on system, was chosen, which allows high levels of gene expression in a time- and concentration dependent manner. Using a bi-directional (pBI) Tet response vector, expression of both tau and APP was achieved from the same plasmid. This system may eventually help to address several questions regarding the relationship between Aβ and tau.

2 MATERIALS AND METHODS

2.1 Behavioral analysis of P301L tau transgenic mice

2.1.1 Animals

The transgenic mice used in this study express the human pathogenic mutation P301L of tau together with the longest human brain tau isoform (htau40) under control of the neuron-specific mThy1.2 promoter. Pronuclear injections were done into C57Bl/6 x DBA/2 F2 oocytes to obtain founder animals that were backcrossed with C57Bl/6 and B6D2F1 mice to establish transgenic lines (Gotz *et al.*, 2001a). Line pR5-183 expressed mutant human tau in many brain areas, however, NFT formation was mainly confined to the amygdala (Gotz *et al.*, 2001a).

For the first study, wild-type (wt) and P301L mice on a B6D2F1 background were sequentially analyzed in two sets which were balanced for the genotype and subjected to an amygdala-dependent test-battery starting at 6 months of age when NFT began to form in the amygdala. Data were pooled, as no statistically significant differences were found between sets.

For the second study, where the mice were tested in a hippocampus-dependent test battery, by an initial breeding with a 50% C57Bl/6 background (P301L/B6D2F1 strain), and by backcrossing five times (N5) with C57Bl/6 mice, animals were obtained with a calculated > 98% C57Bl/6 background. Transgenic mice and littermate controls were tested in two groups at 5 to 6.5 months and 10 to 11 months of age, respectively.

For all studies only male mice were used. The group-housed mice were transferred to individual cages prior to testing and kept under an inverted 12 hour light/dark cycle with a room temperature of 22°C. Food pellets and water were available *ad libitum* unless otherwise noted. 30 min before each test session, the mice were transferred to the behavioral room.

2.1.2 P301L tau mouse genotyping

2.1.2.1 Mouse tail lysis

2 mm of mouse tail were cut and incubated in 20 µl digestion buffer (50 mM Tris pH 8.0, 20 mM NaCl, 1 mM EDTA pH 8.0, 1% SDS) at 1400 rpm in a thermomixer (Vaudaux-Eppendorf AG, Schonenbuch, Switzerland) for 40 min at 55°C, supplemented with 2 µl proteinase K (20 mg/ml). Proteinase K digestion was terminated through denaturation by adding 178 µl double

deionised water (ddH_2O) and incubating the tail lysate at 99°C for 5 min at 500 rpm in the thermomixer.

2.1.2.2 Polymerase chain reaction (PCR)

The polymerase chain reaction technique is a method to amplify DNA-sequences of interest (Mullis, 1990), by using two specific primers which are complementary to the two strands and define the sequence to be amplified. Three major steps are involved: First, denaturation of the DNA to single strands at 95°C. Second, annealing of the primers to their complementary sequence on the DNA. Optimal annealing temperatures are ~ 5 to 10°C lower than the T_m values of the primers. The Primers should be designed in such a way that an annealing temperature of 55 – 65°C is allowed. Third, elongation of the DNA-strand by using a heat stable DNA polymerase adding nucleotides (dNTPs) to the 3'-ends of the primer sequences at 72°C. By repeating these steps several times the DNA sequence of interest is amplified exponentially.

Transgenic P301L tau mice were screened with oligonucleotides tau-I (5'-GGA GTT CGA AGT GAT GGA AG-3') (Pos 18-37, →, 20 bp) and tau-K (5'-GGT TTT TGC TGG AAT CCT GG-3') (Pos 506-525, ←, 20 bp) to obtain an amplified product of ~500 bp. Briefly, 0.5 µl of the tail lysate was added to PCR mix (9.5 µl H_2O, 1.25 µl PCR buffer, 0.25 µl 10 mM dNTP, 0.5 µl oligo tau I/K mixture (0.2 µM), 0.5 µl Red Taq genomic DNA polymerase (Sigma, Fluka, Buchs, Switzerland)). Using a GeneAmp PCR system 9700 machine (Applied Biosystem, Rotkreuz, Switzerland), the reaction was heated to 95°C for 2 min before a series of 35 cycles was initiated (40 sec at 95°C, 60 sec at 64°C, 1 min at 72°C), then kept at 72°C for 7 min and cooled to 4°C.

2.1.2.3 Agarose gel electrophoresis

Analysis or separation of PCR products and digested DNA-fragments was carried out using agarose gel electrophoresis. (TAE-Buffer: 40 mM Tris-acetate, 1 mM EDTA; Gel-loading buffer: 0.25 % bromphenol blue, 0.25 % xylene cyanol FF, 30 % glycerol). An electrical field is used to drag the negatively charged DNA molecules (due to their phosphate groups) through a gel matrix. The migration rate of linear DNA depends mainly on its size and the shorter the DNA molecule the faster it moves through the gel. DNA-fragments were visualized by adding ethidium bromide which intercalates bases of DNA. When exposed to UV-light, ethidium bromide fluorescence a red-orange color.

2.1.3 Histology

Mice were perfused transcardially under deep anesthesia with a mixture of 2% xylazine and 10% ketamine (15 µl/g body weight) (Streuli-Pharma, Uznach, Switzerland). For that, the thorax was opened to expose the heart and major vessels. A cannula was inserted through the left ventricle into the ascending aorta. Right away, the right atrium was punctured with a sharp hook, to allow the efflux of return circulation. To remove the blood, mice were initially perfused with 0.9% NaCl for 5 min until the liver turned beige-yellow, followed by fixation with 4% paraformaldehyde (PFA) in phosphate buffered saline (PBS: 10 x buffer: 80 g NaCl, 2 g KCl, 17.8 g Na_2HPO_4-$2H_2O$ and 2.4 g KH_2PO_4 in 1l H_2O, adjusted to pH 7.4). Brains were then removed, postfixed in the same fixative solution overnight and washed 3 x with 1 x PBS for 24 h. The brains were then dehydrated in an ascending series of ethanol (70%, 96%, 100%; each 3 h, by changing every hour), left overnight in xylol, subsequently immersed in liquid paraffin at 60°C for 5 h and finally embedded in paraffin.

Immunohistochemistry was done on coronal 4-µm thin paraffin sections and brain areas were mapped based on the mouse atlas by Paxinos (Paxinos, 1997). To allow antibodies to penetrate fixed tissue embedded in paraffin, sections were dewaxed in xylol (3 x) and rehydrated in a descending series of ethanol (2 x 100%, 1 x 96%, 1 x 70%) and 2 x in ddH_2O (5 min each). For signal enhancement, sections were microwave treated in citrate-buffer pH 5.8 at 70°C for 15 minutes. Sections were blocked in PBS containing 4% BSA (Bovine serum albumin) or milk and 5% goat serum. Incubation with the primary antibody was done in 50% blocking buffer overnight at 4°C or for 1 h at RT. After washing 3 x with PBS sections were incubated with the secondary antibody in 50% blocking buffer for 1 h at RT. The immunostained sections were washed again and then flat-embedded between glass slides and coverslips with the anti-fading reagent Mowiol (Clariant, Frankfurt am Main, Germany).

For determining the expression pattern of human P301L tau in our mice, the human tau-specific antibody HT7 (Innogenetics Inc, diluted 1:200) and the phosphorylation-dependent anti-tau antibody CP13 (Dr. Peter Davies, diluted 1:200) directed against phosphorylated S202/T205 were used. For the peroxidase/DAB stainings, secondary antibodies were obtained from Vector Laboratories (Vectastain ABC kits PK-6101 and PK-6102).

2.1.4 Amygdala-dependent test battery

2.1.4.1 Motor coordination on the Rotarod

The body weight was determined at 6 and 8 months of age. To test locomotor coordination, the accelerating Rotarod (Udo Basile, Milan, Italy) (Fig. 2.1) was used which consists of a

rotating drum with a diameter of 3 cm covered with knurled Perspex to provide an adequate grip. The mice were first placed on the rod at the lowest speed of 4 rpm for 2 minutes. Only then the rod was switched to acceleration mode and the time on the rod was recorded for up to 5 minutes when the speed reached the maximum of 40 rpm. Mice were assessed daily in two trials on three consecutive days, with an intertrial interval of at least 3 h.

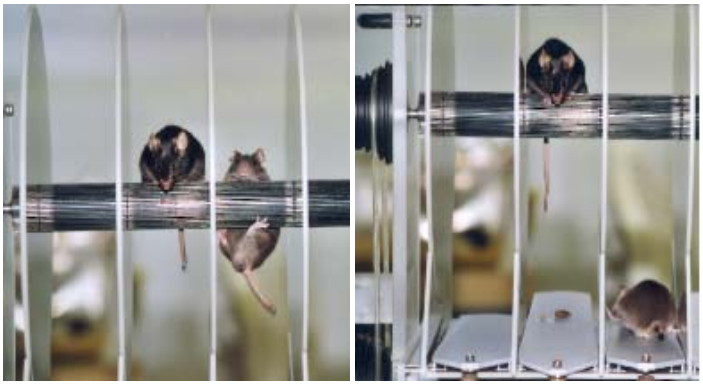

Fig. 2.1 The accelerating Rotarod: The mice are placed on a rotating drum at the lowest speed. Only then the rod is switched to acceleration mode and the time on the rod is recorded (max. 5 min).

2.1.4.2 Open-field test

The open-field test analyzes spontaneous locomotor activity, exploratory behavior, and anomalies of locomotion patterns. Mice were placed at the border of a dimly lit (50 lux) circular arena (diameter of 150 cm) for 10 min followed by a second session on the following day. The arena was divided into an outer zone (within 7 cm of the wall), an inner zone (inner circle with a diameter of 110 cm), and an intermediate zone (Fig. 2.2A). Locomotor activity was assessed by measuring the total distance traveled and the total number of zone transitions. Thigmotaxis, i.e. moving along the wall, was quantified by measuring the time spent in the outer zone. To determine measures of anxiety and exploratory behavior, the following parameters were assessed: number of visits to the inner zone, average distance to the inner zone, and the number of activity state changes. Three activity states were distinguished: progression (periods with a locomotion speed above the progression threshold of 0.085 m/s and a minimal distance moved exceeding 0.05 m), resting (periods lasting at least 2 seconds with a speed below 0.025 m/s) and scanning (periods meeting neither resting nor progression criteria).

2.1.4.3 Light-dark (L/D) test

Unconditioned anxiety-like behavior was tested in the light-dark (L/D) test. The mice were

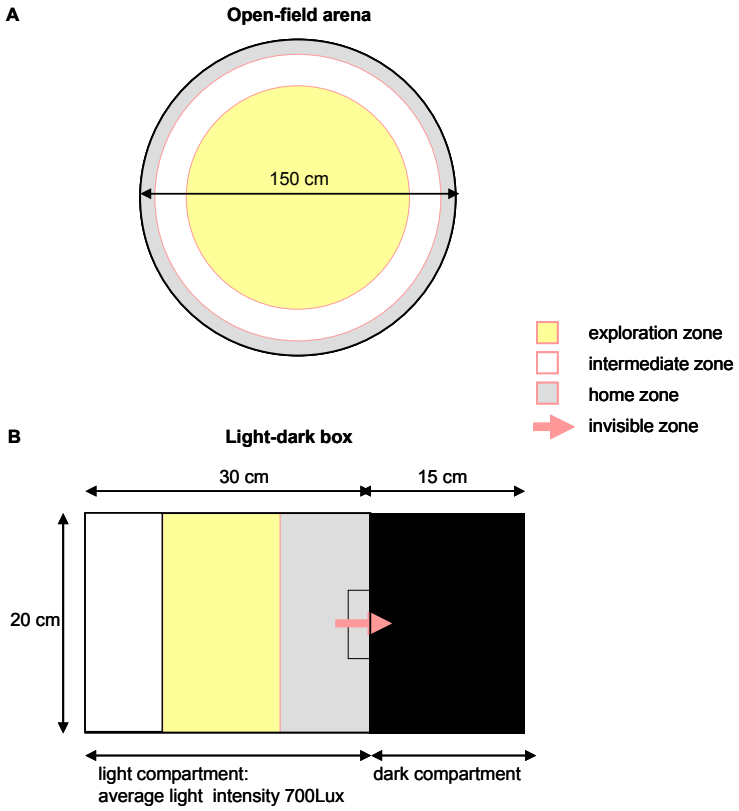

Fig. 2.2 To test levels of spontaneous locomotor activity, anxiety-like behavior and exploration two tests were performed. (A) In the open-field test, the mice were released at the border of a dimly lit circular arena which was divided into an outer zone (home zone; within 7 cm of the wall), an inner zone (exploration zone; inner circle with a diameter of 110 cm), and an intermediate zone. (B) For the light-dark test the mice were placed into the light compartment of the L/D box (average light intensity of 700 lux). A dark compartment was attached opposite to the releasing site with an opening facing the center of the illuminated part.

placed into the 30 cm x 20 cm area of a Perspex L/D box that was illuminated with an average of 700 lux. A dark compartment of 15 cm x 20 cm was attached opposite to the releasing site with an opening facing the center of the illuminated part (Fig. 2.2B). Movements were tracked in the illuminated part over a 5 minutes trial. Anxiety was measured by the latency to enter the dark compartment and the time spent in it. Exploration was defined by the number of rearings in the illuminated part, and the percentage of visited tiles / total of 36 tiles (5 x 3.3 cm) entered with all four paws defined as exploration index.

2.1.4.4 Fear conditioning

The conditioning chamber consisted of a gray opaque box (16.5 x 25 cm) with a grid floor through which shocks could be delivered (0.15 mA) as the unconditioned stimulus (US). The chamber was placed into a dimly lit sound-attenuating box with a speaker on top delivering a 92 dB / 2000 Hz tone as the conditioned stimulus (CS). Two measures were used to quantify freezing as the conditioned reaction: A grid of photobeams (1 x 1 cm) detected the inactivity of the mice, which was defined as no photobeam breaks during at least 2 seconds. Freezing

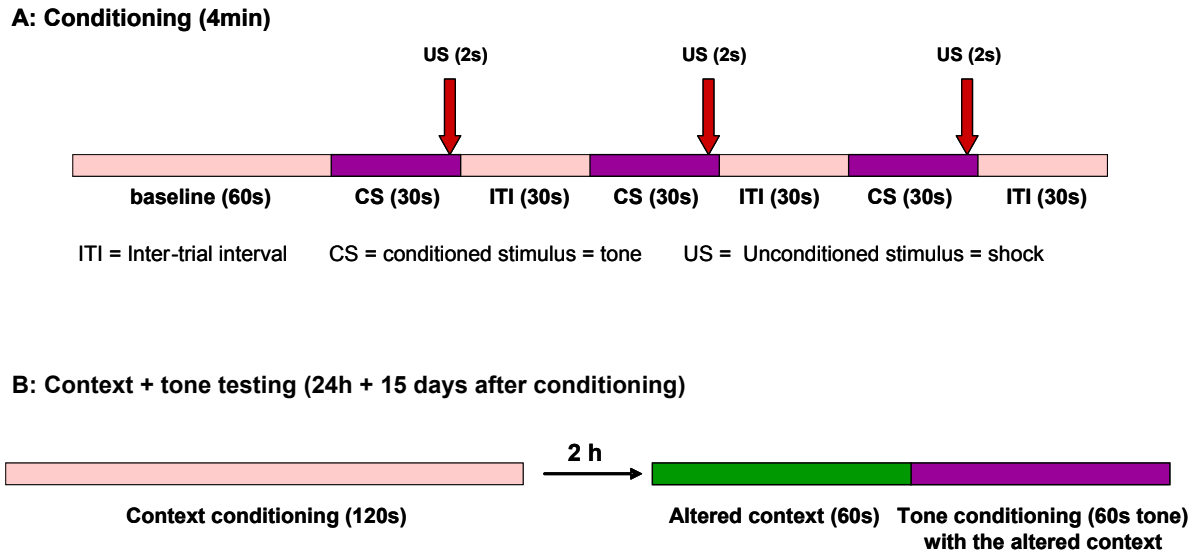

Fig. 2.3 Schematic flowchart illustrating the basic fear conditioning process. (A) For conditioning, a 1-min adaptation period (baseline) was followed by three identical conditioning trials, each trial consisting of 30 seconds CS presentation, with the US being applied during the last two seconds of the CS, separated by intertrial intervals of 30 seconds. (B) To evaluate context conditioning, mice were placed for two minutes in the conditioning chamber. To evaluate conditioning to tone, the physical characteristics of the chamber were changed. Each mouse was then placed for two minutes into this new chamber, and the CS was presented throughout the second minute.

was also detected manually while observing the animal and was defined as no movement except for respiration (as defined and applied by the experimenter). The two measures correlated well with each other. However, the manually detected measurement was finally used due to technical problems with the photobeams during cue testing: Sawdust was used in the new environment and unfortunately, from time to time, the photobeams were concealed, which caused a higher, inappropriate measurement of inactivity.

During the conditioning session, a 1-min adaptation period in the box was followed by three identical conditioning trials, each trial consisting of 30 seconds CS presentation, with the US being applied during the last two seconds of the CS, separated by an intertrial interval of 30 seconds (Fig. 2.3A). Retrieval tests for context conditioning and, two hours later, for conditioning to tone were carried out 24 h and 15 days after the conditioning session by recording freezing as mentioned above. To evaluate context conditioning, mice were placed for two minutes in the conditioning chamber. To evaluate conditioning to tone, the physical characteristics of the chamber were changed (shape, light, smell, and bedding material). Each mouse was then placed for two minutes into this new chamber, and the CS was presented throughout the second minute (Fig. 2.3B).

2.1.4.5 Conditioned taste aversion test (CTA)

For the first four days of the experiment, water-deprived mice were adapted to obtain water only during two daily drinking sessions, a morning session lasting 20 min and an afternoon

session lasting 10 min, with a 4 h intertrial interval. Water was presented in two 15 ml bottles that were weighed before and after the test to measure fluid intake. During the morning session on the conditioning day, mice were only allowed to drink a 0.5% saccharin solution (CS) (saccharin sodium salt hydrate, Fluka Chemie, Buchs, Switzerland) from one bottle. 40 min later, the mice were injected i.p. with a 0.14 M LiCl solution (at 2% of body weight) as the nausea-inducing agent (US).

Two days after conditioning, during the 20-min morning session all mice could drink either tap water from one bottle or the 0.5% saccharin solution from another bottle (two-bottle choice test). The percentage of saccharin consumption per total fluid intake was calculated. Extinction was determined by repeating the choice tests 3 days after conditioning, and on three consecutive days, beginning one week after conditioning. The mice of the second set were analyzed in three additional choice tests starting 5 weeks following conditioning.

To determine whether P301L mice were able to discriminate basic taste qualities, a separate group of water-deprived naive mice was adapted to the drinking schedule as described above. Then, the mice were tested for their natural preference for a sweet taste in a choice test, where one bottle was filled with a 0.5% saccharin solution and the second with tap water. Finally, to determine the natural aversion towards a bitter taste, a choice test between a 0.02% quinine solution (quinine hydrochloride dihydrate, Fluka, Buchs, Switzerland) and water was carried out.

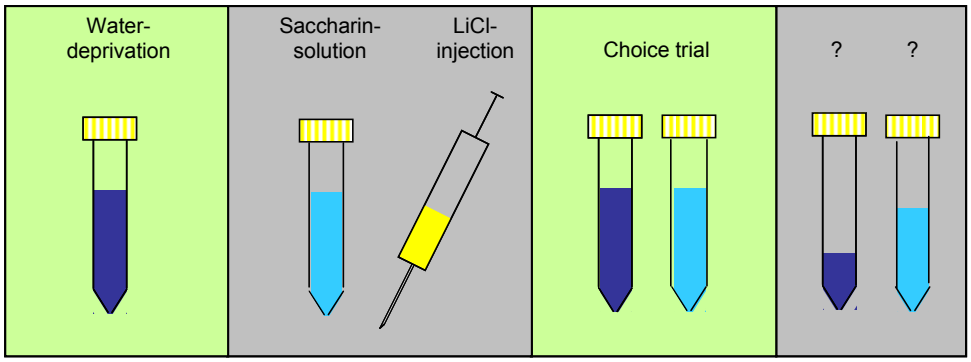

Fig. 2.4 Conditioned taste aversion test (CTA). On the conditioning day, water-deprived mice were allowed to drink a saccharin solution, before they were injected with LiCl as the nausea-inducing agent. Two days after conditioning, the first choice trial was presented and the percentage of saccharin consumption was calculated.

2.1.5 Hippocampus-dependent test battery

2.1.5.1 Open-field and elevated O-maze

In the second study, mice with a calculated > 98% C57Bl/6 background were tested. To identify potential effects of backcrossing on exploratory behavior, anxiety and locomotor activity, the mice were again assessed in the open field, together with the elevated O-maze.

The arena for the open-field test varied from the arena in the first study. Here, the mice were placed at the border of a dimly lit (50 lux) square arena (50 cm x 50 cm) and allowed to explore the arena freely for 30 min (Fig. 2.5A). The arena was divided into an outer (home) zone (within 7 cm of the wall), an inner (exploration) zone (inner square of 24 cm x 24 cm) and an intermediate zone. Locomotor activity was assessed by measuring the total distance moved and the total number of zone transitions. Thigmotaxis, i.e. moving along the wall, was quantified by measuring the time spent in the outer zone. To determine measures of anxiety and exploratory behavior, the following parameters were assessed: time spent in the inner zone, number of visits to the inner zone and the distance traveled in the inner zone.
The elevated O-maze is a runway (diameter 46 cm, width 5.5 cm) elevated to a height of 40 cm above floor level (Fig. 2.5B). It is comprised of two opposing open and two opposing closed sectors. The mice were placed into a closed sector and allowed to explore the maze freely for 5 min. The following parameters were assessed: Percentage of time spent in open sectors, percentage of entries into open sectors compared to total entries, total numbers of head dips, percentage of protected head dips, the total distance moved and the total numbers of zone transitions.

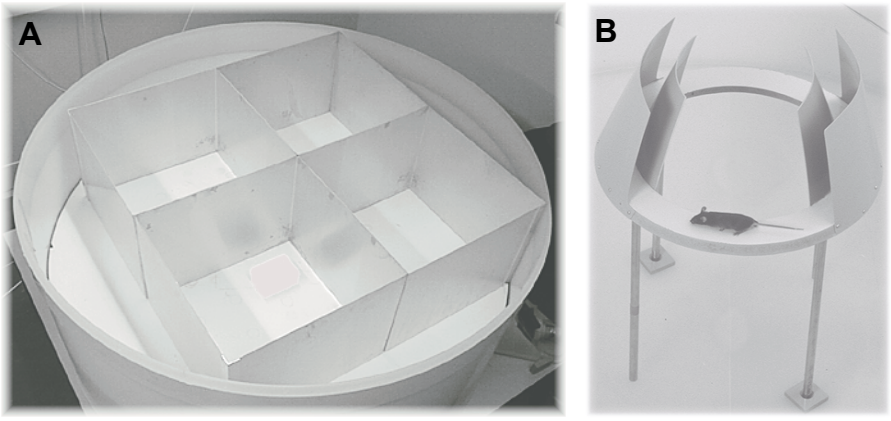

Fig. 2.5 Open-field and O-maze: (A) In the open-field arena, the mice were placed at the border of a dimly lit square arena (50 cm x 50 cm) which is divided into an outer (home) zone (within 7 cm of the wall), an inner (exploration) zone (inner square of 24 cm x 24 cm) and an intermediate zone. (B) The elevated O-maze is a runway elevated to a height of 40 cm above floor level. It is comprised of two opposing open and two opposing closed sectors and the mice were placed into one of the closed sectors. In both tasks, the mice are allowed to freely explore the arena.

2.1.5.2 Y-maze

To determine spontaneous alternation behavior (measure of spatial working memory), the mice were tested in a Y-maze with 40 cm long, 10 cm wide and 20 cm high arms. Each mouse received one trial during which it was placed at the end of one of the three arms and allowed to explore the maze for 5 min. Alternations and total numbers of arm entries were recorded. Spontaneous alternation, expressed as percentage, refers to the ratio of arm choi-

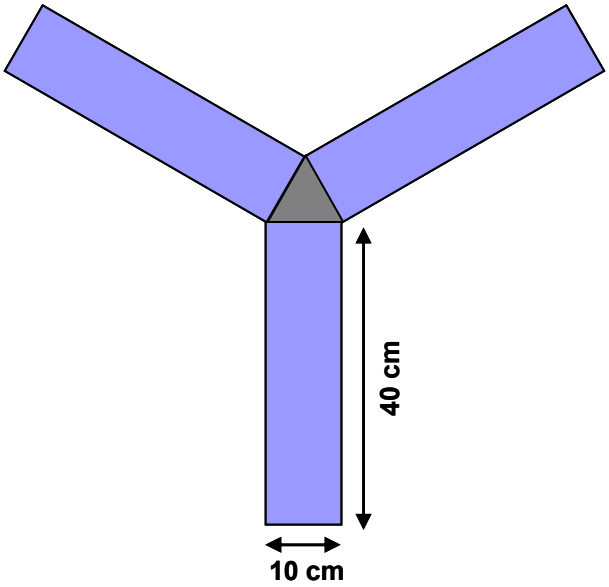

Fig. 2.6 Y-maze paradigm: To test spontaneous alternation behavior, mice were placed at the end of one of the three arms and allowed to explore the maze for 5 min.

ces differing from the previous two choices, to the total number of arm entries. Arm entry was considered to be completed when the hind paws of the mouse had been completely placed in the arm.

2.1.5.3 Morris Water Maze

To measure spatial reference memory, place navigation in the Morris water maze (MWM) was conducted (Morris et al., 1982). Mice were trained in a circular pool of 150 cm diameter made of white Plexiglas, filled with water (24-26°C) and made opaque by adding a white non-toxic paint (Acusol OP 301, Christ Chemie AG, Aesch, Switzerland). Distant visual cues for navigation were provided around the pool. A wire mesh platform (14 x 14 cm) was hidden 0.5 cm below the water surface with a pool perimeter distance of 35 cm. To avoid visual orientation prior to release, mice were transferred in a white plastic cup from their cages to the pool and released with the cup opening towards the wall of the pool. Eight symmetrically placed starting positions at the pool perimeter were varied in a predetermined but not sequential order. Mice were allowed to swim for a maximum of 120 s or until they had found the platform. Finding the platform was defined as staying on the grid for at least 3 s. After removal, mice were placed under an infrared lamp and allowed to warm up and dry off.

The test was divided into two phases, an acquisition phase (18 trials, six/day) followed by a reversal phase during which the platform was moved to the opposite corner (12 trials, six/day) (Fig. 2.7). Intertrial intervals varied from 30 to 90 min. The first 60 s of trial 19 (first reversal trial) was used as probe trial for spatial retention. The following parameters were analyzed both during acquisition and reversal learning: Escape latency, swim speed, time

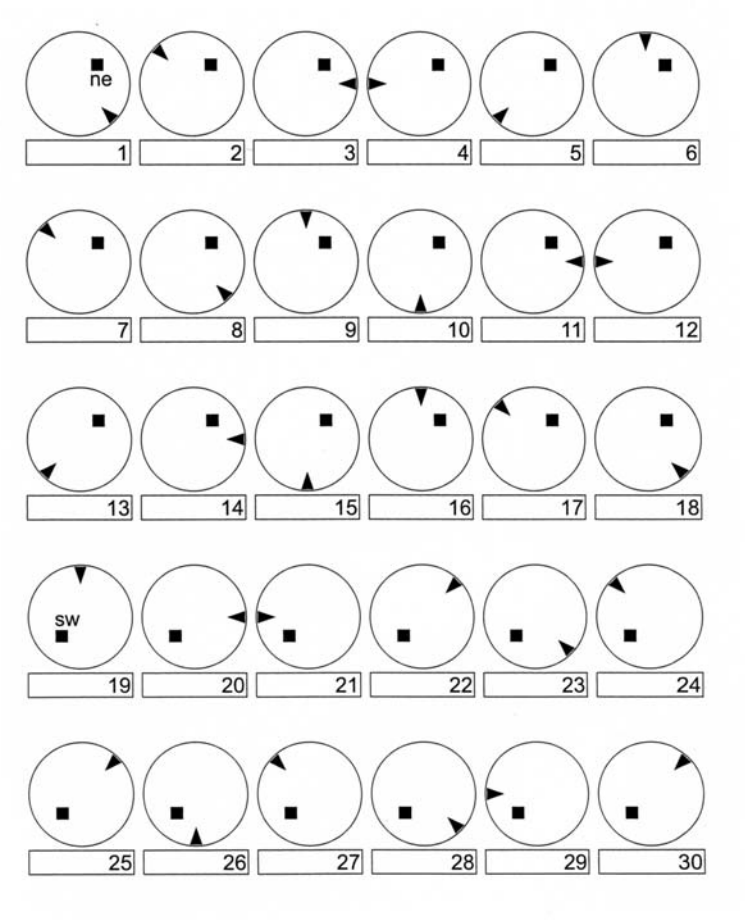

Fig. 2.7 Goal position and starting points in the Morris Water Maze: The figure shows one example out of the four different versions of the protocol. Goal positions are distributed over all four quadrants of the pool and are matched for the genotype, because spontaneous preference for one quadrant can not be excluded. Start points are spread in a pseudo-random manner in such a way that all points are used at a similar frequency. The mice perform 30 trials, 6 per day during 5 days. During the first 18 trials (acquisition phase) they are trained with the hidden platform in a constant position. For the reversal phase (the remaining 12 trials) the platform is moved to the opposite corner (figure adapted from D.P.Wolfer).

floating, wall hugging (thigmotaxis), swim path and the percentage of non-floating time in the current goal quadrant.

For data analysis of these parameters, trials were averaged into blocks of two trials. A second set of variables was used to assess spatial retention during the probe trial: Percentage of time spent in the former goal quadrant (with a chance level of 25%), percentage of time in a circular target zone comprising one-eighth of the pool (chance level of 12.5%) and the number of crossings over the former platform location (annulus crossing). These variables were compared with the average for the adjacent left and right quadrants. The opposite quadrant was not considered because it contained the new goal.

An automated software algorithm was used to classify trials according to the predominant swimming strategy. Seven categories were defined: floating, wall hugging, random swimming, scanning, chaining, focal searching and direct swims (Balschun et al., 2003). Each trial was categorized according to the predominant strategy. The number of trials falling into each category was computed for each mouse.

2.1.6 Video tracking and data analysis

All paths were tracked with an electronic imaging system (EthoVision 2.3, Noldus Information Technology, Wageningen, The Netherlands) at a frequency of 4.2 Hz and a spatial resolution of 256 x 256 pixels. Raw data were transferred to the Wintrack 2.4 software for off-line analysis (Wolfer et al., 2001). For statistical analysis, the SPSS software was used. Between-group comparisons were analyzed using a one-way analysis of variance (ANOVA) or a two-way ANOVA with repeated measures. Significant effects were analyzed post hoc using the Dunnett's test and Fisher's PLSD (protected least significant difference) for pair-wise comparison. All data are represented as mean ± SEM with a statistical significance given at $p < 0.05$.

2.2 Role of different phospho-epitopes and cleavage sites in tau filament formation in tissue culture

2.2.1 Phospho-epitope mapping: Site-directed mutagenesis

The longest human 4-repeat tau isoform, htau40, was cloned into the SpeI-site of the pRc/RSV expression vector (Invitrogen, Basel, Switzerland). Site-directed mutagenesis (Quick Change Kit, Stratagene, La Jolla CA, USA) following the manufacturer's instructions was performed to generate tau mutants with the following sense primers (Microsynth, Balgach, Switzerland):

AT8 (epitope S202/T205 of tau mutated to S202A/T205A): 5'-CAG CCC CGG C**G**C CCC AGG C**G**C TCC CGG CAG-3';

AT100 (epitope T212/S214 of tau mutated to T212A/S214A): 5'-GCC GCT CCC GC**G** CCC CG**G** CCC TTC CAA CCC-3';

T231 (epitope pT231 of tau mutated to T231A): 5'-TGG CAG TGG TCC GT**G** CTC CAC CCA AGT CGC-3'.

Tau Mutagenesis PCR:
5 µl of 10x reaction buffer
1 µl of 10mM dNTP
0.5 µl DNA-template (20 ng/µl)
1.25 µl tau primer forward (10 ng/µl)
1.25 µl tau primer reverse (10 ng/µl)
41 µl ddH_2O to a final volume of 50 µl
Then add
1 µl of PfuTurbo DNA polymerase (2.5 U/µl)

95°C for 30 sec

95°C 30 sec
55°C 60 sec
68°C 12 minutes 18 cycles

68°C for 12 minutes
4°C ∞

2.2.2 Cleavage site mapping: Δ421 truncated tau

Generation of the tau Δ1-421 truncation mutant was done by a three-way ligation procedure. The pRc/RSV expression vector bearing htau40 was digested with the restriction enzymes BstEII (a unique restriction site in tau at position 951) and XbaI (no cleavage site in tau, cuts the RSV vector in the polylinker ~ 150 bp downstream / 3' of the tau insert) (New England Biolabs, Bioconcept, Allschwil, Switzerland) (Fig. 2.8A). This yielded two fragments of ~ 4600 bp and ~ 530 bp, respectively (Fig. 2.8B). Concurrently, a PCR product was created with the RSV-htau40 vector as template and the two following primers (Microsynth, Balgach, Switzerland) (Fig. 2.8C):

Forward primer (28 bp): **Tau BstEII F,** contains the tau segment from bp 924-951 just before the BstEII restriction site: 5'-GTC TAC AAA CCA GTT GAC CTG AGC AAG G-3'.

Reverse primer (35 bp): **Tau 421 XbaI R,** sense strain contains aa 418-421, followed by a stop codon, the XbaI restriction site and aa 425-428:

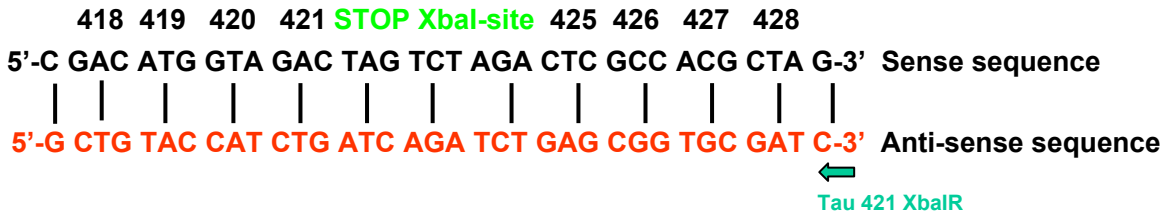

2.2.3 Transformation of chemical competent E. coli cells

To transform chemically competent *E. coli* cells, 1 ng/µl of plasmid DNA or an aliquot of a ligation reaction were added to 50 µl of *E. coli* cells and incubated on ice for 20 min. Following a heat shock for 45 sec at 42°C the cells were chilled on ice for additional 2 min. After adding 950 µl of preheated (42°C) LB-medium (Luria-Bertani medium: 10 g Bacto-Tryptone, 5 g Bacto-yeast extract and 10 g NaCl per 1l H2O adjusted to pH 7.0), the cells were incubated on a shaker at 37°C for 1 hour. After transformation bacteria were plated on LB-agar plates (15 g of Bacto-agar added to 1l of LB-medium) containing the appropriate antibiotic (Ampicillin) and incubated overnight at 37°C.

The next day, single colonies were picked and incubated overnight in 100 ml (for Maxipreps) or in 6 ml (for Minipreps) LB-medium (+ Ampicillin 1:1000) in a bacteria-shaker at 37°C. Transformed bacteria were stored in glycerol (0.3 ml of sterile 100% glycerol to 1.7 ml of bacterial culture) and kept at –80°C.

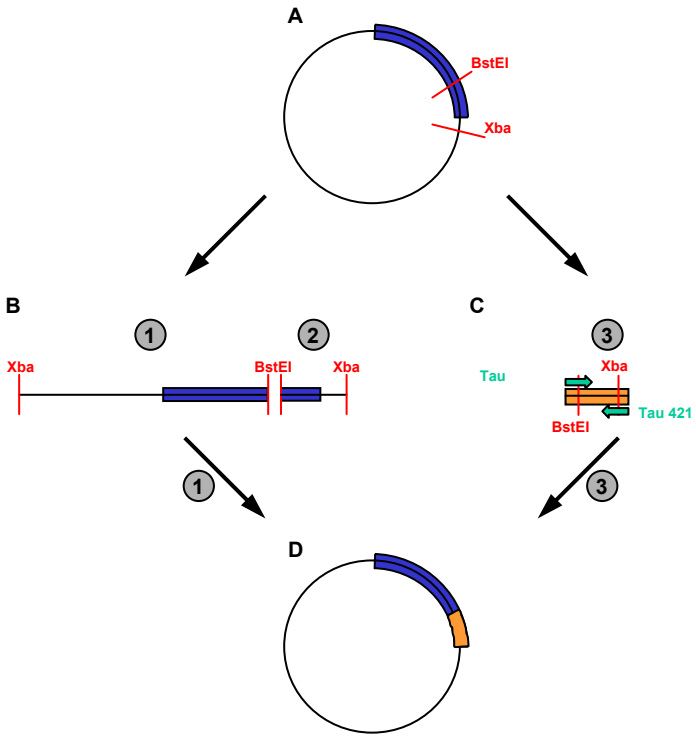

Fig. 2.8 Generation of Δ421 truncated tau: (A) The RSV-htau40 vector was digested with BstEII and XbaI. (B) Two fragments were obtained of the size of ~ 4600 bp and ~ 530 bp, respectively. (C) A PCR fragment with the tau sequence terminated at codon 421 was constructed with the RSV-htau40 vector as template and two specially created primers. (D) Fragments 1 and 3 were ligated, resulting in Δ421 truncated tau.

2.2.4 Isolation of plasmid DNA from E.coli cultures

Plasmid DNA isolation from E. coli cultures was done using the GenElute Plasmid Maxiprep and/or Miniprep Kit (Sigma Aldrich, Buchs, Switzerland). The principle of plasmid isolation is based on an alkaline-SDS lysis procedure followed by adsorption of the DNA onto silica in the presence of high salts. Contaminants were removed by a simple spin-wash step. Finally, the bound DNA was eluted in 10 mM Tris-HCl buffer (1 M Tris: 121,14 g tris(hydroxymethyl)-aminomethane in 1l H_2O, pH 8.0).

If required an ethanol precipitation procedure was used to concentrate the eluted DNA. Adding ethanol depletes its hydration shell and exposes the negatively charged phosphate groups in the backbone of the DNA, so that positively charged ions (e.g. Na^+) bind and a precipitate can form. To one volume of DNA solution, 1/10 volume of 3 M NaOAc (pH 5.2) and 2.5 volumes of 100% ethanol were added. DNA was precipitated for 30 min at –80°C, centrifuged for 30 min at 10'000 rpm at 4°C and washed with 70% ethanol. The DNA pellet was dried at room temperature and finally resuspended in elution buffer.

2.2.5 Recovery of DNA fragments from agarose gels

To isolate DNA-fragments of interest, the appropriate bands were cut out from agarose gels and were recovered using the QIAGEN gel extraction kit according to the manufacturer's instructions (Qiagen, Hombrechtikon, Switzerland). To avoid interference of high EDTA concentrations with enzymatic reactions, a modified TAE-buffer was used for preparation and running of the gel (Modified TAE-Buffer: 40 mM Tris-acetate, 0.1 mM EDTA).

2.2.6 Ligation

Digested DNA or PCR fragments were ligated with a linearized vector using the enzyme T4 DNA ligase (New England Biolabs, Bioconcept, Allschwil, Switzerland). The ligase catalyses the joining of two strands of DNA between the 5'-phosphate and the 3'-hydroxyl groups. The reaction was set up following the manufacturer's instructions. In order to suppress self-ligation of digested plasmid DNA, which contains complementary sticky ends or blunt ends, alkaline phosphatase was used to remove terminal 5'-phosphate groups before the ligation reaction was started.

2.2.7 DNA cycle sequencing

To confirm the presence of the mutated bases or absence of randomly introduced mutations, plasmids were sequenced using the dideoxy method developed by Sanger (Sanger *et al.*, 1977). In the cycle sequencing reaction all four dideoxynucleotides (A, T, G, C) labeled with different fluorescent dyes are added to an excess of deoxynucleotides. When one of the dideoxynucleotides is incorporated into the synthesized strain, the elongation is terminated because of the lack of the 3'-hydroxyl group. The products are then electrophoretically separated in a capillary according to their molecular weight. Different wavelengths are used to excite each dye and thus to identify the sequence of the DNA.
Sequencing was done with the ABI PRISM BigDye Terminator Cycle Sequencing Ready Reaction Kit (Applied Biosystems, Foster City CA, USA): To 200-500 ng DNA-template, 3.2 pmol of primer, 4 µl of Ready Rxn premix and 2 µl of BigDye sequencing buffer were added and filled up to a total volume of 20 µl with H_2O. The following primers were used for sequencing (Microsynth, Balgach, Switzerland):

Tau-G: 5'-ACC TCT GAT GCT AAG AGC AC-3' (Pos 187-206, →, 20 bp)
Tau-O: 5'-CCA ATG CCT GCT TC TTC AG-3' (Pos 308-326, ←, 19 bp)
Tau-E: 5'-TGA AGA AGC AGG CAT TGG AG-3' (Pos 309-328, →, 20 bp)
Tau-K: 5'-GGT TTT TGC TGG AAT CCT GG-3' (Pos 506-525, ←, 20 bp)

Tau-O232: 5'-AAG AAG GTG GCA GTG GTC CGT AC-3' (Pos 670-692, →, 23 bp)
Tau-B: 5'-TGA CAT TCT CCA GGT CTG GC-3' (Pos 750-770, ←, 20 bp)
Tau-F: 5'-AGA CTA TTT GCA CAC TGC CG-3' (Pos 909-928, ←, 20 bp)
Tau-Q: 5'-TGA CCT CCA AGT GTG GCT C-3' (Pos 953-971, →, 19 bp)
Tau-L: 5'-ATC TTC GAC TGG ACT CTG TC-3' (Pos 1042-1061, ←, 20 bp)

The DNA cycle-sequencing reaction was carried out using the following program: 96°C for 1min; 25 cycles (96°C for 10 s, 50°C for 5 s, 60°C for 4 min); hold at 4°C. DNA was precipitated in 100% ethanol and washed with 70% ethanol. The air dried DNA pellet was resuspended in 20 µl HPLC-upgrade H_2O. For the capillary gel run and detection of fluorescent dyes the ABI PRISM 310 Genetic analyzer (Applied Biosystems, Foster City CA, USA) was used.

2.2.8 Cell culture

Human SH-SY5Y neuroblastoma cells (DSMZ, Braunschweig, Germany; DSMZ No. ACC 209) were grown in Dulbecco's modified Eagle's medium F-12 (DMEM: F-12) supplemented with 2 mM L-glutamine, 1% penicillin/streptomycin, 10% fetal calf serum (FCS) and 5% horse serum (HS) (GIBCO, Basel, Switzerland). HEK 293 cells (human embryonal kidney cells; LGC Promochem, Molsheim Cedex, France; ATCC No. CRL-1573) were cultured in DMEM medium (GIBCO, Basel, Switzerland) supplemented with 10% FCS. All cells were maintained at 37°C in a saturated humidity atmosphere containing 5% CO_2.
Transfections with either wild-type or mutant htau40 cDNA constructs were done using LipofectAMINE 2000 (Invitrogen, Basel, Switzerland) or Metafectene (Biontex, Munich, Germany) and clones selected with 125 µg/ml G418 (VWR International AG, Calbiochem, Lucerne, Switzerland) for 30 days. To induce neuronal differentiation, cells were seeded on collagen type I-coated dishes (4 x 10^5 cells / 10 cm Petri dish) and sequentially treated for 5 days with retinoic acid (RA, 20 µM; Sigma Aldrich, Buchs, Switzerland) in standard culture medium, followed by 5 days with brain-derived neurotrophic factor (BDNF; 50 ng/ml; Peprotech, Lucerne, Switzerland) in serum-free medium (Encinas *et al.*, 2000). These neuronally differentiated cells were cultured in serum-free medium with BDNF for another 5 days adding pre-aggregated $A\beta_{42}$ (10 µM; Bachem, Bubendorf, Switzerland) or PBS. For that, $A\beta_{42}$ was reconstituted in PBS at a calculated concentration of 220 µM and shaken at 1000 rpm for 24 hours at 37°C. This fibril preparation contains a mixture of species such as Aβ-monomers and oligomers but also SDS-stable oligomers (Hartley *et al.*, 1999). Suspensions of fibrillar $A\beta_{42}$ preparations corresponding to 10 µM soluble peptide were added to the cultures for five days. Once $A\beta_{42}$ had been added to the cells, the medium was not changed anymore.

2.2.9 Immunocytochemistry

For immunocytochemistry, cells were grown on collagen-coated coverslips and fixed with 4% PFA for 30 min, followed by permeabilization with 0.3% Triton-X-100 for 10 min. Coverslips were blocked for 1h in 1x PBS containing 5% BSA and 2% goat serum. The first antibody was diluted in blocking buffer and cells were incubated for 1h in a humified chamber. After washing 2 x with PBS, cells were incubated with the according secondary antibody for another hour. After washing with PBS and H_2O, coverslips were mounted with Mowiol on microscope slides. Primary antibodies used for immunocytochemistry (IC) are listed in table 2.1. Secondary antibodies were obtained from Jackson ImmunoResearch (Milan Analytica, LaRoche, Switzerland).

2.2.10 MTT assay

To measure the proliferation rate of SH-SY5Y cells, an MTT assay was performed. MTT (3-(4,5-Dimethylthiazol-2-yl)-2,5-diphenyl-tetrazolium bromide; Thiazolyl blue) (Sigma Aldrich, Buchs, Switzerland) is a water soluble tetrazolium salt that can be converted to insoluble purple formazan by cleavage of dehydrogenase enzymes of living cells. SH-SY5Y cells were plated on 12 well plates at a density of 4 x 10^4 cells / well and differentiated with RA and BDNF as described above. Cell density was measured at different time points over differentiation (T_0, T_{2d}, T_{5d}, T_{7d}, and T_{9d}) by adding MTT (0.5 mg/ml dissolved in phenol red free DMEM: F-12 medium) to each culture (1 ml / well) and incubating for 3 hours at 37°C. Subsequently, medium was removed and the precipitated formazan was solubilized using 0.1 N HCl in 100% isopropanol. After 15 min shacking, the absorbance of the converted dye was measured at a wavelength of 595 nm using a Wallac Victor 2 (1420) Multi-label counter (PerkinElmer, Monza (Milan), Italy). Background absorbance was measured at 695 nm.

2.2.11 Cell lysis and protein extraction

The levels and solubility of tau protein were determined by extracting Aβ-treated and control cells using buffers with increasing ionic strength. The medium was exhausted and the cells were washed once with ice-cold PBS. Cells were scrapped and homogenized on ice with a Microlance 25 GA1 tip (BD Bioscience, Basel, Switzerland) in 150 µl RAB (high-salt reassembly) buffer (0.1 M MES pH 7.2, 1 mM EGTA, 0.5 mM MgSO4, 0.75 M NaCl, 0.02 M NaF, 1 mM PMSF, 0.1 mM EDTA), supplemented with a Complete EDTA-free protease inhibitor cocktail (1 tablet / 1 ml; 1:25) (Roche, Basel, Switzerland) and 1 mM PMSF. The cells were incubated for 20 min on ice, followed by centrifugation for 20 min at 10'000 g at 4°C. The supernatant was carefully removed (RAB fraction) and the RAB-insoluble pellet was extrac-

Table 2.1: Primary antibodies used for IC and WB

Anti-body	Specificity	Source	IC	WB
APP C-terminal	Recognizes aa 676-695 on APP C-terminus, α-rabbit	Sigma Aldrich, Buchs, Switzerland		1:2000
AT100	Phosphorylation-dependent human tau antibody against phosphorylated T212/S214, monoclonal α-mouse	Innogenetics, Gent, Belgium	1:200	
AT8	Phosphorylation-dependent human tau antibody against phosphorylated S202/T205, monoclonal α-mouse	Innogenetics, Gent, Belgium	1:200	
CP13	Phosphorylation-dependent human tau antibody against phosphorylated S202/T205, monoclonal α-mouse	P. Davies, A. Einstein College of Med, New York, USA	1:200	1:50
ET2	Specific for exon 10 of tau (recognizes only 4R-tau), monoclonal α-mouse	P. Davies, A. Einstein College of Med, New York, USA		1:25
HT7	Phosphorylation-independent human tau antibody, aa 159-163, monoclonal α-mouse	Innogenetics, Gent, Belgium	1:200	1:500-1:1000
Tau 5A6	Phosphorylation-independent human tau antibody, aa 19-46, monoclonal α-mouse	Developmental Studies Hybridoma Bank, Johnson, University of Iowa, Iowa City, USA	1:300	1:1000
Tau-133	N-terminal tau-specific antiserum (aa 1-16), α-rabbit	M. Goedert, MRC Laboratory of Molecular Biology, Cambridge, UK		1:200
Tau-134	C-terminal tau-specific antiserum (aa 428-441), α-rabbit	M. Goedert, MRC Laboratory of Molecular Biology, Cambridge, UK		1:200
Tau5	Phosphorylation-independent human tau antibody, aa 200-220, monoclonal α-mouse	Biosource, LucernaChem, Lucerne, Switzerland		1:500-1:1000
Tau-C3	Specific for caspase-3 cleaved tau at aa 421, monoclonal α-mouse	L. Binder, Northwestern University, Chicago, USA		1:500
α-14-3-3	Recognize a mixture of GST-14-3-3 proteins, polyclonal α-rabbit	Abcam Ltd., Cambridge, UK		1:1000
α-GFP	Anti green fluorescent protein, α-rabbit	Biosource, LucernaChem, Lucerne, Switzerland		1:1000
α-RhoGDI	Anti RhoGDI, polyclonal α-rabbit	Abcam Ltd., Cambridge, UK		1:1000

ted in 150 µl RIPA buffer (50 mM Tris pH 8.0, 150 mM NaCl, 5 mM EDTA, 0.1% SDS, 0.5% sodium deoxycholate SDO, 1% NP-40) with a Microlance 26 GA5/8 tip. After incubation for 20 min on ice and centrifugation for 20 min at 10'000 g at 4°C, the supernatant was recovered (RIPA fraction). The RIPA insoluble pellet was transferred with a pipette tip to a Beckman centrifuge tube. The pellet was extracted in 70% formic acid (FA) with a Microlance 26 GA5/8 tip and incubated for 20 min on ice. The FA-solution was centrifuged for 30 min at 50'000 g in an Optima TLX ultracentrifuge using a Beckmann TLA 120.2 rotor (Beckmann, Nyon, Switzerland) at 4°C. The supernatant was transferred onto a Millipore dialyze membrane (Millipore, Volketswil, Switzerland) and dialyzed against 50 mM Tris (pH 7.4), 1 mM DTT (DiThioThreitol), and 0.1 mM PMSF for 1h at room temperature (FA fraction). All fractions were stored at -80°C.

2.2.12 Western Blot analysis

Protein concentrations of the samples were determined with the DC Protein Assay (Bio-Rad, Reinach, Switzerland). Same amount of protein separated on 10-20% Tricine gels (Invitrogen, Basel, Switzerland) (10 x running buffer: 121 g TrisBase, 179 g Tricine, 10 g SDS per 1l H_2O adjusted to pH 8.3) and then transferred onto nitrocellulose membranes (0.1 µm) (Schleicher & Schuell BioScience, Dassel, Germany) (10 x transfer buffer: 144,2 g Glycine and 30,4 g TrisBase per 1l H_2O). The blots were blocked in TBS-Tween (TBST) containing 5% non-fat milk for 1h and incubated with the primary antibody overnight at 4°C or for 2h at room temperature. Primary antibodies used for western blotting (WB) are listed in table 2.1.
After three 5 min washes with TBST, the membranes were incubated with the appropriate secondary antibody conjugated to HRP (Horseradish Peroxidase) (Amersham Biosciences, Otelfingen, Switzerland) for 1h and washed afterwards with TBS at least three times. The blots were developed using ECL Western Blotting detection reagents (Amersham Biosciences, Otelfingen, Switzerland) or SuperSignal West Femto Luminol / Enhancer Solution (Pierce, Perbio Science, Lausanne, Switzerland). Same exposure times were chosen for all blots. The films (X-OMAT LS, Kodak/Sigma, Buchs, Switzerland) were scanned and images were analyzed using the ImageJ analysis program developed at the National Institutes of Health (http://rsb.info.nih.gov/ij/). If needed, the blots were stripped for 30 min at 50°C using a Western Blot Stripping Buffer (2% SDS, 0.0625 M Tris and 0.1 M β-Mercaptoethanol) and reprobed.

2.2.13 Immunoprecipitation

Immunoprecipitation was done using the Seize Primary Immunoprecipitation Kit (Pierce, Perbio Science, Lausanne, Switzerland) following the manufacturer's instructions. Thereby, the purified antibody is immobilized directly onto an agarose gel column, where it can form an immune complex with the antigen of interest. After removal of non-bound material by washing, the bound antigen can be dissociated from the antibody and collected by centrifugation. The advantage of this method is that it enables the reuse of primary antibody and results in purified antigen free of antibody contamination.

2.2.14 Silver staining

Silver staining allows the detection of most proteins on polyacrylamide gels. Thereby, the gel is impregnated with soluble silver ions and developed by treatment with formaldehyde, which reduces silver ions to form an insoluble brown precipitate of metallic silver. This reduction is promoted by proteins. A modified staining protocol from Blum *et al*. was used (Blum *et al.*, 1987). Protein fractions were run on a 10-20% Tricine gel. The gel was than fixed in 40% ethanol and 10% acetic acid overnight at 4°C. Following two washes in 30% ethanol and one wash in H_2O, each for 20 min, the gel was sensitized in 0.02% sodium thiosulfate ($Na_2S_2O_3$) for 1 min. The gel was washed 3 x 20 sec in H_2O, incubated in ice-cold 0.1% silver nitrate ($AgNO_3$) for 20 min at 4°C and washed again 3 x 20 sec in H_2O. To develop the gel a solution containing 3% sodium carbonate (Na_2CO_3) and 0.05% formalin was used. If the developer turned yellow the solution was renewed. As soon as the staining was sufficient, it was terminated in 1% glycine for 10 min. Finally, the gel was washed 3 x 10 min and stored in H_2O.

2.2.15 Mass spectrometry analysis

Since extraction of proteins from the gel is difficult, in-gel digestion of proteins with proteases (mostly trypsin) is used to generate peptide fragments. These peptide fragments were analyzed by matrix-assisted laser desorption/ionization tandem time-of-flight mass spectrometry (MALDI-TOF / TOF). The mass spectra were further analyzed with the software Mascot (Matrix Science, available at www.matrixscience.com) using a combined MS and MS/MS search. This search was carried out against the human UniProt complete proteome set database to identify proteins by comparing the peptide masses. Analysis was done at the Functional Genomics Center Zurich (FGCZ user centre) by Della David from the same laboratory.

2.2.16 Tet-system

The Tet-system uses a transactivator which is expressed from a constitutive promoter (regulatory plasmid) to regulate the transcription of a gene of interest from a silent promoter (response plasmid) (Fig. 2.9). In the Tet-On system the transactivator (rtTA) binds to a Tet-response element (TRE) on the response plasmid and activates transcription in the presence of an inducer. The current inducer of choice is doxycycline (DOX) because of its low cost, commercial availability, and because it efficiently activates rtTA at doses that are well below cytotoxic levels. Transfected cells were treated for 24h with doxycycline (10 µg/ml).

The regulator plasmid pUHD 29-1 that encodes the reverse-tetracycline-controlled transactivator was obtained from Dr. Bujard (ZMBH, Heidelberg, Germany). The pBI Tet Vector (BD Biosciences Clontech, Palo Alto, CA, USA) is a response plasmid that can be used to express two genes of interest from one bidirectional promoter (P_{bi-1}), regulated by the rtTA protein. P_{bi-1} contains a TRE element, which consists of seven copies of the 42-bp tet operator sequence (tetO). The TRE element is located between two minimal CMV promoters (CMV_{min}), which lack the enhancer that is part of the complete CMV promoter. Each of the two CMV_{min}-promoters controls the expression of two separate genes of interest (Fig. 2.9).

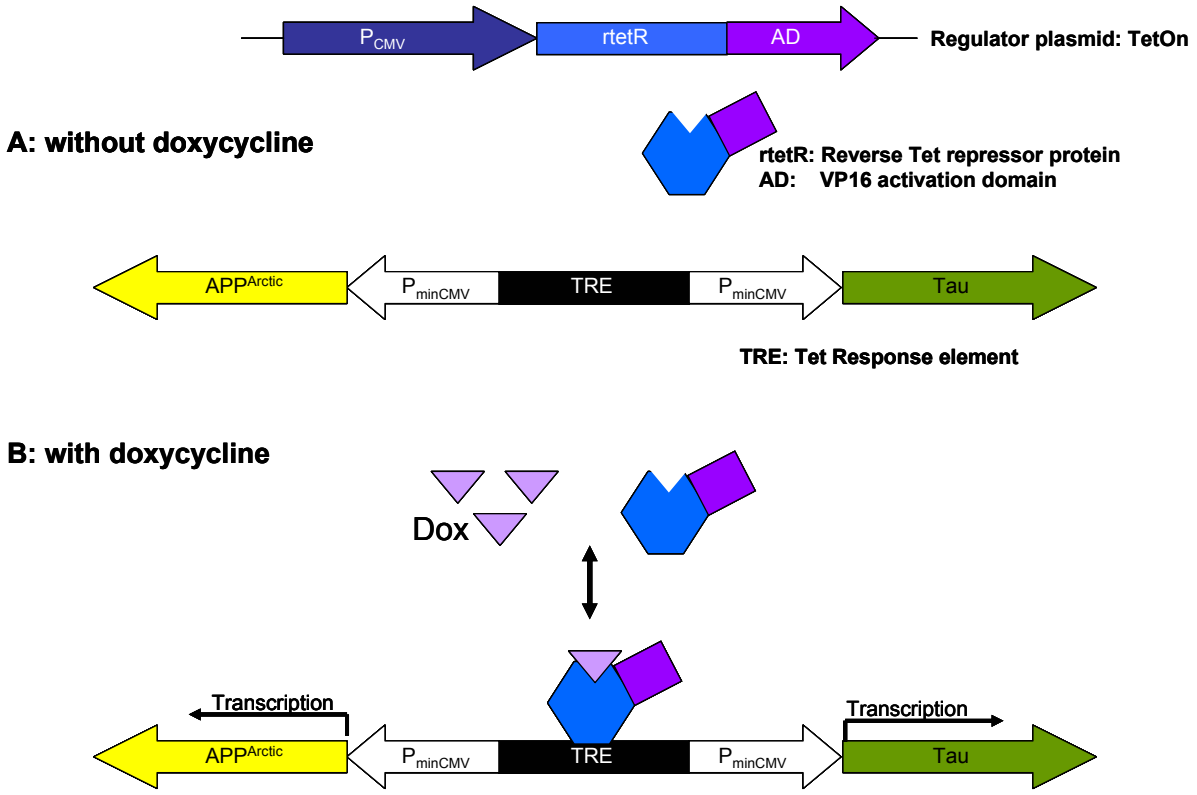

Fig. 2.9 Tet-on-system: A regulator plasmid encodes the reverse-tetracycline-controlled transactivator (rtTA; consisting of rtetR and AD) under the control of a constitutive promoter. As a response plasmid the pBI Tet vector is used which express two genes of interest (Tau and APP^{ARC}) each under the control of one minimal CMV promoter. (B) Only in the presence of an inducer (doxycycline) the transactivator binds to a Tet-response element (TRE) located on the response plasmid and activates thereby transcription of the genes of interest.

2.2.16.1 β-galactosidase assay

SH-SY5Y and HEK 293 cells were plated on 6 well plates at a density of 4 x 10^5 cells / well and co-transfected with the rtTA-plasmid and a pBI-GL control vector (BD Biosciences Clontech, Palo Alto, CA, USA), which is a response plasmid that can be used to express luciferase and β-galactosidase. After 24h treatment with doxycycline (10 µg/ml) cells were washed in PBS and fixed for 15 min in 0.05% glutaraldehyde in PBS. After 3 x washing for 5 min in PBS, they were stained in X-gal stain solution (1 mg/ml X-gal, 5 mM $C_6FeK_3N_6$, 5 mM $C_6FeK_4N_6$, 2 mM $MgCl_2$, PBS pH 7.3) for 3 hours at 37°C.

3 RESULTS

3.1 Behavioral analysis of P301L tau transgenic mice

3.1.1 Amygdala-dependent test battery

3.1.1.1 Expression pattern of P301L tau

To determine the expression pattern of human P301L tau in more detail, with special emphasis on brain areas involved in the CTA task, frontal sections of four P301L tau expressing mice were analyzed by immunohistochemistry using the human tau-specific antibody HT7 and the phosphorylation-dependent anti-tau antibody CP13 (Fig. 3.1). Expression of human tau was found in the motor, somatosensory and insular cortex (IC) and in the claustrum at position AP +1.1 mm. At AP –0.82, tau was present in cortical motor and somatosensory neurons and to a variable degree in the posterior part of the agranular insular cortex (AIP), in the anterior cortical amygdaloid nucleus (ACo) and different regions of the thalamus. At position AP –1.34, expression was found in the cortex, in the basolateral (BLA) and the basomedial nucleus of the amygdala (BM), in the dorsal endopiriform nucleus (DEn) and in the ACo. No tau expression was found in the lateral nucleus (LA) and the central nucleus of the amygdala (CE). HT7 staining revealed also a strong expression of human tau in the hippocampus (CA1, CA3 and dentate gyrus), whereas staining of these brain areas with the CP13 antibody was very weak. However, both antibodies strongly stained the posterior part of these hippocampal regions at position AP –2.92 (where human tau was also expressed in cortical neurons), the posterior part of the basolateral amygdala, and to a variable degree neurons in the red nucleus (parvocellular part, RPC), the ventral tegmental area (VTA) and the posteromedial cortical amygdaloid nucleus (PMCo). At AP –4.60, tau was present in cortical neurons, especially in the lateral entorhinal cortex and the external cortex of the inferior colliculus (ECIC) and to a variable degree in the oral pontine reticular nucleus (PnO), the rostral periolivary region (RPO) and the reticulotegmental nucleus pons (RtTG). Particularly high levels of expression were found in the brain stem (AP –7.20), predominantly in the inferior olive (IO), the ambiguus nucleus (Amb), and in various parts of the reticular formation and medulla. In contrast to the tau expression in the BLA, IC and some thalamic nuclei, no expression was found in CTA-relevant areas such as the ventral posteromedial nucleus of the thalamus (VPM), the parabrachial nucleus (PBN) and the nucleus of the solitary tract (NTS).

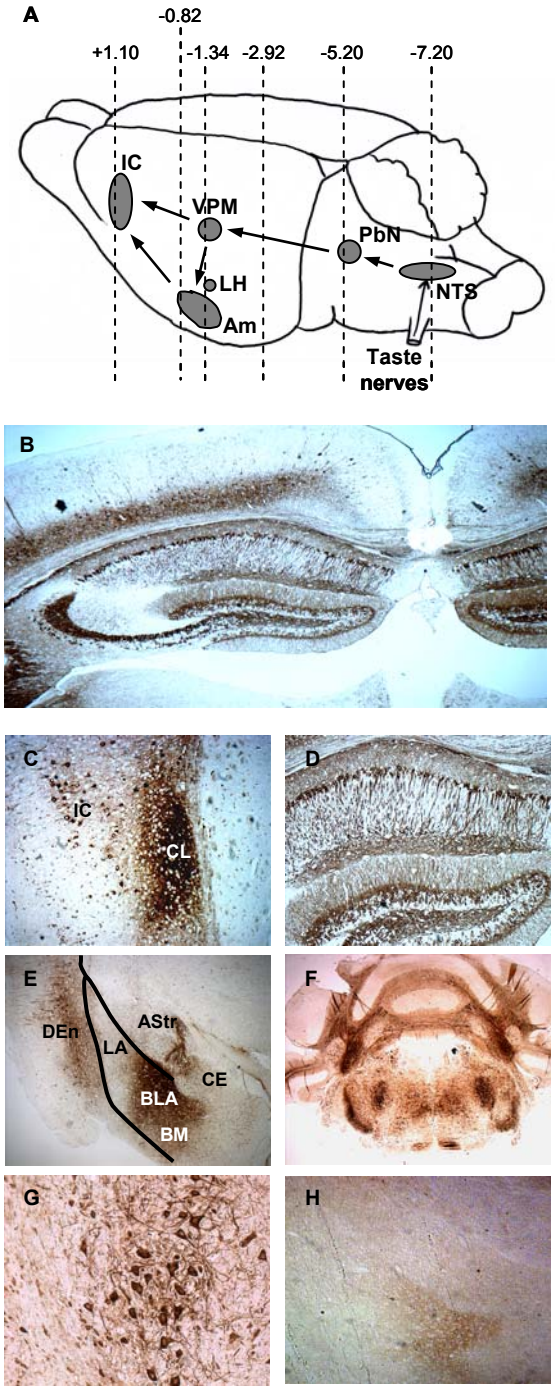

Fig. 3.1 Expression pattern of tau in P301L tau transgenic mice. (A) Areas involved in CTA are shown in gray: IC, insular cortex; VPM, ventral posteromedial nucleus of the thalamus; LH, lateral hypothalamus; Am, amygdala; PbN, parabrachial nucleus and NTS, nucleus of the solitary tract. (B) Tau was expressed in the cortex, hippocampus and adjacent brain areas. (C) Higher magnification of tau expression in the IC and CL (claustrum), (D) the hippocampus, (E) the DEn (dorsal endopiriform nucleus), the BLA (basolateral nucleus) and BM (basomedial nucleus) of the amygdala, the Astr (amygdalostriatal transition area), but not in the lateral nucleus (LA) and the central nucleus of the amygdala (CE). (F) Tau was expressed in the brain stem. (G) Higher magnification of (F) shows high tau expression in motor neurons of the brain stem. (H) The amygdala of a wt mouse is shown as a negative control. The sections were stained with the human tau-specific antibody HT7 (B, D, F, G, H) and the phospho-tau specific antibody CP13 (C, E).

3.1.1.2 Weight reduction and motor coordination of P301L tau transgenic mice

At 6 months of age when the experiments were initiated, body weights of wild-types (38.2 ± 2.2 g) were significantly higher than that of P301L tau transgenic mice (33.0 ± 1.2 g; $p < 0.04$) (wt: N=21; P301L: N=20). This difference was even more pronounced during the CTA task, where the mice were water-deprived (wt: 36.4 ± 1.2 g; P301L: 30.2 ± 0.8 g; $p < 0.001$) (Fig. 3.2). To test whether expression of the transgene affected locomotor coordination the accelerating Rotarod test was performed (N=11/group). P301L mice stayed significantly longer on the Rotarod than wt mice (wt: 124.3 ± 14.2 sec; P301L: 178.2 ± 17.5 sec; $F(1,20) = 5.316$, $p < 0.032$) and therefore reached a significantly higher average speed (wt: 18.7 ± 2.0 rpm; P301L: 25.3 ± 2.3 rpm; $F(1,20) = 4.647$, $p < 0.043$) before slipping off the rod. However, when the data were normalized for weight (by calculating a weight coefficient), the differences between the two groups disappeared ($F(1,20) = 0.364$, $p > 0.553$), demonstrating a correlation between weight and performance on the Rotarod (Fig. 3.3).

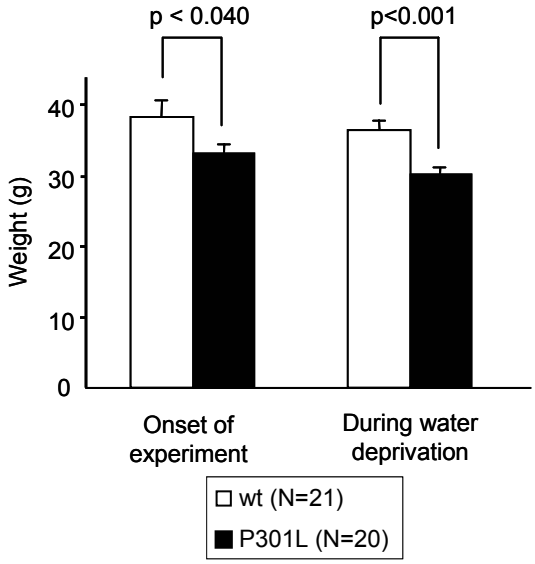

Fig. 3.2 Weight reduction of P301L mice. The weight of the P301L mice was significantly reduced at the onset of the experiment ($p < 0.04$) and, more pronounced, during the CTA task ($p < 0.001$). The values represent the mean ± SEM.

3.1.1.3 Slightly increased exploration of P301L mice in the open-field and light-dark test

Levels of spontaneous locomotor activity, anxiety-like behavior and exploration were assessed in the open-field and light-dark (L/D) tests. In the open-field test (N=21/group), no genotype effect was found for measures of locomotor activity [total distance traveled: $F(1,40) = 2.587$, $p > 0.116$; total number of zone transitions: $F(1,40) = 0.003$, $p > 0.956$]. Simi-

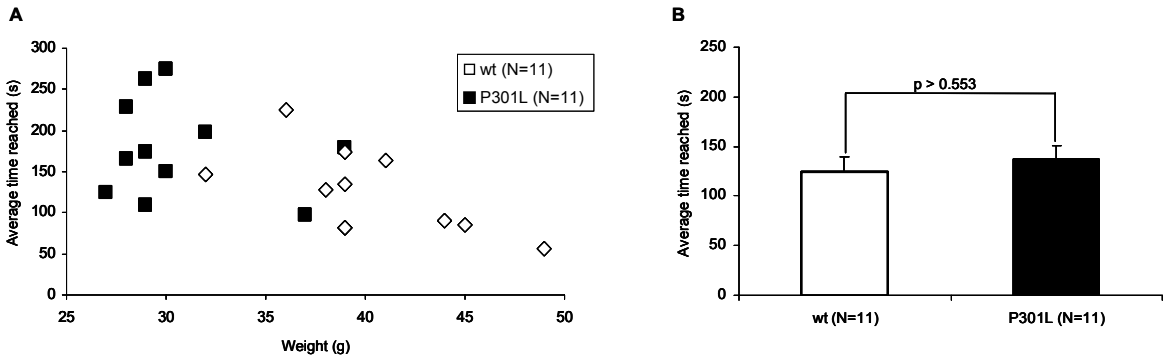

Fig. 3.3 Correlation between weight and performance on the Rotarod. (A) P301L mice stayed significantly longer on the Rotarod than wt mice. (B) However, when the data were normalized for weight (by calculating a weight coefficient), the differences between the two groups disappeared. The values represent the mean ± SEM.

larly, no differences were found for measures of anxiety such as thigmotaxis ($F(1,40) = 0.119$, $p > 0.732$), the time spent in the inner zone ($F(1,40) = 0.473$, $p > 0.496$), and the average distance to the inner zone ($F(1,40) = 0.347$, $p > 0.559$). Only for the total number of activity state changes a significant genotype effect was detected ($F(1,40) = 6.469$, $p < 0.015$) (Fig. 3.4).

No significant differences were found in the L/D test (wt: N=20; P301L: N=21) for measures of anxiety such as the latency to enter the dark compartment ($F(1,39) = 0.082$, $p > 0.776$) and the time spent in the dark compartment ($F(1,39) = 0.040$, $p > 0.843$). In contrast, additional parameters for exploration such as the number of rearings ($F(1,39) = 4.624$, $p < 0.038$) and the exploration index ($F(1,39) = 4.078$, $p < 0.050$) were significantly increased in P301L tau transgenic mice (Fig. 3.5).

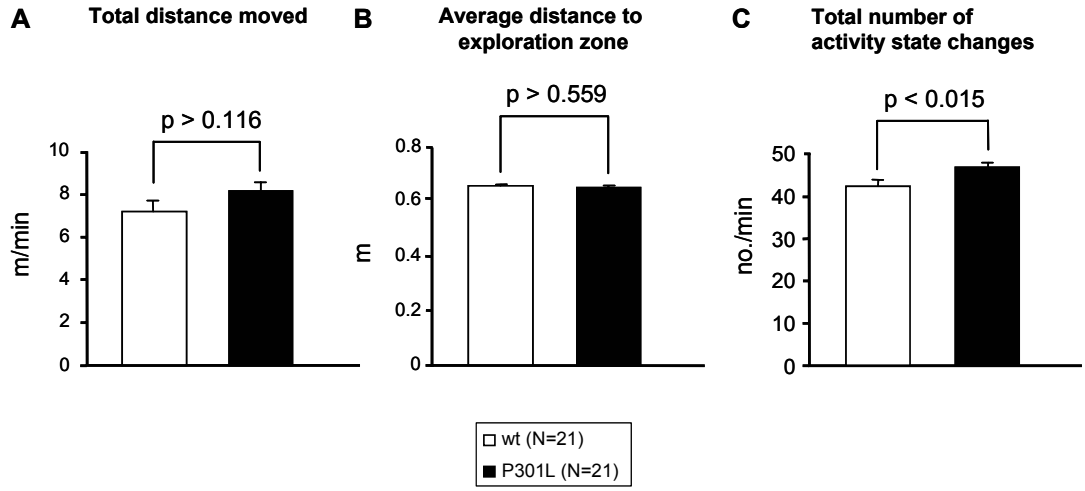

Fig. 3.4 No altered activity levels of P301L mice in the open-field test but slightly increased exploratory behavior. (A) Total distance moved; (B) average distance to exploration zone; and (C) total number of activity state changes. Values represent the mean ± SEM.

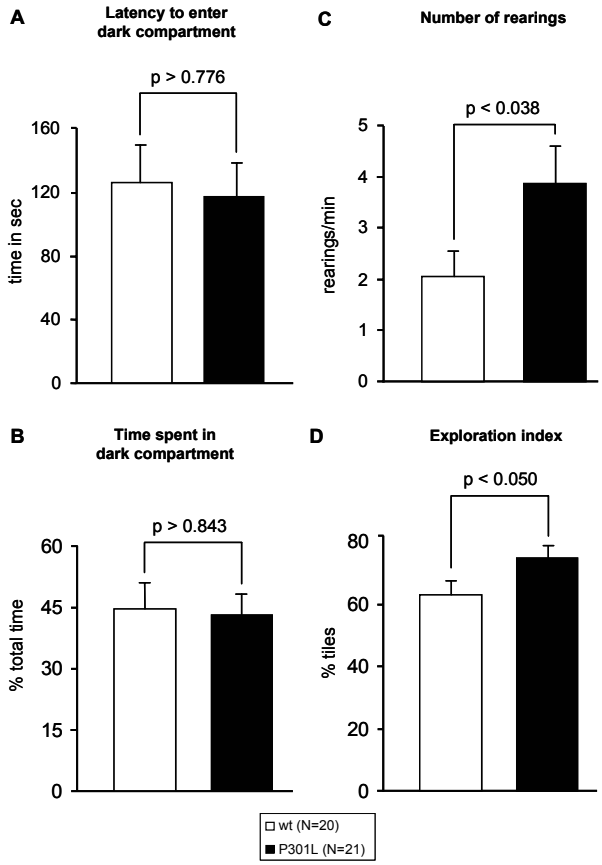

Fig. 3.5 No altered anxiety levels of P301L mice in the light-dark test but slightly increased exploratory behavior. (A) Latency to enter the dark compartment; (B) time spent in the dark compartment; (C) number of rearings; and (D) exploration index. Values represent the mean ± SEM.

3.1.1.4 No altered fear conditioning in P301L mice

To test the ability of P301L mice to acquire a conditioned fear response, freezing was recorded during the conditioning session as well as the retrieval sessions for conditioning to context or tone. During conditioning, freezing increased significantly in both groups after the first US has been delivered ($F(7,273) = 38.022$, $p < 0.001$; wt: N=21; P301L: N=20; Fig 3.6A). Neither genotype nor genotype x interval significantly affected freezing during conditioning (genotype: $F(1,39) = 2.857$, $p > 0.099$; genotype x interval: $F(7,273) = 1.436$, $p > 0.191$), although freezing levels of transgenic mice consistently were below that of wt mice (Fig. 3.6A).

During the retrieval test for context conditioning, no significant differences between transgenic and wt mice could be found 24 h ($F(1,39) = 0.344$, $p > 0.561$) (wt: N=21; P301L: N=20) as well as 15 days ($F(1,19) = 0.242$, $p > 0.629$) (wt: N=11; P301L: N=10) post-conditioning (Fig. 3.6B). No significant genotype effect was observed in freezing during the retrieval test for conditioning to tone, neither at 24 h ($F(1,39) = 0.013$, $p > 0.911$) nor at 15 days ($F(1,19) = 0.068$, $p > 0.798$) post-conditioning. Freezing significantly increased in response to tone presentation (second minute of the test) in both groups (24h: $F(3,117) = 34.287$, $p < 0.001$, 15d: $F(3,57) = 112.458$, $p < 0.001$) demonstrating that wt as well as

P301L mice learned to associate the tone with the US. Tone presentation elicited a similar increase of freezing in both groups (genotype x interval interaction: 24h: F (3,117) = 0.776, p > 0.510, 15d: F (3,57) = 0.512, p > 0.676) (Fig. 3.6C).

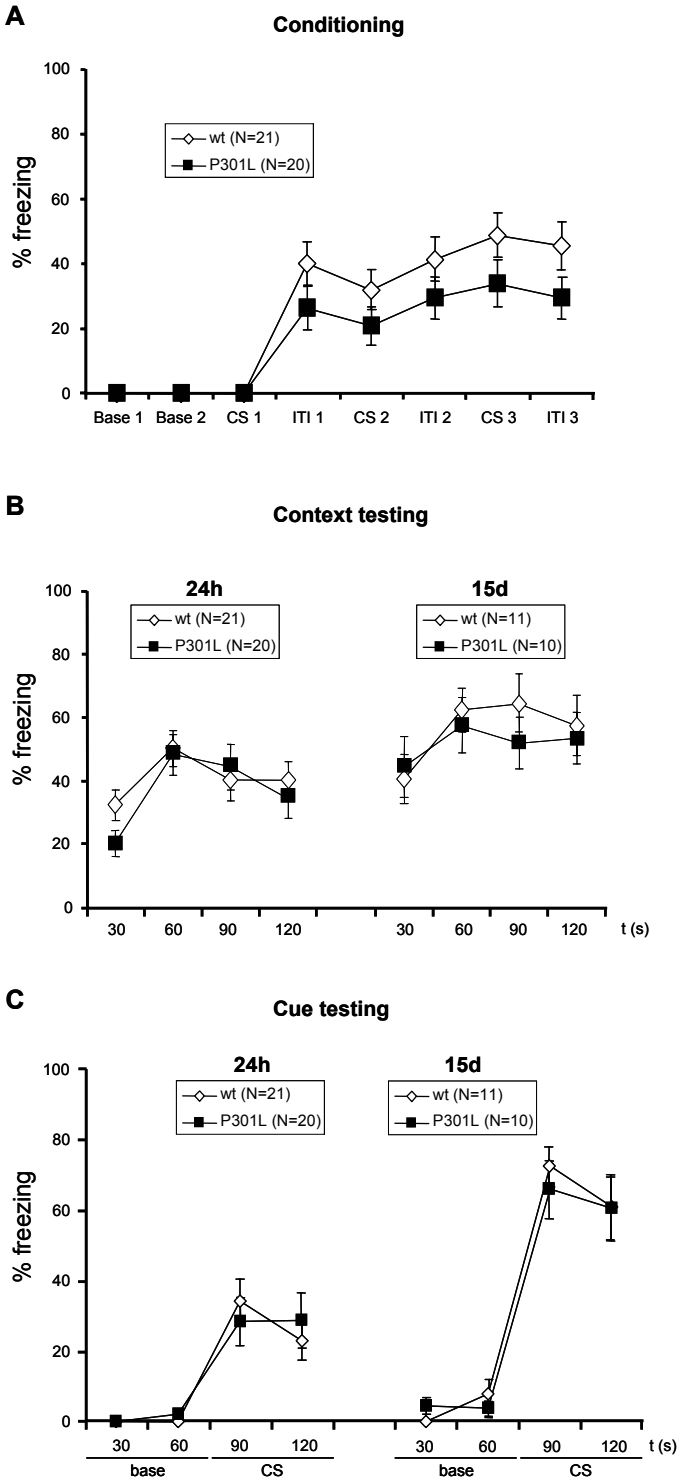

Fig. 3.6 No altered fear conditioning in P301L mice. (A) Genotype did not significantly affect freezing during conditioning ($p > 0.099$). Base, baseline activity; CS, tone presentation; ITI, inter-trial interval. (B) In the context test, no significant differences between genotypes were detected, neither at 24 h ($p > 0.561$) nor at 15 days ($p > 0.629$) post-conditioning. (C) In the cue test, no significant differences between genotypes were detected, neither at 24 h ($p > 0.911$) nor at 15 days ($p > 0.798$) post-conditioning. The values represent the mean ± SEM.

3.1.1.5 Enhanced extinction of CTA in P301L mice

To test the ability to develop a taste aversion, P301L mice and wild-type littermate controls (N=19/group) were exposed to the novel taste saccharin (CS) followed by a single injection of LiCl (US). A two-way ANOVA with repeated measures over the choice tests conducted 48 h, 72 h and one week after conditioning showed a significant main effect of genotype ($F(1,36) = 8.167$, $p < 0.007$), choice test ($F(4,144) = 8.352$, $p < 0.001$) and genotype x choice test interaction ($F(4,144) = 3.266$, $p < 0.013$) (Fig. 3.7A). Post-hoc pair-wise comparisons revealed that during the first choice test 48 h after conditioning both groups developed a strong taste aversion for saccharin (percentage of saccharin consumed: wt: 5.6 ± 1.0%;

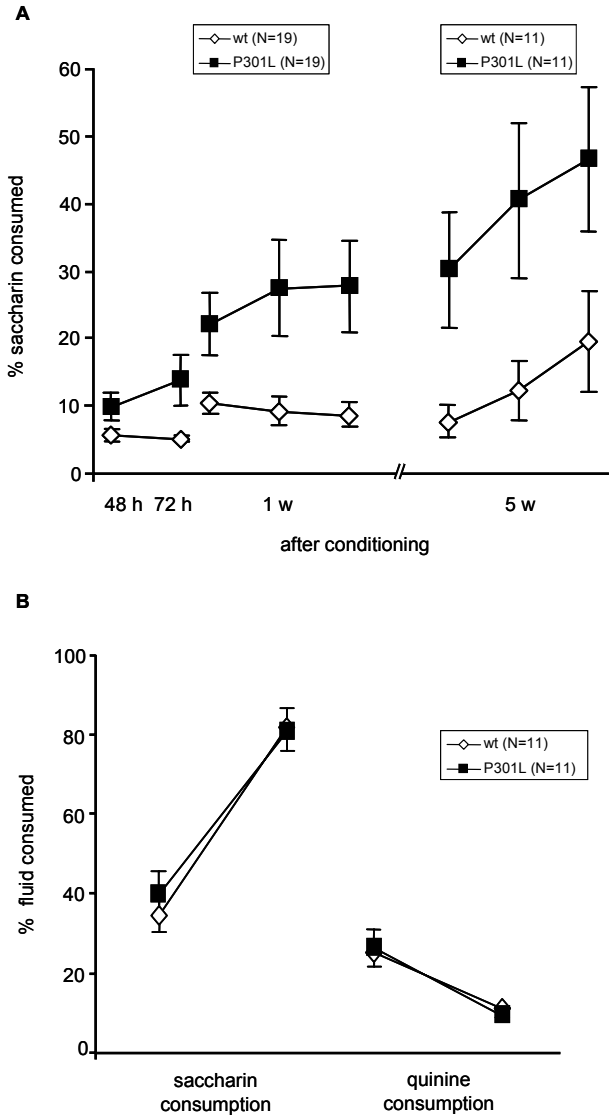

Fig. 3.7 Accelerated extinction of CTA in P301L mice. (A) During the first choice test 48 h after conditioning no significant genotype effect was observed ($p > 0.094$). However, during all subsequent choice tests, 72 h and one week after conditioning, P301L mice consumed significantly more saccharin (N=19/group). Additionally, a subset of mice (N=11/group) was again tested five weeks after conditioning. P301L mice continued to show a significantly accelerated extinction. (B) Basic taste qualities in naive mice were not impaired by the tau pathology. Values represent the mean ± SEM.

P301L: 9.8 ± 2.1%; p > 0.094), indicating that acquisition and consolidation of a taste aversion was not significantly impaired by the tau pathology. However, during the second choice test, P301L mice began to consume significantly more saccharin than wild-types (p < 0.017) demonstrating a faster extinction of the taste aversion. Repetition of these choice tests on 3 consecutive days starting 1 week after conditioning showed that CTA memory in wild-type mice extinguished slowly, whereas extinction was significantly faster in transgenic mice. A subset of mice (N=11/group) was again exposed five weeks after conditioning to three such choice tests. P301L mice still continued to show a significantly accelerated extinction (main effect of genotype: F (1,20) = 5.404, p < 0.031) (Fig. 3.7A). Neither the amount of water intake during the last adaptation day before conditioning (wt: 1.34 ± 0.07 g; P301L: 1.41 ± 0.05 g; F (1,36) = 0.592, p > 0.447), nor the amount of saccharin consumed on the conditioning day itself (wt: 1.27 ± 0.11 g; P301L: 1.35 ± 0.06 g; F (1,36) = 0.339, p > 0.564) revealed a significant effect of the transgene. In addition, total liquid intake (water plus saccharin) of P301L mice did not differ significantly from wild-type controls at any time point during the choice tests (F (1,36) = 0.094, p > 0.761).

Basic taste qualities were assessed in water-deprived naive mice (N=11/group) by presenting saccharin and quinine solutions. This did not reveal any significant differences between transgenic and control mice (for saccharin: F (1,20) = 0.147, p > 0.706; and for quinine: F (1,20) = 0.002, p > 0.968), indicating that P301L mice possess a normal taste sensitivity (Fig. 3.7B).

3.1.2 Hippocampus-dependent test battery

3.1.2.1 Increased exploratory behavior of P301L mice in the open-field and elevated O-maze

In a second set of experiments P301L mice were used with a calculated > 98% C57Bl/6 background. To assess levels of spontaneous locomotor activity, anxiety-like behavior and exploration, two tasks were performed.

In the open-field, at 6 months of age (N=12/group), no genotype effect was found for measures of locomotor activity such as total distance traveled (F (1,22) = 0.088, p > 0.769) (Fig. 3.8A) and total number of zone transitions (F (1,22) = 0.378, p > 0.545). In contrast, a significant genotype effect was detected for measures of anxiety and exploration such as the time spent in the inner (exploration) zone (F (1,22) = 9.650, p < 0.005) (Fig. 3.8B), number of visits to the inner zone (F (1,22) = 6.014, p < 0.023) (Fig. 3.8C), and the distance traveled in the inner zone (F (1,22) = 6.725, p < 0.017). Evidence that this zone was indeed anxiogenic for

the control group was confirmed by the finding that they spent only 70% of the calculated expected time in this zone, whereas P301L mice performed at chance level.

At 11 months of age (N=12 (wt); N=9 (P301L)), a significantly different locomotor behavior was revealed between genotypes (total distance traveled ($F(1,19) = 8.384$, $p < 0.009$) (Fig. 3.8A); total number of zone transitions ($F(1,19) = 8.452$, $p < 0.009$)), showing enhanced activity in P301L mice compared to wild-type controls. In contrast to 6 months old mice, no significant differences were found in the time spent in the inner (exploration) zone ($F(1,19) = 0.140$, $p > 0.712$) (Fig. 3.8B). However, P301L mice still performed more visits to the inner zone ($F(1,19) = 6.365$, $p < 0.021$) (Fig. 3.8C) where they showed higher activity levels ($F(1,19) = 6.565$, $p < 0.019$). In addition, further analysis revealed that wild-type mice spent sig-

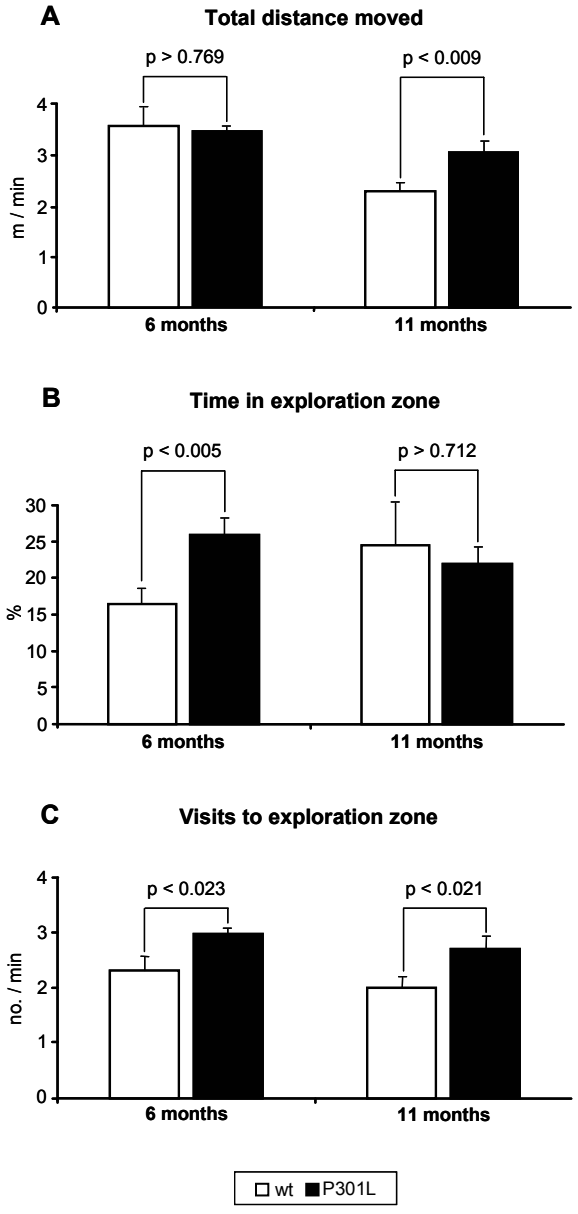

Fig.3.8 Increased exploration and reduced anxiety levels of P301L mice in the open-field. (A) Total distance traveled, (B) time spent in the inner (exploration) zone, and (C) total number of visits to the exploration zone. N=12/group at 6 months; N=12 (wt); N=9 (P301L) at 11 months. Values represent the mean ± SEM.

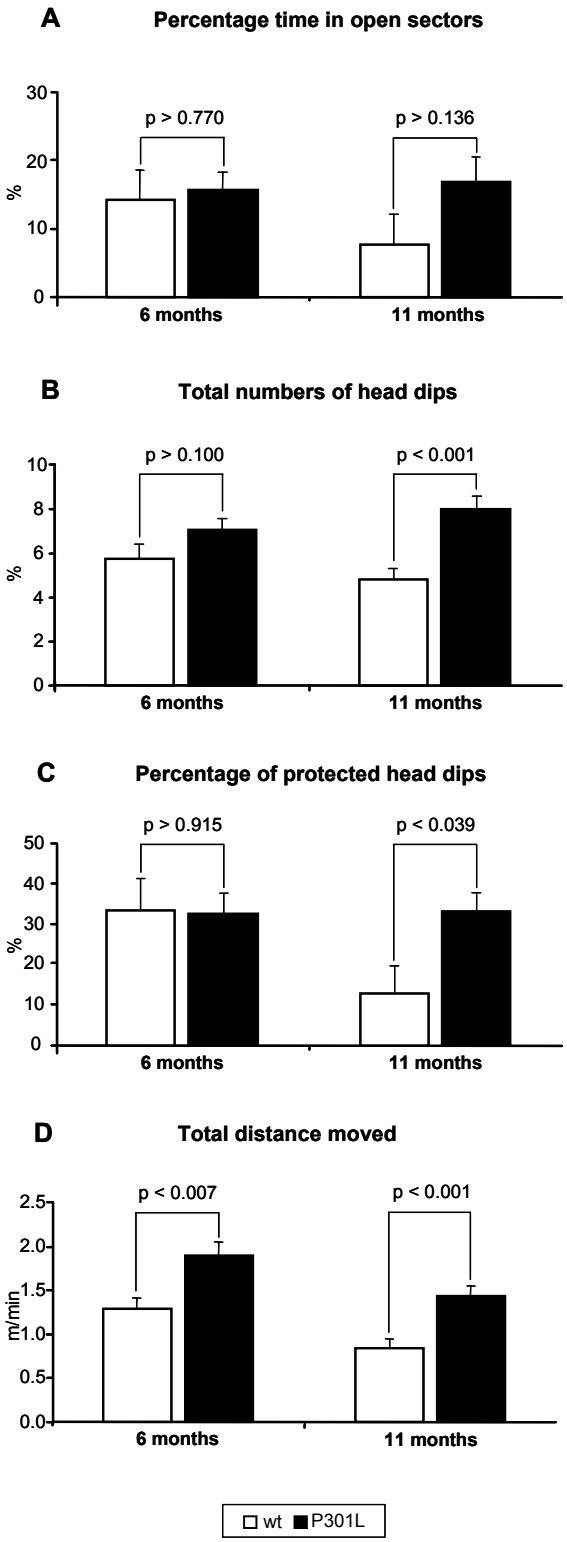

Fig. 3.9 Increased exploration of P301L mice in the elevated 0-maze. (A) Percentage of time spent in open sectors, (B) total number of head dips, (C) percentage of protected head dips, and (D) total distance traveled. N=12/group at 6 months; N=12 (wt); N=10 (P301L) at 11 months. Values represent the mean ± SEM.

nificantly more time resting in the exploration zone (periods with >2s with speed <0.025m/s (system noise threshold)) than P301L mice ($F(1,19) = 5.378$, $p < 0.032$), possibly demonstrating a more anxiety-like behavior. No differences were found in thigmotaxis ($F(1,22) = 2.533$, $p > 0.126$) at either age.

In the elevated O-maze, no significant differences were found for measures of anxiety such as the percentage of time spent in open sectors (6 months (N=12/group): $F(1,22) = 0.088$, $p > 0.770$; 11 months (N=12 (wt); N=10 (P301L)): $F(1,20) = 2.407$, $p > 0.136$) (Fig. 3.9A), and the percentage of entries into open sectors compared to total entries (6 months: $F(1,22) = 1.226$, $p > 0.280$; 11 months: $F(1,20) = 1.948$, $p > 0.178$). Furthermore, the total number of head dips ($F(1,22) = 2.942$, $p > 0.100$) (Fig. 3.9B) and the percentage of protected head dips ($F(1,22) = 0.012$, $p > 0.915$) (Fig. 3.9C) did not differ at 6 months of age. In contrast, these measures varied significantly at 11 months (Total number of head dips ($F(1,20) = 18.075$, $p < 0.001$) (Fig. 3.9B); percentage of protected head dips ($F(1,20) = 4.890$, $p < 0.039$) (Fig. 3.9C). Additional exploratory measures in the O-maze such as the total distance traveled (6 months: $F(1,22) = 8.903$, $p < 0.007$; 11 months: $F(1,20) = 14.054$, $p < 0.001$) (Fig. 3.9D) and the total number of zone transitions (6 months: $F(1,22) = 7.180$, $p < 0.014$; 11 months: $F(1,20) = 16.092$, $p < 0.001$) were significantly increased in P301L mice at both ages tested.

3.1.2.2 No altered spatial working memory in P301L mice

To test spatial working memory, spontaneous alternation behavior was analyzed in the Y-maze. All groups (6 months: N=12/group; 11 months: N=12 (wt); N=10 (P301L)) expressed a reliable spatial working memory by performing above chance level (> 58.9%). P301L mice did not differ in their alternation behavior from wild-type controls (6 months: $F(1,22) = 0.169$, $p > 0.685$; 11 months: $F(1,20) = 3.995$, $p > 0.059$) (Fig. 3.10A). They even showed a slightly more pronounced alternation behavior at 11 months, which may be due to their higher exploratory drive. No differences were found in the number of arm entries indicating equivalent total activity and motivation states (6 months: $F(1,22) = 0.019$, $p > 0.891$; 11 months: $F(1,20) = 0.825$, $p > 0.375$) (Fig. 3.10B). Together, this shows that P301L mice are not impaired in spatial working memory.

3.1.2.3 Deficits in spatial reference memory in P301L mice

To assess spatial reference memory, P301L mice and wild-type littermate controls were tested in the Morris water maze paradigm. All groups learned to locate the hidden platform position as shown by decreased escape latencies during the acquisition phase (6 months (N=12/group): time effect: $F(8,176) = 17.779$, $p < 0.001$; genotype effect: $F(1,22) = 0.270$, $p > 0.609$; genotype x time effect: $F(8,176) = 0.466$, $p > 0.879$; 11 months (N=12 (wt); N=10 (P301L)): time effect: $F(8,160) = 4.587$, $p < 0.001$; genotype effect: $F(1,20) = 0.036$, $p > 0.851$; genotype x time effect: $F(8,160) = 0.804$, $p > 0.600$) (Fig. 3.11A). The escape latencies increased notably in both genotypes at 6 months of age after replacing the platform for

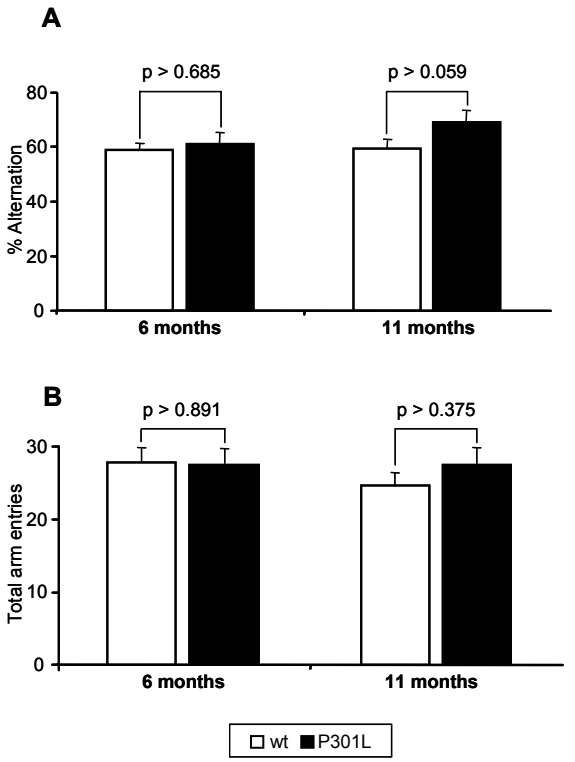

Fig. 3.10 No deficits in spatial working memory of P301L mice in the Y-maze. (A) Percentage of spontaneous alternation behavior, and (B) total numbers of arm entries. N=12/group at 6 months; N=12 (wt); N=10 (P301L) at 11 months. Values represent the mean ± SEM.

the reversal phase, confirming that the animals had adapted their escape strategy to the specific platform position. Nevertheless, both groups were able to adapt to the new platform position (time effect: $F(5,110) = 6.951$, $p < 0.001$; genotype effect: $F(1,22) = 1.387$, $p > 0.252$; genotype x time effect: $F(5,110) = 1.234$, $p > 0.298$) (Fig. 3.11A). At 11 months, no significant improvement in the escape latencies over time was revealed, mostly due to the lower escape latencies already at the beginning of the reversal phase (time effect: $F(5,100) = 1.267$, $p > 0.284$; genotype effect: $F(1,20) = 0.730$, $p > 0.403$; genotype x time effect: $F(5,100) = 0.928$, $p > 0.466$) (Fig. 3.11A), indicating a weaker orientation towards the former platform position compared to the younger mice. Additional measures such as percentage of time in the current goal quadrant (genotype effect; 6 months: $F(1,22) = 1.162$, $p > 0.293$; 11 months: $F(1,20) = 0.364$, $p > 0.553$) (Fig. 3.11B) or total distance traveled (genotype effect; 6 months: $F(1,22) = 0.857$, $p > 0.365$; 11 months: $F(1,20) = 0.048$, $p > 0.829$) did not differ between genotypes. Average swim speed, floating time and wall hugging (thigmotaxis) were also not affected by the mutation (data not shown).

To test spatial reference memory of the former platform location a probe trial (first 60 s of the first reversal trial) was conducted. A two-way ANOVA with repeated measures over the quadrant places showed a significant main effect of place ($F(2,44) = 9.187$, $p < 0.001$) and place x genotype interaction ($F(2,44) = 3.201$, $p < 0.050$) at 6 months of age. *Post hoc* pair-wise comparisons revealed a significant place effect in wild-type mice ($p < 0.001$), whereas

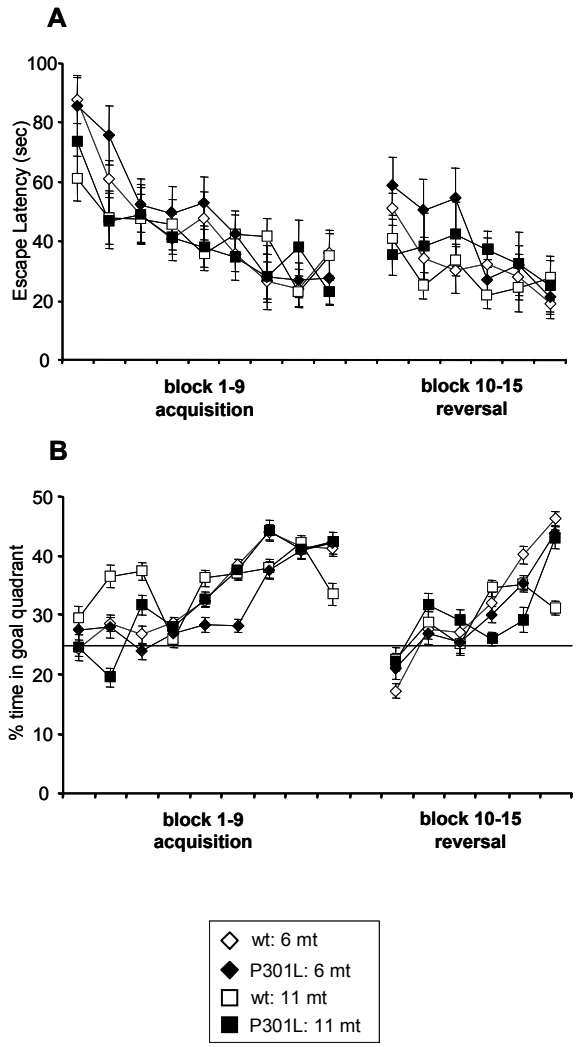

Fig. 3.11 Acquisition and reversal learning in the Morris water maze. (A) Both P301L mice and wild-type littermate controls learn to locate the hidden platform position equally well, as shown by decreasing escape latencies in the acquisition phase. The escape latencies raise notably in both genotypes at 6 months of age after replacing the platform for the reversal phase, confirming that the animals have adapted their escape strategy to the specific platform position. At 11 months of age this effect is slightly less pronounced, indicating lower adaptation to the former platform location. However, all groups show a reasonable escape performance for the new platform position during the reversal phase. (B) Additional measure: percentage of time spent in the present goal quadrant. N=12/group at 6 months; N=12 (wt); N=10 (P301L) at 11 months. Values represent the mean ± SEM.

no such place effect was observed in P301L mice ($p > 0.277$). A further comparison revealed that P301L mice spent significantly less time in the former goal quadrant than wild-type control mice ($F(1,22) = 6.820$, $p < 0.016$) (Fig. 3.12A). A similar outcome was revealed by a more stringent measure of spatial selectivity when the percentage of time spent in a circular target zone (comprising one-eighth of the pool surface) was determined ($F(1,22) = 7.831$, $p < 0.010$) (Fig. 3.12B). Similarly, a significant difference was found for the annulus crossing ($F(1,22) = 4.517$, $p < 0.045$) (Fig. 3.12C). At 11 months of age, neither group showed a significant preference for the former platform location (main effect of place: $F(2,40) = 1.481$, $p > 0.240$); place x genotype interaction: $F(2,40) = 1.117$, $p > 0.337$). Therefore, no significant differences between the genotypes could be revealed at this age (time in the former goal quadrant: $F(1,20) = 0.169$, $p > 0.685$ (Fig. 3.12A); percentage of time spent in the target zo-

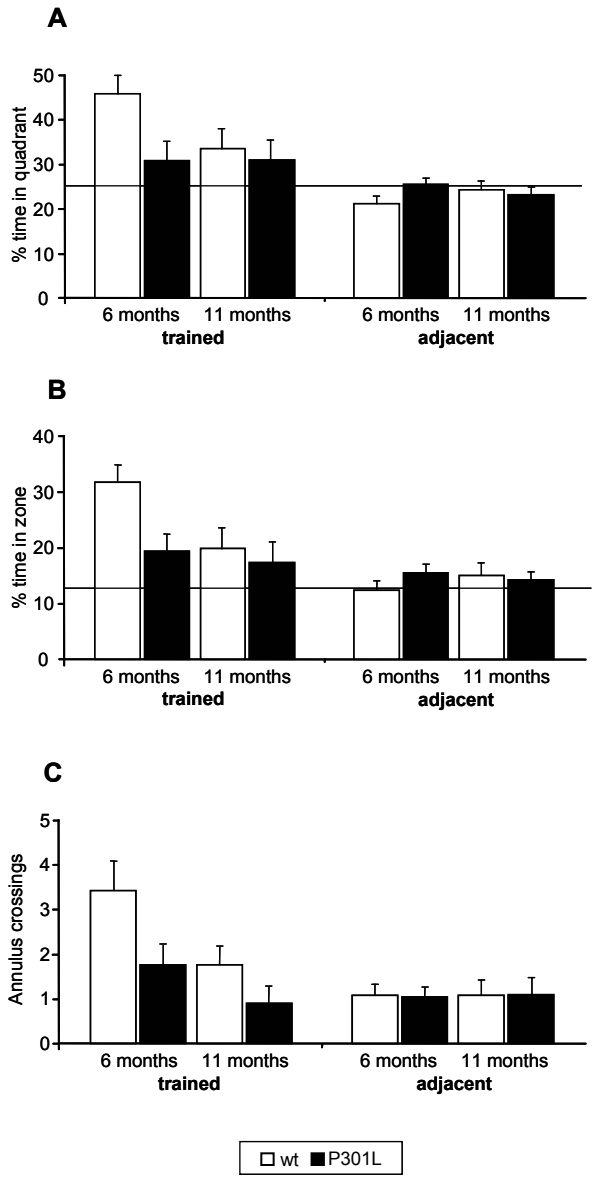

Fig. 3.12 Probe trial in the Morris water maze reveals deficits in spatial reference memory in P301L mice. (A) A two-way ANOVA with repeated measures over the quadrant places shows a significant main effect of place ($p < 0.001$) and place x genotype interaction ($p < 0.050$) at 6 months of age. *Post hoc* pairwise comparison reveals a significant place effect for wild-type mice ($p < 0.001$), whereas no such place effect is observed in P301L mice ($p > 0.277$). Further comparison reveals that P301L mice spend significantly less time in the former goal quadrant than wild-type control mice ($p < 0.016$). At 11 months of age, neither group shows a significant preference for the former platform location (main effect of place: $p > 0.240$; place x genotype interaction: $p > 0.337$). Due to a floor effect as evidenced by a poor performance of the wild-type control group during the probe trial, with no significant preference above chance level for the former platform location, no significant differences could be revealed between the genotypes at this age ($p > 0.685$). A similar outcome is revealed by more stringent measures of spatial selectivity such as (B) percentage of time spent in a circular target zone (comprising one-eighth of the pool surface) (6 months: $p < 0.010$; 11 months: $p > 0.626$), and (C) annulus crossing (6 months: $p < 0.045$; 11 months: $p > 0.139$). N=12/group at 6 months; N=12 (wt); N=10 (P301L) at 11 months. Values represent the mean ± SEM.

ne: $F(1,20) = 0.245$, $p > 0.626$ (Fig. 3.12B) and annulus crossing $F(1,20) = 2.378$, $p > 0.139$ (Fig. 3.12C)). Together, these results indicate an impaired memory retrieval of P301L mice in the water maze paradigm, which is masked in the older group by the poor performance of the wild-type control mice.

Finally, we analyzed the swim strategy of the mice during acquisition and reversal learning by categorizing each individual trial according to the predominant swimming pattern (Fig. 3.13A). This revealed that the overall distribution of strategies did not differ between genotypes (6 months: $F(1,22) = 1.987$, $p > 0.173$; 11 months: $F(1,20) = 0.378$, $p > 0.546$) (Fig. 3.13B). In addition, no differences in the search strategy were found during reversal learning (6 months: $F(1,22) = 0.033$, $p > 0.858$; 11 months: $F(1,20) = 0.687$, $p > 0.417$) (Fig. 3.13C). Together, these data show that P301L mice do not use completely different search strategies than wild-type mice to escape from the water.

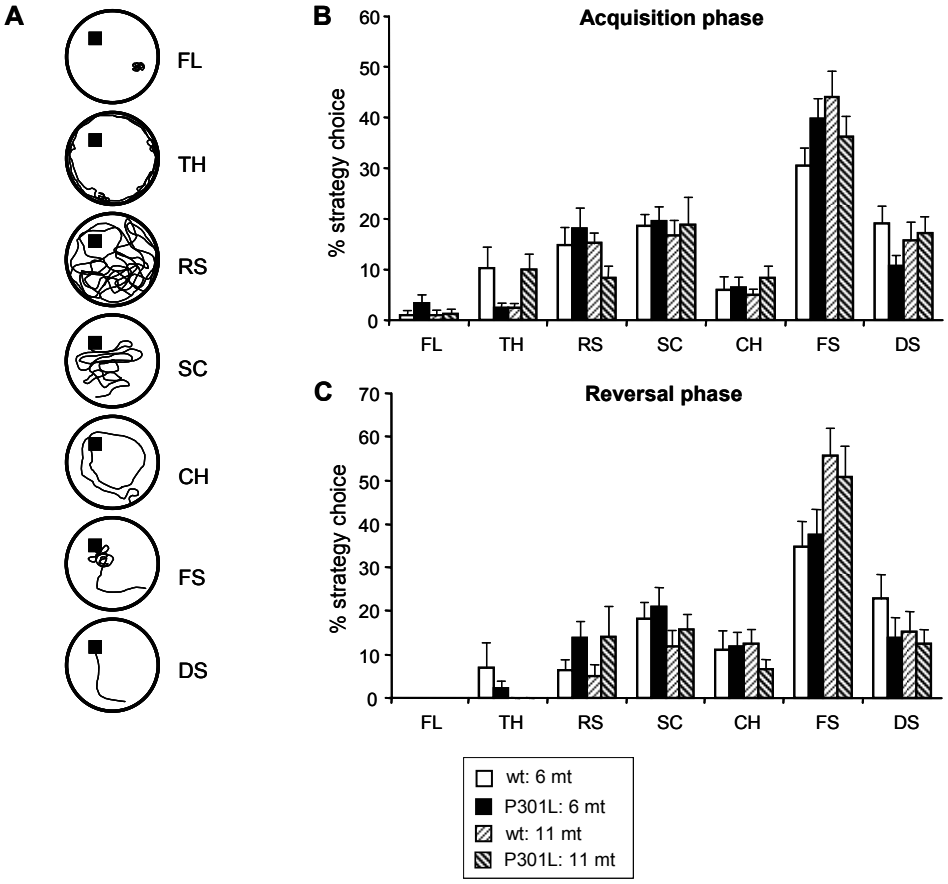

Fig. 3.13 Swim strategy during acquisition and reversal learning in the Morris water maze. (A) Swim strategies of the mice were analyzed during acquisition and reversal learning by categorizing each individual trial according to the predominant swimming pattern (FL, floating; TH, thigmotaxis; RS, random swim; SC, scanning; CH, chaining; FS, focal swim; DS, direct swim). The overall distribution of strategies does not differ between genotypes at any age (B) during acquisition (6 months: $p > 0.173$; 11 months: $p > 0.546$), and (C) during reversal learning (6 months: $p > 0.858$; 11 months: $p > 0.417$). N=12/group at 6 months; N=12 (wt); N=10 (P301L) at 11 months. Values represent the mean ± SEM.

3.2 Role of different phospho-epitopes and cleavage sites in tau filament formation in tissue culture

3.2.1. Analysis of DNA constructs

To map phospho-epitopes of tau involved in filament formation in our human SH-SY5Y tissue culture system, the pRc/RSV expression vector containing the longest human 4-repeat tau isoform was utilized (Fig 3.14). The following epitopes in tau were mutated by site-directed mutagenesis: AT8 (S202A/T205A), AT100 (T212A/S214A) and T231A. The introduction of the designated point mutations and the correct orientation of the ligation products were verified by DNA cycle sequencing (Fig 3.15). In addition, a previously made tau construct bearing the S422A mutation was included in the analysis. Besides the phospho-mutants, an isoform of tau truncated at position 421 was generated and analyzed by DNA cycle sequencing and restriction digests (Fig. 3.16).

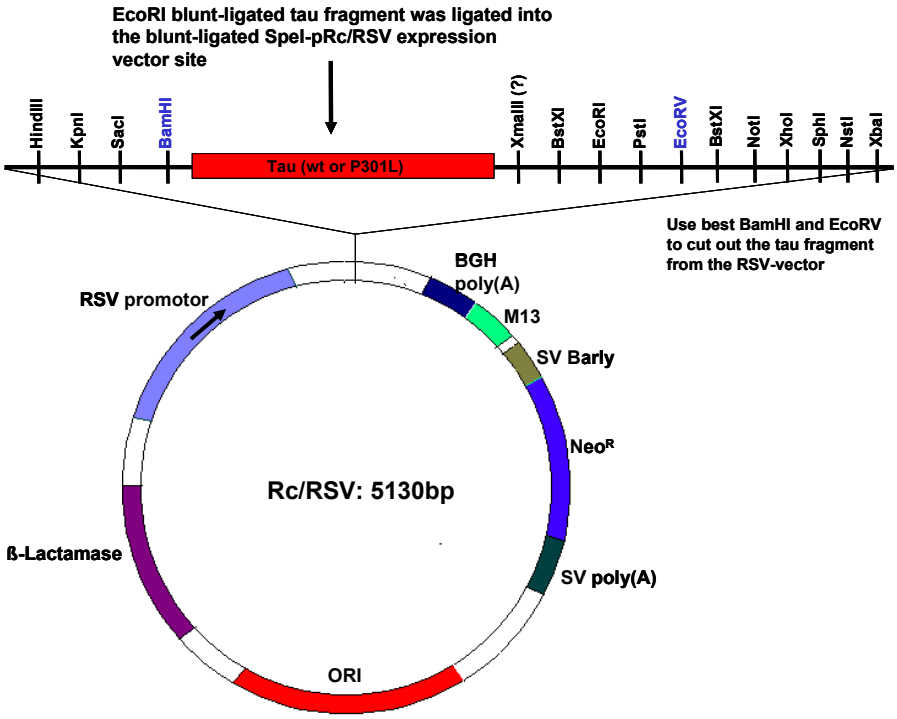

Fig. 3.14 Tau plasmid: The longest human 4-repeat tau isoform (htau40) was blunt-end ligated into the multiple cloning site of the pRc/RSV expression vector. The total size of the tau bearing vector is ~ 6570 bp! To check for plasmid size, HindIII was used. This enzyme has one restriction site on tau (Pos 1021; numbering according to the longest tau isoform) and one on the vector (~ Pos 600) which yields two bands of ~ 1050 bp and 5500 bp. To release the tau fragment from the plasmid, BamHI and EcoRV can be used: There are three sites for BamHI and two for EcoRV on the vector, which yields five bands which can be distinguished by their size (~ 300 bp, ~ 800 bp, ~ 1150 bp, ~ 1450 bp (the tau fragment), and 2800 bp, respectively).

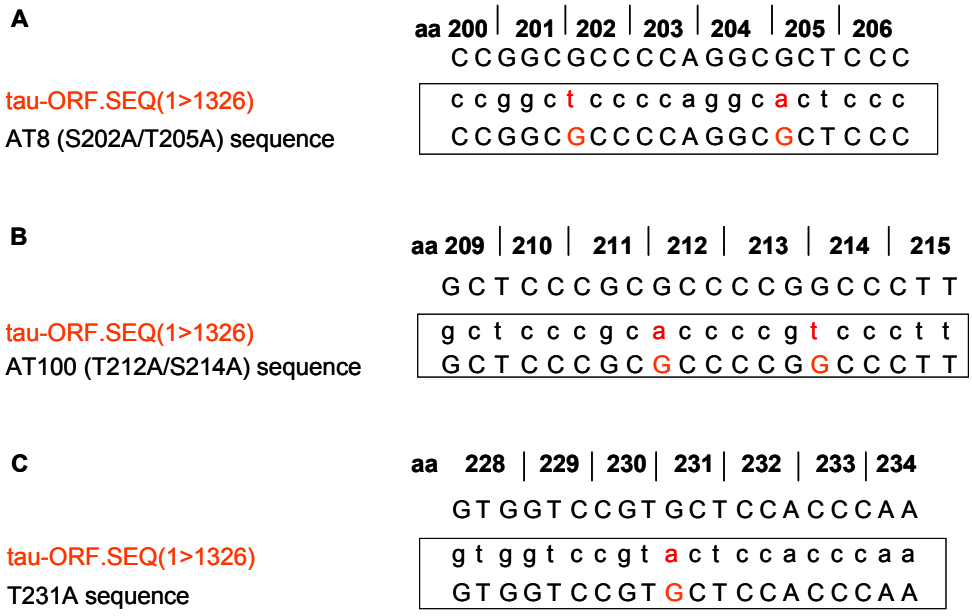

Fig. 3.15 Analysis of single base pair substitutions by DNA cycle sequencing. (A) Mutagenesis of the AT8-epitope (Ser-202/Thr-205 mutated to S202A/T205A). (B) Mutagenesis of the AT100-epitope (Thr-212/Ser-214 mutated to T212A/S214A). (C) Mutagenesis of the pThr231-epitope (mutated to T231A).

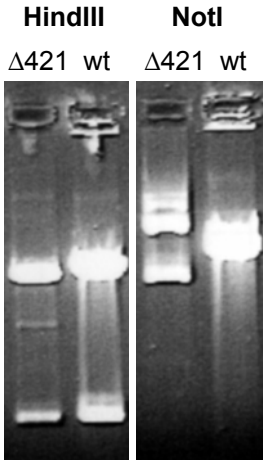

Fig. 3.16 Restriction analysis of Δ421 truncated tau: Digestion with HindIII yields two fragments for both Δ421 truncated and wt tau. In contrast, digestion with NotI yields a single cut band only with the wt-tau plasmid as the NotI-site has been removed by the truncation procedure.

3.2.2. Overexpression of tau constructs in human SH-SY5Y cells

The different tau constructs were stably expressed in human SH-SY5Y neuroblastoma cells and their expression was confirmed by immunocytochemistry (Fig. 3.17) and Western blotting (Fig. 3.18). The selective advantage of SH-SY5Y neuroblastoma cells is that they can be differentiated into neuron-like cells by sequential treatment with RA and BDNF. Thus, they mimic more closely the situation in the brain than other non-neuronal cell-types. As expected, sequential RA/BDNF treatment caused a neuron-like phenotype with neurite outgrowth and establishment of a complex neuronal network (Fig. 3.19). To elucidate the impact of tau overexpression on the proliferation rate of SH-SY5Y cells, an MTT assay was performed for dif-

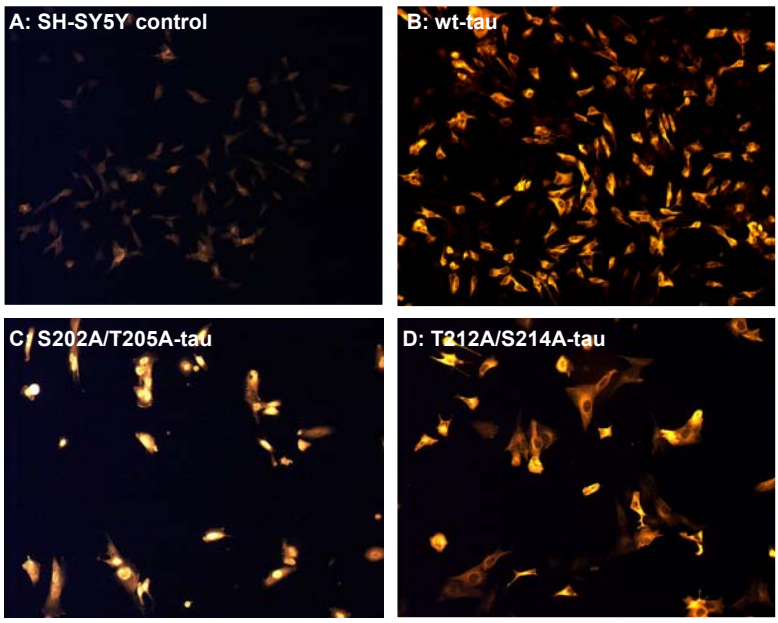

Fig. 3.17 Immunofluorescence staining of SH-SY5Y cells with the human tau-specific antibody HT7 (1:200). SH-SY5Y cells were (A) untransfected or transfected with (B) wt-tau, (C) S202A/T205A-tau and (D) T212A/S214A-tau constructs, respectively.

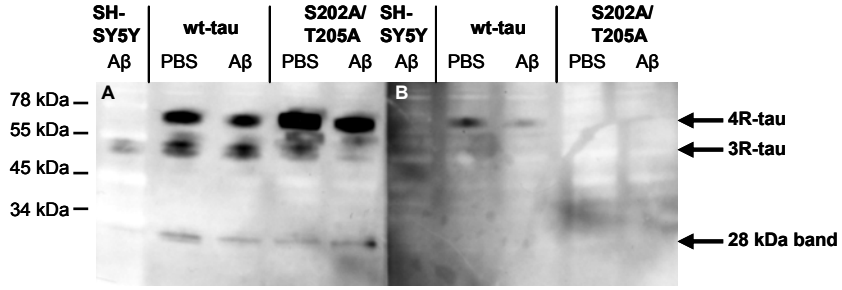

Fig. 3.18 Western blot analysis of RAB extracts: (A) Probing with the HT7 antibody (1:1000) reveals a prominent overexpression of htau40 in transfected cells compared to untransfected SH-SY5Y control cells independent of mutations or Aβ-treatment. (B) In contrast, CP13 antibody (1:50) against tau-phospho-epitope AT8 (Ser-202/Thr-205) weakly labels wt-tau htau40, whereas the S202A/T205A tau mutant and endogenous tau is not detected.

ferent time points of differentiation. During the 5 days of RA treatment, wt-tau overexpressing cells proliferated slightly faster than P301L mutant tau expressing and SH-SY5Y control cells (Fig. 3.20). Addition of BDNF terminated the proliferation of cells overexpressing tau and cell numbers were reduced as the S-type (flat) cells died off during the 5 days with BDNF. In contrast, SH-SY5Y control cells continued to proliferate throughout the entire differentiation period.

After ten days of RA/BDNF differentiation, SH-SY5Y cells were exposed for additional five days to fibrillar preparations of $A\beta_{42}$. This treatment was not accompanied by any obvious increases in cell death (Ferrari et al., 2003). Once $A\beta_{42}$ had been added to the cells, the medium was not changed. This, in addition to the stickiness of fibrillar $A\beta_{42}$, may explain why $A\beta_{42}$ formed large clumps on the cell bodies and processes of differentiated cells (Fig. 3.21).

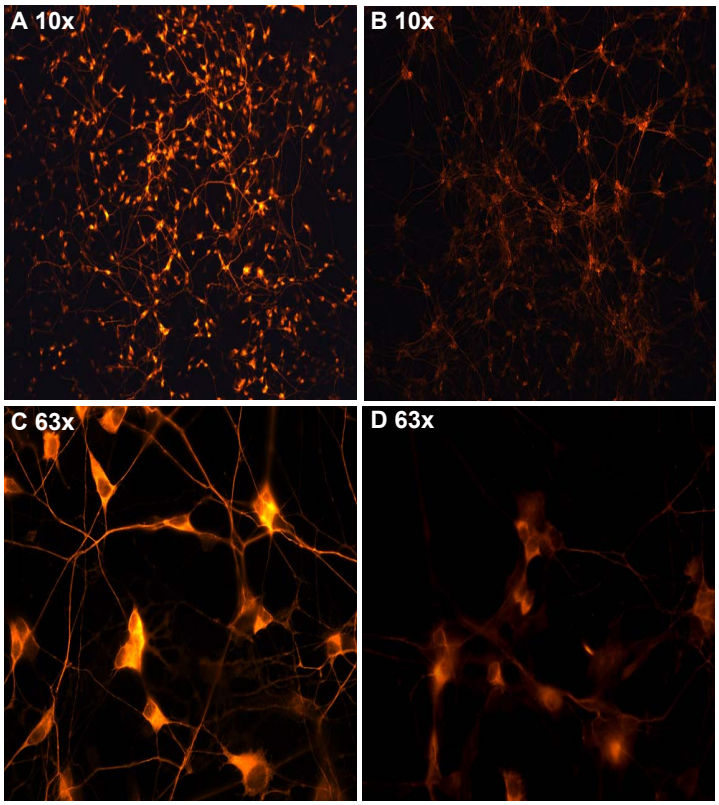

Fig. 3.19 Immunofluorescence staining of neuronally differentiated wt-tau (A+C) and SH-SY5Y control (B+D) cells with the human tau-specific antibody HT7 (1:200).

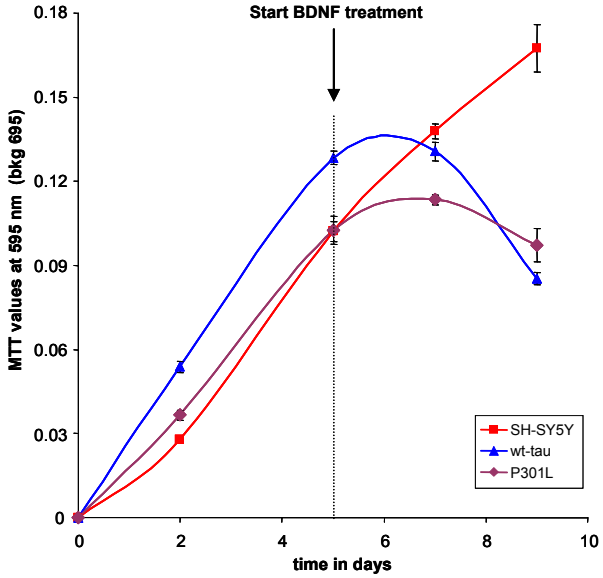

Fig. 3.20 Cell proliferation: Wt-tau overexpressing cells proliferate slightly faster than P301L mutant tau expressing and SH-SY5Y control cells during the phase of RA-treatment. Addition of BDNF terminates the proliferation of tau overexpressing cells, whereas SH-SY5Y control cells continue to proliferate throughout the entire period of differentiation. The data represent the mean of three replicates for each time point.

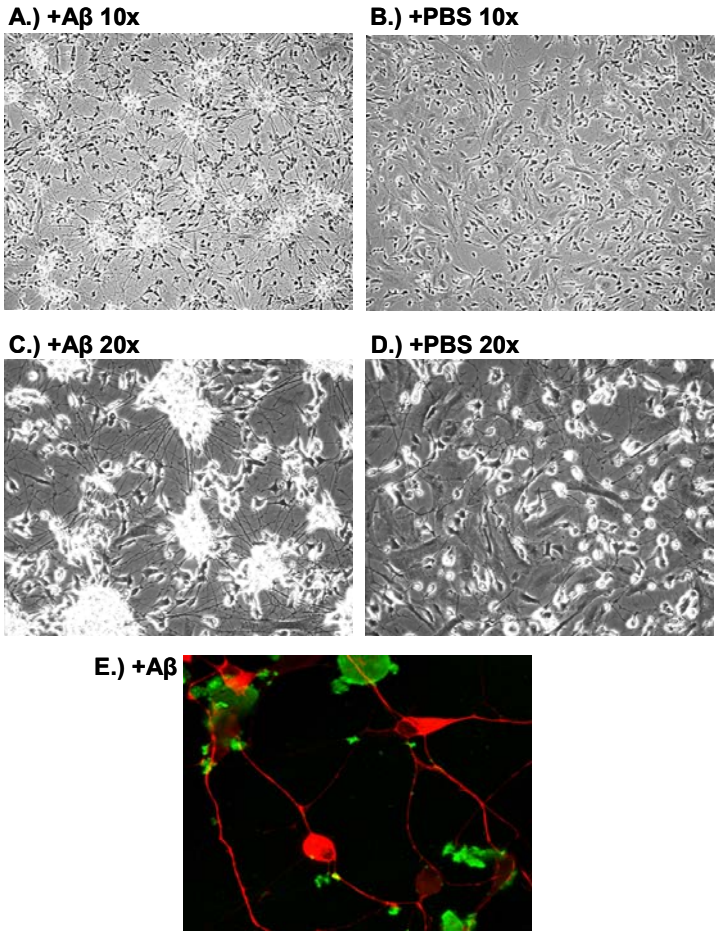

Fig. 3.21 (A-D) Light-microscopic and (E) confocal images show that Aβ42 (4G8, green, Ferrari *et al.*, 2003) forms large clumps on the cell bodies and processes of differentiated wt-tau expressing SH-SY5Y cells (HT7, red).

3.2.3. $A\beta_{42}$-treatment of tau overexpressing SH-SY5Y cells: Western Blot analysis and quantification

Our group has shown recently that treatment of wild-type and P301L mutant tau overexpressing cells with fibrillar $A\beta_{42}$ caused a substantial shift of tau from the RAB- and RIPA-fraction into the FA-fraction, demonstrating increased levels of insoluble tau (Ferrari *et al.*, 2003).

To confirm these previous *in vitro* findings and to determine whether mutating distinct phospho-epitopes of tau will abrogate the β-amyloid-induced decrease in tau solubility, FA-fractions of different cell extracts were analyzed by Western blotting (Fig. 3.22). As only highly insoluble proteins are shifted into the FA-fraction, not enough material is available to exactly determine the protein concentration of the solution. Therefore, relative volumes of FA-fractions were loaded normalized for the total volumes obtained. The ratio of the intensities of Aβ- vs. PBS-treated full length tau bands (~ 60 kDa) on the FA-blots was analyzed using ImageJ software. In addition to full-length tau, a low-molecular weight band at 28 kDa was detected by the HT7 antibody, which was used to detect tau on Western blots. Due to

uncertainty of the origin of this band (see chapter 3.2.4 below) it was not included in the quantification. At least three independent experiments were performed for each construct. As shown in figure 3.23, $A\beta_{42}$-treatment of SH-SY5Y control cells caused a ~ 5.5 fold decrease in tau solubility compared to PBS-treated cells (baseline level), demonstrating the capability of endogenous tau to aggregate as well as transfected tau. Overexpressing wt-tau (htau40) in these cells led to an additional ~ 2.8 fold increase in $A\beta_{42}$-mediated tau insolubility compared to baseline induction level (~ 15.5 fold total increase upon treatment with $A\beta_{42}$). By mutating the Ser-422 phospho-epitope into alanine, induction of tau insolubility dropped to baseline levels confirming previous findings (Ferrari *et al.*, 2003). Furthermore, mutating the phospho-epitopes AT8 and pThr231 of tau prevented the decrease in tau solubility as well and may even be inhibitory to aggregation of endogenous tau, as shown by a ~ 60 % decrease in tau insolubility compared to baseline. Unfortunately, the data for the AT100 mutant had finally to be excluded due to a loss of the tau transgene as revealed by Western blot analysis of RAB-fractions. However, taken together, our results indicate a role of different

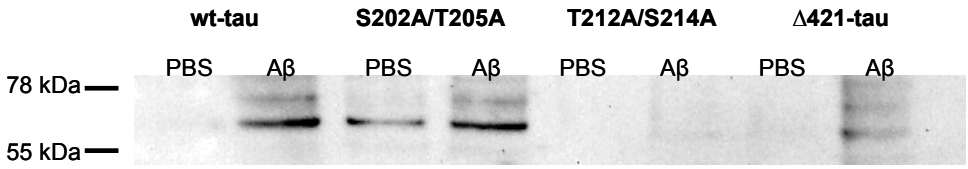

Fig. 3.22 Representative Western blot of FA-fractions: $A\beta_{42}$ decreases the solubility of wt-tau significantly. Mutating specific phospho-epitopes of tau prevent this decrease in tau solubility compared to PBS-treated fractions. Note that no overexpressed tau was found in the RAB-fraction of T212A/S214A tau extracted cells (AT100 mutant). Hence the data of this mutant cell-line is excluded from the analysis. WB labeled with HT7 (1:500 for FA-blots).

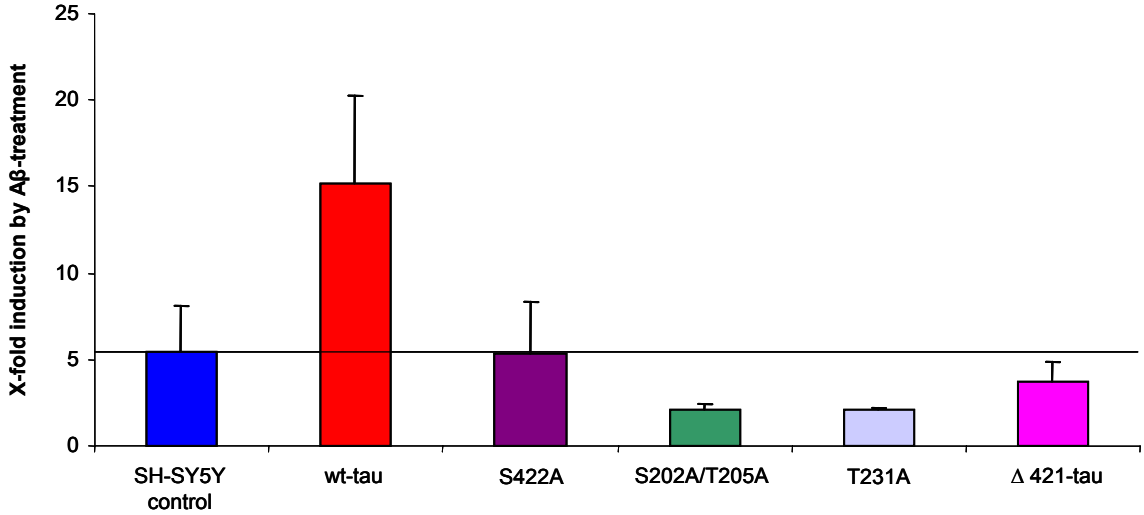

Fig. 3.23 Quantification of tau in FA-fractions. $A\beta_{42}$-treatment of SH-SY5Y control cells caused a ~ 5.5 fold decrease in tau solubility compared to PBS-treated cells (baseline level), demonstrating the capability of endogenous tau to aggregate as well. Overexpressing wt-tau in these cells led to an additional ~ 2.8 fold increase in $A\beta_{42}$-mediated tau insolubility compared to the baseline induction level. In contrast, mutating different phospho-epitopes of tau (Ser-422, Ser-202/Thr-205 and Thr-231) prevented this decrease in tau solubility. Surprisingly, truncation of the C-terminal region of tau at position 421 prevented the $A\beta_{42}$-mediated decrease in tau solubility as well. Bars represent the means ± SEM of at least three independent experiments.

epitopes in tau filament formation.

Tau constructs truncated at Asp-421 assemble much faster than wild-type tau in vitro, demonstrating that the carboxy-terminal tail of the tau molecule inhibits filament formation (Abraha et al., 2000; Berry et al., 2003). Surprisingly, truncation of the C-terminal region of tau at position 421 prevented the $A\beta_{42}$-mediated decrease in tau solubility in our SH-SY5Y tissue culture system as well (Fig. 3.23).

3.2.4. Characterization of tau isoforms in SH-SY5Y cells:

To better characterize the tau isoforms extracted from SH-SY5Y cells, a Western blot analysis of RAB-fractions with different tau antibodies was carried out (Fig. 3.24). In cells transfected with the longest 4R-tau isoform, at least two bands between ~ 60-65 kDa could be detected (e.g. with the exon 10 specific antibody ET2). A faint band was also visible with the ET2-antibody in SH-SY5Y control cells, demonstrating the existence of endogenous 4R-tau isoforms in these cells, at least upon differentiation. The predominant endogenous tau species in SH-SY5Y cells was the shortest 3R isoform (fetal tau) (Zhong *et al.*, 1999). During

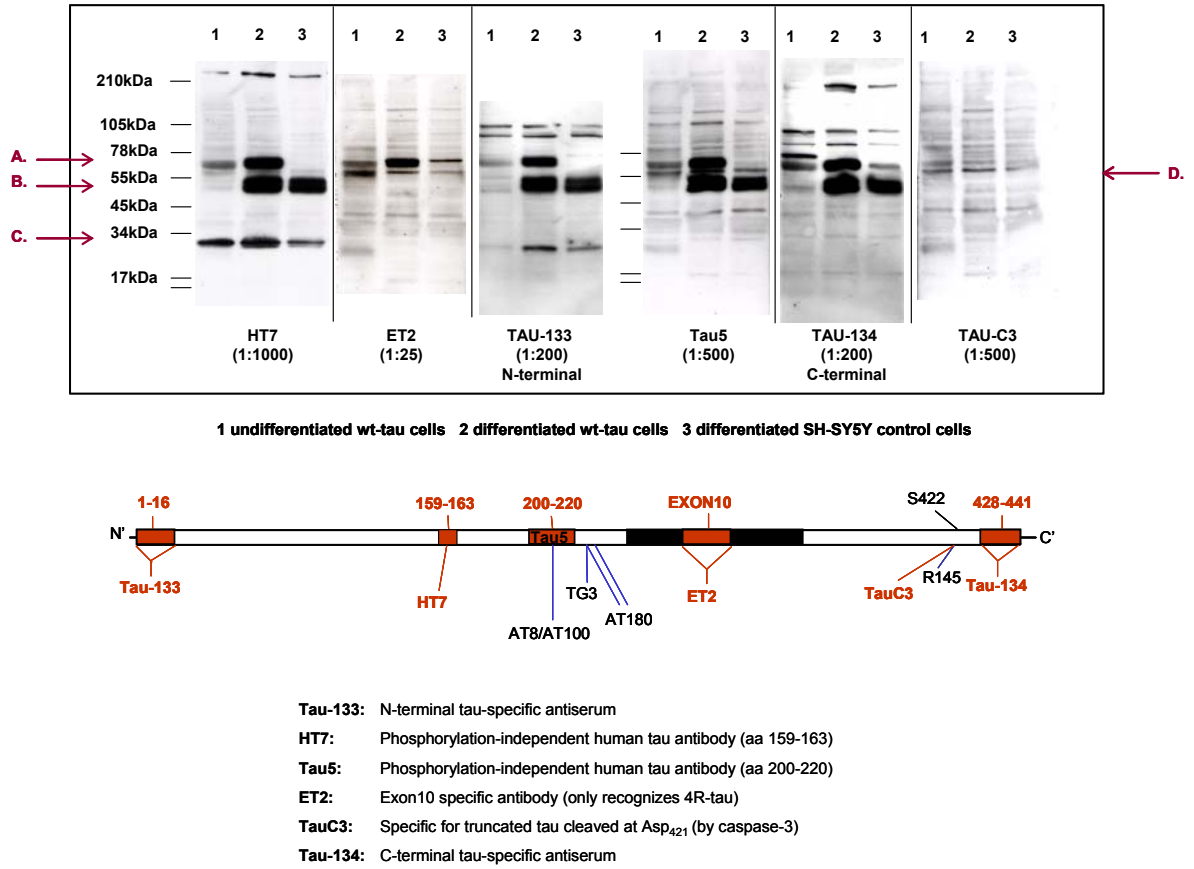

Tau-133: N-terminal tau-specific antiserum
HT7: Phosphorylation-independent human tau antibody (aa 159-163)
Tau5: Phosphorylation-independent human tau antibody (aa 200-220)
ET2: Exon10 specific antibody (only recognizes 4R-tau)
TauC3: Specific for truncated tau cleaved at Asp_{421} (by caspase-3)
Tau-134: C-terminal tau-specific antiserum

Fig. 3.24 Western profiling using different tau antibodies (RAB-fractions). (A) 4R-tau overexpressing band. (B) During differentiation the endogenous 3R-tau level increases dramatically (not detected with the exon 10 specific antibody ET2). (C) Low-molecular tau band (~28kDa), only labeled with antibodies with epitopes in the N-terminal half of tau (< aa 200). (D) Weak bands representing caspase-3 cleaved tau.

differentiation, endogenous 3R-tau level increased dramatically, due to neurite outgrowth. The low molecular weight band of 28 kDa which is detected by the HT7 antibody, was additionally visualized with Tau-133, an antiserum specific for the N-terminal part of tau. In contrast, all other antibodies, reactive with the C-terminal half of tau beyond position 200, did not recognize this band. These results may indicate that the 28 kDa band is an N-terminally truncated fragment of tau (cleaved between aa 163 (HT7-epitope) and 200 (Tau5- epitope)) (Fig 3.24). Moreover, weak bands, possibly representing caspase-3 cleaved tau at position 421, were seen with the truncation-specific antibody Tau-C3.

To get more information about the molecular nature of the 28 kDa band, an immunoprecipitation procedure was carried out. Thereby, an RAB-fraction of wt-tau overexpressing SH-SY5Y cells was loaded onto two tau-specific affinity columns, one coupled with HT7 and the other with Tau5A6 (directed against tau epitope aa 19-46). The different fractions were analyzed by Western blotting using HT7 as primary antibody. The 28 kDa band was only found in the flow-through (Fig.3.25; B4-lanes), whereas full-length tau was mainly found in the elution fractions (at least for HT7). Thus, the 28 kDa fragment does not bind to the tau antibodies including HT7 on the IP-column, while it is detected by HT7 on Western blots. One possible explanation for this finding is that HT7 can only recognize the 28 kDa epitope when the fragment is denatured, which is the case after boiling the samples for the Western blotting procedure.

To test this hypothesis, a pre-boiled RAB-fraction of wt-tau overexpressing cells was loaded onto the columns. Neither in the flow-trough, nor in the eluates was the 28 kDa band found, implicating that it is bound to the column. Therefore, the whole column was boiled twice to pull down everything, and the fractions were again loaded onto a gel (Fig. 3.26). In the boiled column fractions the 28 kDa band appeared once again, together with a slightly lower band

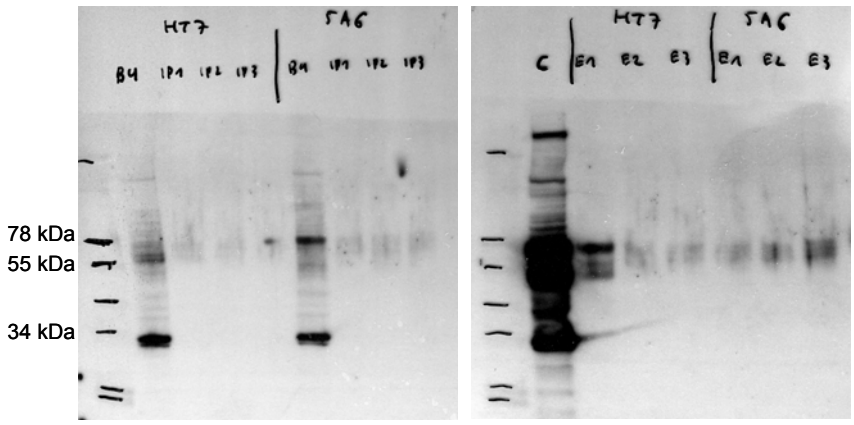

Fig. 3.25 Immunoprecipitation (IP) of tau. RAB-fraction of wt-tau overexpressing SH-SY5Y cells are loaded onto tau-specific IP-columns, generated with HT7 and Tau5A6 antibodies. B4: flow-through; IP1-3: wash steps after flow-through, to get rid of every unbound material; C: control fraction before loaded onto the IP-column; E 1-3: elution-fractions of the desired antigen. The 28 kDa band is only found in the flow-through and the control lanes (WB labeled with HT7 (1:1000)).

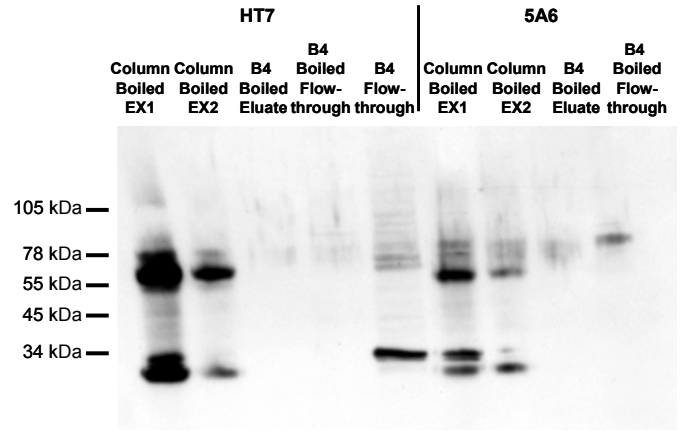

Fig. 3.26 Immunoprecipitation (IP) of the tau immune complex. To pull down everything which was sticking to the agarose gel / antibody complex, the whole column was boiled and fractions were loaded onto a 10-20 % tricine gel. In the boiled fraction the 28 kDa band appears again (compare with the B4 flow-through). Slightly below, a second band is visible, representing the light chain of the co-precipitated antibody. (WB labeled with HT7 (1:1000)).

(the light chain of the antibodies), indicating an highly hydrophobic structure of this band, but a conclusion pro or contra a tau origin can still not be drawn. A schematic overview of the IP-experiments is illustrated in table 3.1.

To isolate and analyze the 28 kDa band, IP-fractions were further separated by gel electrophoresis. The proteins were silver stained and the indicated bands were cut out (Fig. 3.27). After trypsinization, protein digests were identified by matrix-assisted laser desorption ionization tandem time-of-flight mass spectrometry (MALDI-TOF / TOF). No tau fragments were revealed by this analysis, however, two interesting candidates, the adaptor protein14-3-3γ and Rho GDP-dissociation inhibitor (RhoGDI-1) were discovered (for all identified bands see table 3.2).

Tab. 3.1: Schematic overview of the tau IP-experiments

Sample	Fraction	60 kDa band	28 kDa band
IP-RAB fractions	Flow-through	**(+)**	**+**
	Eluate	**+**	**-**
IP-Boiled RAB fractions	Flow-through	**-**	**-**
	Eluate	**+**	**-**
Column boiled	Eluate	**+**	**+**

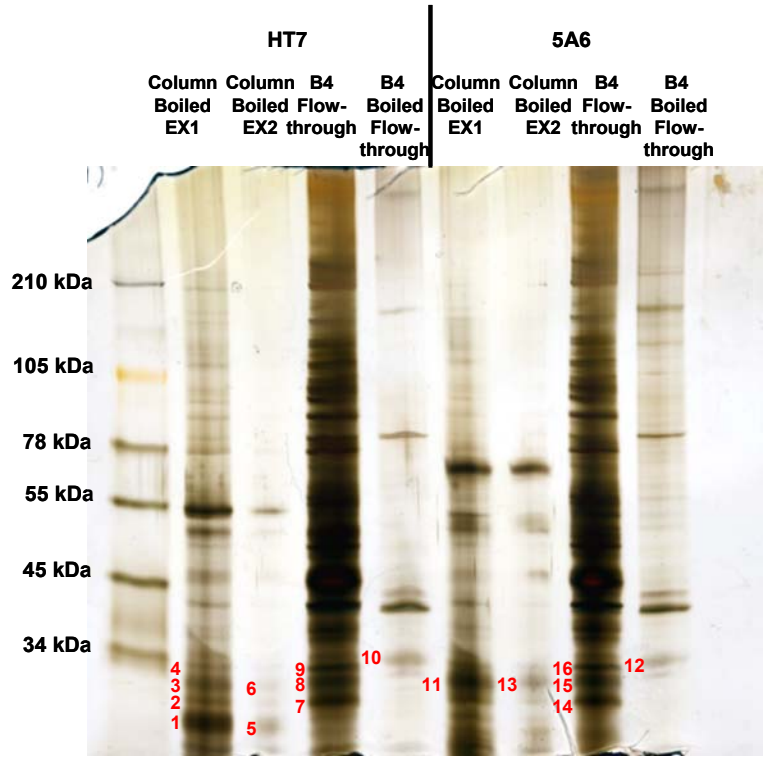

Fig. 3.27 Silver staining of IP-fractions. The bands indicated below the 34 kDa marker band were cut out and analyzed by mass spectrometry. The 28 kDa is expected in the first three lanes of each tau-specific antibody column. The B4 boiled flow-through lanes served as controls.

Tab. 3.2: Mascot search results: MALDI-TOF / TOF analysis

Band number	Protein number	Protein name
1 + 5	P01837	Ig kappa chain C region
2 + 6 + 7 + 14	P52565	Rho GDP-dissociation inhibitor 1 (RhoGDI1)
3 + 13	-	Not detected
4 + 12	Q15657	Tropomyosin isoform
8 + 11 +15	P35214	14-3-3 protein gamma (Protein kinase C inhibitor protein-1)
9	P42655	14-3-3 protein epsilon (Mitochondrial import stimulation factor L subunit)
10 + 16	Q8TCG3	TPMsk3 (Fragment)

To confirm a role of these proteins in our tissue culture system, FA-blots were stripped and reprobed with antibodies specific for 14-3-3γ and RhoGDI. Significant amounts of RhoGDI in the $A\beta_{42}$-treated FA-fractions were revealed, whereas no labeling was achieved against 14-3-3γ on the FA-blot. This indicates a specific effect of $A\beta_{42}$ on RhoGDI solubility (Fig. 3.28). The band migrated with an apparent molecular mass of close to 28 kDa, however, a direct comparison with the HT7 blot suggested that the RhoGDI band is not congruent with the HT7 band. Unfortunately, an IP with the RhoGDI antibody did not work, meaning that a final confirmation is still lacking. Nevertheless, RhoGDI is an interesting candidate to follow-up in subsequent studies (see discussion part 4.2).

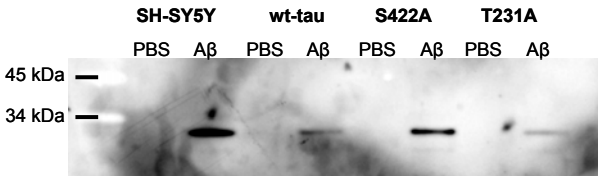

Fig. 3.28 FA-blot reprobed with RhoGDI. A FA-blot was stripped and reprobed with a Rho-GDI specific antibody. Approximately at 28 kDa strong bands appear in the Aβ-treated fractions, indicating an effect of fibrillar-Aβ on RhoGDI.

3.2.5 Tet-system

In light of the interaction of Aβ/APP and tau in AD, it is useful to have a system available where expression of these genes is tightly regulated in a time- and concentration-dependent manner. Therefore, we created a bi-directional (pBI) Tet response system, with co-expression of both tau and APP expected to provide new insights into the relationship of these two proteins.

First, to be able to select positive clones, a neomycin-resistance sequence was cloned into the PvuII-site of the pUHD 29-1 regulator plasmid (Bujard, ZMBH, Heidelberg, Germany) that encodes the reverse-tetracycline-controlled transactivator (rtTA) (Fig. 3.29). Two pBI-constructs were generated: wt-tau/GFP and wt-tau/APP^{Arc} (Fig. 2.9). The Arctic mutation was chosen, because Aß carrying this mutation forms protofibrils at a much higher rate and in larger quantities than wild-type Aß (Nilsberth *et al.*, 2001). To generate these constructs, wt-htau40-cDNA (cloned into the pRc/RSV expression vector) and a GFP-fragment (located on a GFP-expressing plasmid) were first removed by digestion with BamHI/EcoRV and EcoRI/NheI, respectively. The fragments were ligated (blunt-ended) into the multiple cloning site I (MCSI: EcoRV-site) of the pBI-vector.

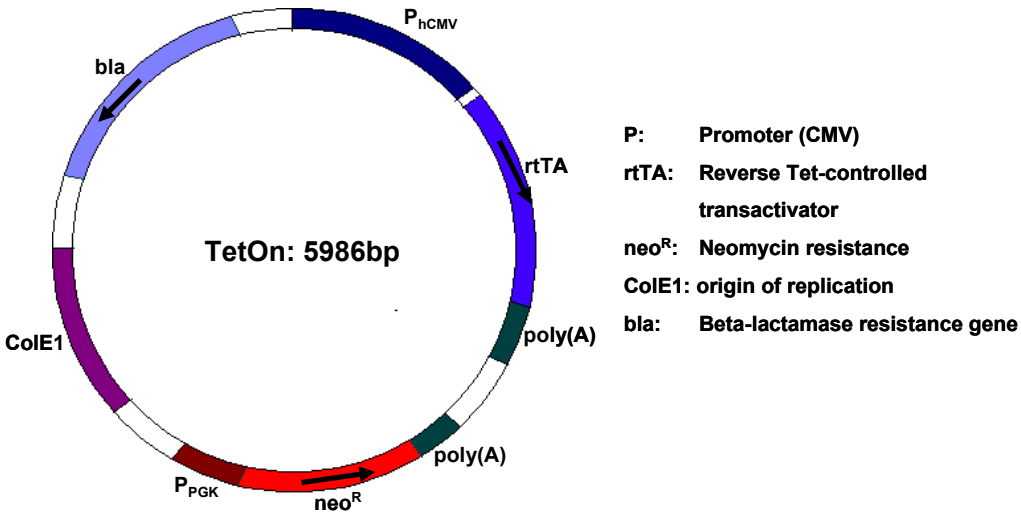

Fig. 3.29 Tet-on regulator plasmid pUHD 29-1. A neomycin-resistance sequence is cloned into the PvuII-site of the regulator plasmid that encodes the reverse-tetracycline-controlled transactivator (rtTA) under expression of a constitutive CMV-promoter.

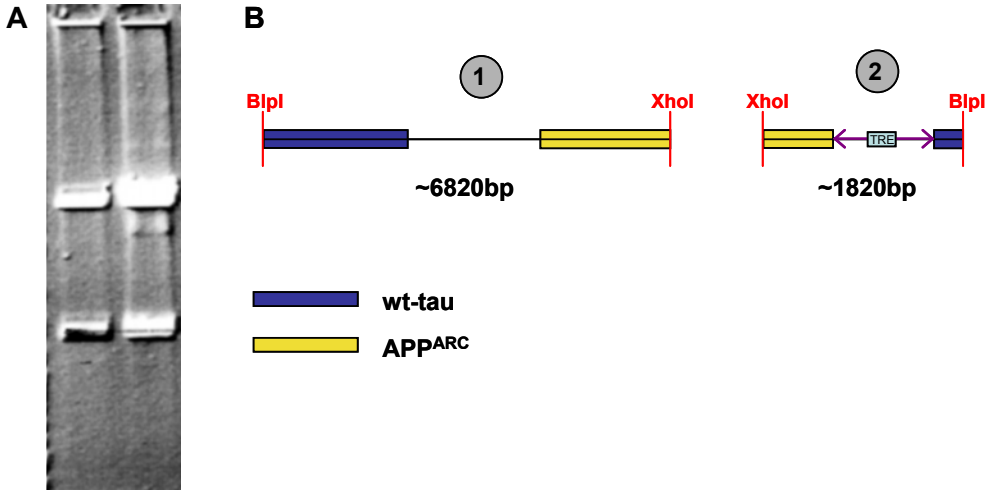

Fig. 3.30 Restriction size analysis of the wt-tau/APP^{ARC} response plasmid. Correct orientation of the ligation product is checked by double-digestion with BlpI (one restriction site in tau) and XhoI (one restriction site in APP). Correct ligation yields two fragments of the approximately sizes of 6820 and 1820 bp, respectively.

The APP^{Arc} mutation was introduced into the human APP$_{695}$ cDNA, which was cloned into the pGEM-9Zf vector. APP fragments were removed by digestion with HindIII and ligated (end-blunted) into the MCSII-site (NotI) of the GFP-pBI or wt-tau-pBI vector. Similarly, wt-htau40 cDNA was ligated into the GFP-pBI vector to obtain the wt-tau/GFP-vector. The correct sequence and orientation of all constructs was verified by DNA cycle sequencing and restriction enzyme size analysis (Fig. 3.30).

In a first attempt, a stable founder Tet-On cell line was generated by transfecting SH-SY5Y cells with the regulator plasmid encoding the reverse-tetracycline-controlled transactivator (rtTA). The pBI-constructs were transfected (together with a pTK-Hyg selection vector) into the stably expressing founder Tet-On-SH-SY5Y cells to obtain double-stable Tet-On cell lines. However, no overexpression of the proteins of interest was achieved as determined by immunocytochemistry, Western blotting and GFP-fluorescence analysis. In addition, co-transfection of the rtTA-plasmid with the response plasmids led to the same negative result (data not shown).

To check Transfections efficiency and to determine whether the regulator plasmid was functional, SH-SY5Y and HEK 293 cells were co-transfected with the rtTA-plasmid or with a new Tet-On regulator plasmid obtained from BD Biosciences and a pBI-GL control vector (BD Biosciences Clontech, Palo Alto, CA, USA), which is a response plasmid that can be used to express luciferase and β-galactosidase. After doxycycline treatment for 24h, the β-galactosidase activity was measured by counting numbers of positive cells per visible field using light microscopy (Fig. 3.31). In HEK 293 cells a reliable expression of β-galactosidase was detected, demonstrating the functionality of the rtTA-plasmid. In contrast, only a few SH-

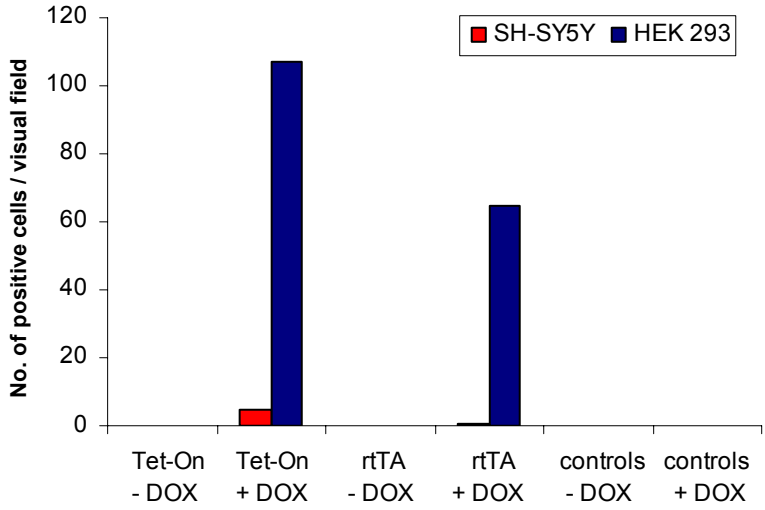

Fig. 3.31 β-galactosidase activity measurement. SH-SY5Y and HEK 293 cells were co-transfected with the rtTA-plasmid and a pBI-GL-control vector, which express β-galactosidase upon treatment with doxycycline. After 24h treatment cells were fixed and incubated with an X-gal staining solution for 3h at 37°C. The numbers of positive cells per visible field were counted. Whereas HEK 293 cells show a reliable expression, only a few SH-SY5Y cells are labeled. At least three independent fields per cell-line were analyzed.

SY5Y cells were labeled, indicating poor transfection efficiencies in these cells which may explain our negative findings shown above. A possible reason for this low transfection rate is the relatively large size of the plasmids (e.g. ~ 8400 bp for the wt-tau/APP^{Arc} construct) causing difficulties with cells, such as neuroblastoma cells.

Next, to verify the response constructs (wt-tau/GFP and wt-tau/APP^{Arc}), HEK 293 cells were transiently transfected and 4h after transfection doxycycline was added for 24h. Transfected wt-tau/GFP cells showed a reliable GFP expression as revealed under the fluorescence microscope (Fig.3.32). Cells were then extracted in RAB-buffer and lysates analyzed by Western blotting (Fig. 3.33). HT7-labelling revealed a strong overexpression of tau (16-30 fold) in transfected, non-treated cells compared to untransfected HEK 293 cells, showing an intrinsic

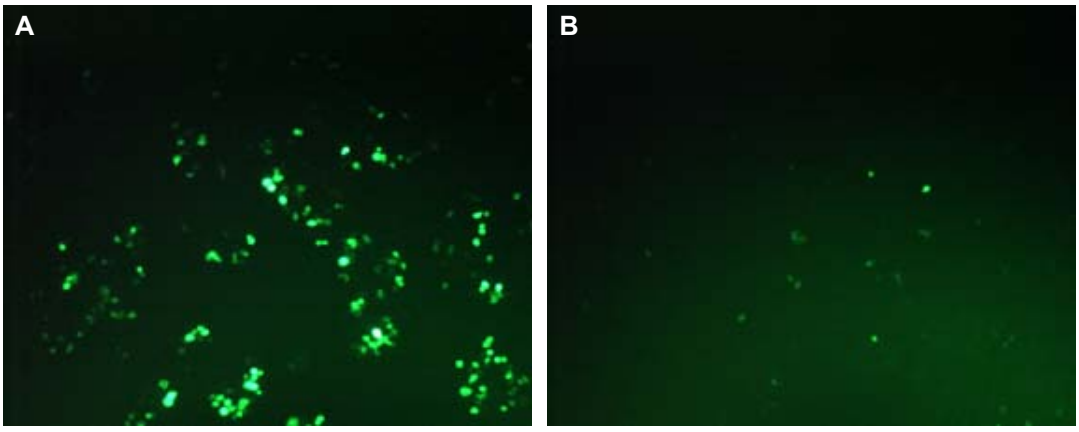

Fig. 3.32 Tet-system: HEK 293 cells transiently transfected with rtTA-regulator plasmid and the response wt-tau/GFP construct (A) GFP-expression upon doxycycline-treatment for 24h. (B) Transfected cells without doxycycline showing some basic background activity.

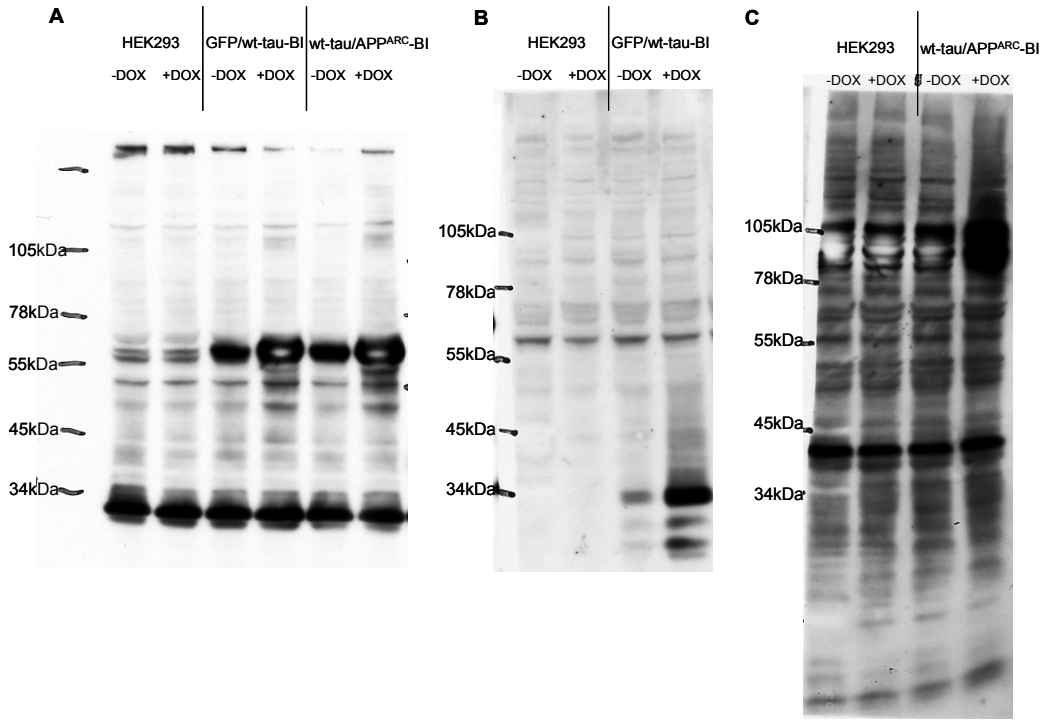

Fig. 3.33 Tet-system: HEK 293 cells transiently transfected with the rtTA-regulator plasmid and the response constructs wt-tau/GFP and wt-tau/APP^{ARC}, respectively. (A) The HT7 antibody (1:1000) is used to detect tau over-expression. Background expression of tau is found in transfected cells without Dox-treatment. Upon treatment with doxycycline tau expression increase 4-7 fold compared to untreated cells. (B) A similar result is obtained by probing with α-GFP (1:1000) against GFP. (C) APP C-terminal antibody (1:2000) against APP revealed only a slightly higher APP expression in transfected cells due to high APP expression levels in untransfected cells.

basal activity of tau. However, upon doxycycline (Dox) treatment the expression level of tau rose further (~ 95 fold compared with untransfected, Dox-treated cells and 4-7 fold compared with transfected, untreated cells). GFP expression showed a more regulated pattern, where basal levels were 6.5 fold higher than in untransfected cells. Dox treatment increased this basal transcription activity significantly (~ 26 fold). APP expression, however, was only slightly higher in transfected cells (~ 1.2 fold), since a prominent labeling was already seen in untransfected cells.

Together, these results show that the regulator and response plasmids are functional. However, several additional experiments and perhaps also modifications of the system are necessary to finally develop a functional TET-system in which the relationship between Aß and tau can be properly addressed. Some of these possibilities are brought up in the discussion part (4.3).

4 DISCUSSION

4.1 Behavioral analysis of P301L tau transgenic mice

I assessed P301L tau transgenic mice as a model for the tau pathology in AD and related disorders, first in using an amygdala-dependent test battery (fear conditioning and CTA) and secondly, using a hippocampus-dependent test battery (Y-maze and Morris water maze) (Table 4.1). Moreover, in both studies exploration, anxiety and locomotor activities were determined, which were independent of the mouse background (Rotarod, open field test, light-dark test, O-maze) (Table 4.1). Together, the data reveal a behavioral impairment of P301L tau transgenic mice, which can be correlated with the expression pattern of the human tau transgene. The data of the first study have been published 2004 in Neurobiology of Disease (Pennanen et al., 2004) and the results of the second study are in press in Genes, Brain and Behavior (Pennanen *et al.*, 2005, in revision).

4.1.1 Amygdala-dependent test battery

The immunohistochemical and behavioral analysis of P301L tau transgenic mice revealed a widespread aggregation of tau in the forebrain that is accompanied by selective changes in behavior. Behavioral changes include a small increase in exploratory behavior and an accelerated extinction of an aversion against a taste that has been previously paired with nausea. No changes with respect to wild-types were found in locomotor activity, fear conditioning, taste neophobia, and unconditioned natural taste preference for a sweet solution and natural taste aversion against a bitter solution. Tau aggregation was found in the forebrain in nuclei of the amygdalar complex, the hippocampus and all areas of the neocortex investigated (sensory, motor and associative areas). Aggregates were also present in several brain stem areas including the red nucleus, ventral tegmental area, and parts of the reticular formation, inferior olive, and ambiguus nucleus. NFT formation, as a final stage of tau aggregation, is initiated in a subset of amygdaloid neurons at around six months of age, possibly reflecting high relative levels of tau expression and/or selective vulnerability of distinct amygdaloid nuclei (Gotz *et al.*, 2001a; Gotz and Nitsch, 2001).

The study also revealed that the body weight of P301L mice was slightly lower than that of wild-types already at the beginning of the behavioral testing at 6 months of age. This weight difference was even larger during the final (CTA) task of the test battery, when the mice were water-deprived. Such a weight loss could be due to disturbances in different brain areas. Lesion studies, for instance, established that certain hypothalamic nuclei regulate food intake

Tab. 4.1: Behavioral analysis of P301L tau transgenic mice

TASK	TESTING	RESULTS
1st study, amygdala-dependent test battery: P301L mice (B6D2F1 background; starting at 6 mt of age)		
Weight	Body weight	P301L mice ↓
Rotarod	Locomotor coordination	P301L mice ↑
Open-field	Locomotor activity, anxiety-like behavior and exploration	Activity: P301L mice ↔ Anxiety: P301L mice ↔ Exploration P301L mice ↑
Light-dark test	Anxiety-like behavior and exploration	Anxiety: P301L mice ↔ Exploration P301L mice ↑
Fear condition-ing	Conditioned fear response to tone and context	Conditioning:P301L mice ↔ Context testing:P301L mice ↔ Tone testing:P301L mice ↔
Conditioned taste aversion (CTA)	Conditioned taste aversion	Acquisition and consolidation: P301L mice ↔ Extinction: P301L mice ↑ Basic taste qualities: P301L mice ↔
2nd study, hippocampus dependent-test battery: P301L mice backcrossed to C57BL/6		
Open-field	Locomotor activity, anxiety-like behavior and exploration	6 months of age: Activity: P301L mice ↔ Anxiety: P301L mice ↓ Exploration P301L mice ↑ 11 months of age: Activity: P301L mice ↑ Anxiety: P301L mice ↓ Exploration P301L mice ↑
O-maze	Locomotor activity, anxiety-like behavior and exploration	6 months of age: Activity: P301L mice ↑ Anxiety: P301L mice ↔ Exploration P301L mice ↑ 11 months of age: Activity: P301L mice ↑ Anxiety: P301L mice ↔ Exploration P301L mice ↑
Y-maze	Spontaneous alternation behavior to test spatial working memory	6 + 11 months of age: Alternation behavior: P301L mice ↔ Number of arm entries: P301L mice ↔
Morris water maze (MWM)	Spatial reference memory , swimming navigation and search strategies	6 months of age: Acquisition learning: P301L mice ↔ Reversal learning: P301L mice ↔ Probe trial: P301L mice ↓ Search strategies: P301L mice ↔ 11 months of age: Acquisition learning: P301L mice ↔ Reversal learning: P301L mice ↔ Probe trial: P301L mice ↓ (but also wt mice ↓) Search strategies: P301L mice ↔

↑ = upregulated, ↓ = downregulated; ↔ = no significant differences

and body weight (Kishi and Elmquist, 2005). However, no tau aggregates were found in the hypothalamus. Damage to amygdaloid nuclei, an area with tau aggregates, has been reported in rats to cause either no change or the opposite, i.e. a gain of weight (Rollins *et al.*, 2001). However, in our mice an altered emotion caused by amygdala dysfunction, such as increased exploratory behavior, could have pronounced effects on food uptake and thereby on body weight.

In the open-field, P301L and wild-type mice moved equal distances, but P301L mice changed their activity state somewhat more often from progression to resting to scanning. Furthermore, in the light-dark box they were more active and clearly increased the frequency of rearing, all of which are signs for greater exploratory behavior. Both, in the open-field and light-dark test, measures of anxiety were unchanged. Several brain structures have been found to be involved in exploratory behavior including the hippocampus and amygdala. That the amygdala might be affected in our transgenic mice is suggested by the observation that amygdala lesions increase exploratory behavior (Kelley *et al.*, 1989). Dysfunction of the amygdala, however, would not affect unconditioned anxiety as measured with an anxiety test (elevated plus-maze) in rats (Treit and Menard, 1997).

Expression of the transgene and formation of tau aggregates in the forebrain did not impair fear conditioning to tone or context. When tested 15 days after conditioning, wild-types as well as P301L mice also showed no signs of extinction and froze even more in response to the conditioned stimuli (context, auditory cue). The non-significant tendency of reduced freezing of P301L mice only during conditioning remains puzzling, and no treatment with a similar selective effect has been described. Anyhow, it is difficult to imagine how emotional or cognitive changes could affect freezing during conditioning but not during retrieval.

That P301L mice had no deficits in fear conditioning to a tone is in agreement with the expression pattern of tau aggregates in their brain (Fig. 4.1). Conditioning to an auditory CS is

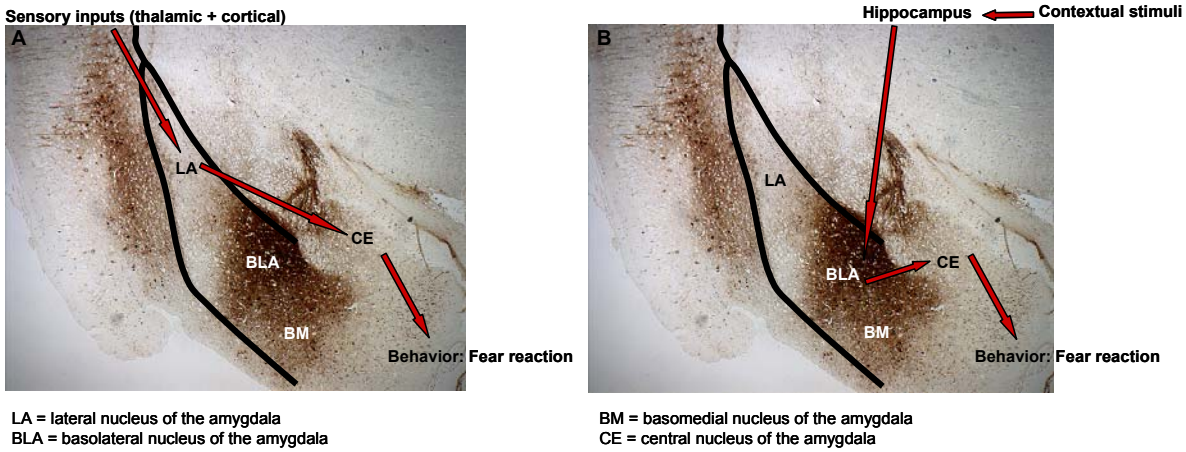

Fig. 4.1 Neuroanatomy of fear conditioning. (A) Conditioning to sensory inputs (e.g. tone) is dependent on functionally intact lateral and central nuclei of the amygdala, sites that were free of tau aggregates (B) Context fear conditioning depends on an intact hippocampus which projects to the BLA. However, despite a prominent expression of P301L tau in the hippocampus and the BLA, no deficits were found in context fear conditioning.

dependent on functionally intact lateral and central nuclei of the amygdala (LeDoux, 2000), sites that were free of tau aggregates in our transgenic mice. The involvement of the basolateral amygdala (BLA), a site with tau aggregates in P301L mice, is less well established (but see also (Goosens and Maren, 2001). In contrast to fear conditioning to a tone, successful context fear conditioning depends on an intact hippocampus which projects to the BLA (LeDoux, 2000). However, despite a prominent expression of P301L tau in the hippocampus and the BLA of P301L mice, no deficits were found in context fear conditioning compared with control mice. This may be due to the design of the fear conditioning task that was probably not sensitive enough to reveal differences between the two groups. Similar to our P301L mice, aged APP^{Swe} mutant mice also showed no deficits in fear conditioning to a tone or a context when compared to corresponding wild-types (Corcoran *et al.*, 2002). These APP^{Swe} mice had β-amyloid plaques in the hippocampus as well as the amygdala and a reduction in function might have been expected. Only when the salience of the context CS was reduced, an indication of impairment in APP^{Swe} mice appeared. The general lack of massive neurodegeneration in animal models of AD may explain the largely normal performance of both P301L and APP^{Swe} mice in fear conditioning, which is in contrast to the reported impaired fear conditioning in AD patients (Hamann *et al.*, 2002). This demonstrates the importance to design highly sensitive protocols for the measurement of different behavioral tasks.

P301L mice acquired a taste aversion indistinguishable from that of wild-types; that is, when given a choice to drink either a saccharin solution or water 2 days after pairing saccharin drinking with nausea, both genotypes greatly preferred water and avoided the saccharin solution. However, repeated exposure to such a choice situation attenuated the aversion, and this extinction was drastically accelerated in P301L mice compared to wild-types. The possibility has to be considered that a stronger conditioning in wild-type mice might not have shown due to a ceiling effect, that is, wild-type mice performed already close to an optimum with no further capacity of improvement.

The CTA deficit in P301L mice cannot be explained by a reduced neophobia, an increased sweet preference or a reduced aversion for unpleasantly tasting solutions. With respect to these three traits, no genotype differences could be found. P301L, as well as wild-type mice reduced their fluid intake, when first exposed to the saccharin solution (neophobia), developed a strong preference for the sweet solution when drinking was not followed by nausea, and avoided a bitter tasting quinine solution to the same degree. Furthermore, despite their slightly reduced body weight, P301L mice did not consume less saccharin solution on the conditioning day, that is, exposure to the conditioned stimulus was comparable in both groups.

It has been suggested that lesions of the BLA have a general effect on the response to novel stimuli (such as food) by decreasing neophobia (Dunn and Everitt, 1988). However, in our

study no attenuation of a taste neophobia was found. Thus, the observed formation of tau aggregates in the amygdala in P301L mice very unlikely caused a severe functional impairment of this structure.

Tau was expressed in brain areas which have been shown to be involved in CTA including the BLA, the insular cortex and some thalamic nuclei (Welzl *et al.*, 2001). No expression was found in other CTA-relevant areas such as the ventral posteromedial nucleus of the thalamus (VPM), the parabrachial nucleus (PBN) and the nucleus of the solitary tract (NTS).

Little is known about what might accelerate extinction of CTA. Several studies implicated hormonal systems, neurotransmitter systems or specific brain structures in CTA extinction (for review, see (Bures *et al.*, 1998); but in general these studies described retarded, but not accelerated, extinction upon treatments. For example, whereas hippocampal lesions affected acquisition of CTA only mildly or not at all (Best and Orr, 1973; Yamamoto *et al.*, 1995), they slowed extinction of an already conditioned aversion (Kimble *et al.*, 1979). In one study, excitotoxic lesions of the VPM had little effect on the acquisition of CTA but markedly accelerated its extinction similar to what we observed in our transgenic mice (Yamamoto *et al.*, 1995). However, tau is not expressed in the VPM of P301L mice.

Numerous studies support a critical involvement of the amygdala in CTA (Aja *et al.*, 2000; Lamprecht *et al.*, 1997; Yamamoto *et al.*, 1995). Similar to its effect on other aversive memories, the amygdala could modulate consolidation processes (e.g. of CTA) in other brain areas via its projections to these areas (McGaugh *et al.*, 2002). Such a modulation could be achieved by pathways from the amygdala to the insular cortex, a structure critical for storage of a CTA. Stimulation in the BLA induced LTP in the insular cortex which enhanced retention of CTA memory in subsequent extinction trials (Escobar and Bermudez-Rattoni, 2000). Overexpression of P301L tau in the BLA could impair this modulatory effect resulting in accelerated extinction, either directly or by weakening the strength of the memory trace.

Interestingly, a recent study showed that the BLA is essential for extinction of CTA memory whereas acquisition is dependent on an intact central nucleus (Bahar *et al.*, 2003). The differential effect of tau aggregates on fear conditioning and CTA fits well with their distribution pattern in the amygdala. We observed the aggregates in the basolateral but not the lateral and central nucleus. In contrast to CTA, fear conditioning is not dependent on an intact BLA, but an intact lateral and central nucleus (for review, see (Bures *et al.*, 1998; LeDoux, 2000). It also seems noteworthy to mention that, again, APP^{Swe} mice resemble to some degree P301L mice. APP^{Swe} mice expressed amyloid plaques in the amygdala and also showed an accelerated extinction of the CTA memory. However, in contrast to the P301L mice, the APP^{Swe} mice already had deficits in the acquisition of the task (Janus *et al.*, 2004).

AD patients exhibit an impairment at all levels of gustatory information processing, in line with the notion of a dissociation between preservation of olfactory and gustatory thresholds

and an alteration in odor identification in patients with mild stage AD, suggesting that the alteration is central rather than peripheral (Broggio *et al.*, 2001). Significant losses in the ability to detect the taste of glutamic acid and to recognize odorants were found in demented AD and non-AD patients when compared with age-matched controls (Schiffman *et al.*, 1990). These findings are consistent with our transgenic model as the P301L mice share features of AD and FTD.

In summary, the distribution of mutant tau in P301L mice is widespread and comes close to the pattern of tau pathology observed in patients. These mice also lack the motor disturbances observed in other tau mutants, disturbances which are not characteristic of AD (see below 4.1.3). P301L mice share, however, some characteristics with behavioral disturbances observed in APP mutant mice. Furthermore, disturbances can be detected already when mice are 6 months old. Thus, we believe that P301L mice are a good model to investigate the contribution of tau pathology, as observed in AD and FTDP-17, to behavioral disturbances.

Although this investigation raised a number of questions that have to be addressed in future studies, a number of conclusions on the early effects of tau aggregation in transgenic P301L mutant tau mice can be drawn. Firstly, in the open field and light-dark box subtle signs for increased exploratory behavior were manifest in P301L mice. Secondly, fear conditioning to tone or to context remained unaffected, probably due to the specific distribution of tau aggregates in the amygdala. Thirdly, a selective alteration in the extinction of a taste aversion could be seen in P301L mice. This, again, resembles data collected in APP^{Swe} mice subjected to a similar paradigm. Thus, CTA suggests itself as a sensitive measure of altered brain function in response to the formation of tau aggregates. One possible common factor for all these results could be a dysfunction of specific nuclei of the amygdala.

4.1.2 Hippocampus-dependent test battery

As shown in the first study, P301L tau is differentially expressed in cortical areas, in the basolateral (BLA) and the basomedial (BM) nuclei of the amygdala, in the hippocampus (CA1, CA3 and dentate gyrus), and in other brain areas. To elucidate the impact of tau aggregation on hippocampus-dependent cognition, I used, in a second study, P301L mice backcrossed onto a C57Bl/6 background. An immunohistological comparison of brains of transgenic mice on a more mixed background (B6D2F1) with transgenic mice onto a C57Bl/6 background at both 7 and 13 months of age revealed no obvious differences in the expression pattern and phosphorylation of tau (data not shown). Consistent with these findings, in the open-field, confirming the previous data obtained with P301L mice on the B6D2F1 background (Pennanen et al., 2004), increased exploratory behavior compared to wild-type controls was

found for both ages tested. In addition, older P301L mice showed less anxiety and a higher locomotor activity than their littermates. In the elevated O-maze the P301L mice showed increased activity at all ages. Anxiety levels were not altered at 6 months, but at 11 months of age. These findings are similar to those obtained in the open-field, where P301L mice showed a less anxious behavior than wild-types. The increase in activity as observed in the O-maze may be taken as additional evidence for an altered exploratory drive. Obviously, P301L mice exhibit a modest disinhibition of exploratory behavior which manifests in the open field, for example, as more time spent in the inner (exploration) zone and in the O-maze as an increase in the total distance traveled. These effects are even more pronounced when the mice get older and are accompanied by reduced anxiety levels. Disinhibition of exploratory behaviors is not uncommon in rodents with deficits of hippocampal function (Hausheer-Zarmakupi *et al.*, 1996; Laghmouch *et al.*, 1997; McDaniel *et al.*, 1994; Wright *et al.*, 2004).

In the Y-maze all groups showed a reliable expression of spatial working memory as demonstrated by spontaneous alternation behavior above chance level. The two genotypes did not differ at either age, suggesting intact spatial working memory of P301L mice.

This result is supported by the fact that acquisition and reversal learning in the water maze was not altered in P301L mice, as illustrated by similar learning curves for all groups. However, in the probe trial, at 6 months of age, the P301L mice spent less time in the former platform quadrant or in the goal zone indicating impairment in spatial reference memory compared to controls. At least theoretically, less persistent searching may also reflect increased exploratory drive. Analysis of a shorter time window during the probe trial yielded a similar outcome (data not shown), providing further evidence that the deficits are cognitive in nature. The significant difference in spatial retention, which was observed between P301L and control mice at 6 months, was not seen at 11 months of age. This was due to a floor effect as evidenced by a poor performance of the wild-type control group during the probe trial, with no significant preference above chance level for the former platform location (Fig. 3.12). Although, in general, C57Bl/6 mice are fairly good learners of swimming navigation (Upchurch and Wehner, 1988, 1989), there are reports showing that these mice, as a group, can occasionally perform poor probe trial scores, even when they had learned to adapt a special escape strategy to the former platform location (Wolfer et al., 1997).

At both ages tested, P301L mice were not capable of developing a significant preference for the former platform location as revealed in the probe trial, therefore a further decline at 11 months of age was not detectable. Only for the annulus crossings as the most sensitive measure, a reduced performance was shown which, however, was not statistically significant (Fig. 3.12C).

Triple transgenic mice (APP^{SWE} x P301L x $PS1_{M146V}$) developed cognitive impairments in the MWM as early as 4 months of age (at least homozygous 3xTg mice) which were comparable

to the manifested retention/retrieval deficits in our P301L mice, whereas acquisition of the hidden platform position was unaffected (Billings *et al.*, 2005). As in our mouse model, these deficits occurred prior to the formation of any plaque or tangle pathology.

In addition, the results obtained in P301L mice are in agreement with findings in rats with CA3 lesions (a brain area in P301L mice where tau aggregates are found), which are impaired in the retention of spatial memory in the water maze paradigm (Roozendaal et al., 2001). The observed deficits in spatial reference memory in the P301L mice may be due to aggregation of tau in the hippocampus and the BLA. The hippocampus is dependent on the BLA in glucocorticoid-induced impairment of spatial memory retrieval (Roozendaal et al., 2003). Anatomical evidence further indicates a role for the BLA in regulating hippocampal processes, as the BLA is known to project extensively to discrete hippocampal subfields (Petrovich et al., 2001). For example, electrophysiological data demonstrated that information which was processed within the amygdala reached the hippocampal formation, where it appeared to modulate synaptic activity. Therefore, the presence of tau aggregates in the BLA of our P301L mice may have contributed to the observed spatial memory impairment.

The results from our P301L mice share some characteristics with behavioral disturbances observed in APP mutant mice. Deficits in spatial reference memory have been reported in several lines, albeit the onset of cognitive deficits varies between different studies, even within the same strain (for a review: (Ashe, 2001)). Deterioration of spatial working memory in two different lines of APP transgenic mice could not be detected before 13 -15 months of age, although conversion of detergent-soluble into insoluble Aβ and thus plaque formation occurred much earlier (~ at 6 months) (Chen *et al.*, 2000; Morgan *et al.*, 2000). Together, it is possible that spatial working memory is preserved longer than spatial reference memory and is unrelated to the initial conversion into insoluble Aβ-plaques or NFT-formation. However, it is also likely that the dynamic ranges of the used paradigms to measure spatial working memory may miss the more subtle abnormalities developing in younger mice.

The behavioral impairment of P301L tau transgenic mice, which can be correlated with the expression pattern of P301L tau, is also consistent with findings in human disease. For example, depending on the brain area affected by neuronal loss, the clinical phenotype in FTDP-17 patients can differ with variable cognitive and behavioral features (Kramer et al., 2003). Carriers of the P301L mutation showed significant differences in tasks reflecting the relatively focal deficit in frontal systems in these patients (Geschwind et al., 2001). The decrement appeared as early as in the second and third decades of life, many years before neurodegeneration manifests itself clinically. Similarly, in our P301L tau transgenic mice selective behavioral deficits are observed well before overt NFT formation.

In summary, we found in the present study that tau aggregation, in the absence of overt NFT formation, caused deficits in spatial reference memory as determined in the Morris water

maze and a modest disinhibition of exploratory behavior at 6 months of age. The difference in the exploratory drive is even more pronounced during aging, whereas no further decline in spatial reference memory was detected at 11 months of age. No impairment was found in acquisition and reversal learning in the water maze and in spatial working memory as assessed by spontaneous alternation behavior in the Y-maze. These data suggest, together with the previous findings, that tau aggregation in distinct brain areas directly affects the performance in memory tests controlled by these brain areas. They also showed that tau aggregation, even in the absence of NFT formation, is sufficient to cause behavioral deficits.

4.1.3 Behavioral analysis of other tau transgenic mouse models

Additional tau transgenic mouse strains have been investigated in a range of behavioral tests. For example, transgenic mice which express the same mutant form of tau (P301L), but a different tau isoform, under control of the PrP promoter, strongly overexpress the tau transgene in several neuronal cell-types, including motor neurons. These mice have been analyzed at 5 to 7 months of age as they develop a progressive motor phenotype by 9 to 10 months of age, thus preventing behavioral testing at this later age (Lewis et al., 2000). Although the transgenic mice were unimpaired as a group in any behavioral measure, when numbers of tau-bearing neurons were determined in neocortex and hippocampus, these were correlated with a poorer cognitive performance in the individual mice (Arendash et al., 2004). V337M tau mutant mice which express the transgene only in the hippocampus displayed increased locomotor activity and exploratory behavior in the elevated plus maze, increased spontaneous locomotion in the open-field, but no significant impairment in the Morris water maze (Tanemura et al., 2002). Transgenic mice expressing human tau with the R406W mutation had highest levels of the transgene in the hippocampus and, to a lesser extent, in other cortical and subcortical brain areas. In the amygdala, only a few cells strongly expressed mutant tau, even in old animals (Tatebayashi et al., 2002). These mice showed a slight decrease in locomotor activity in the open field, and a significant impairment in contextual and cued fear conditioning. Obviously, the form of mutant tau expressed and the type of promoter controlling its expression, together with the genetic background on which the transgene is expressed have a major impact on the outcome of the behavioral analysis (Wolfer and Lipp, 2000).

4.2 Tissue culture system

The relationship between Aβ and tau and their relative contribution to the clinical features of AD is one of the main topics in AD research. Recently, our group has demonstrated pathological interactions between these two major players in AD. *In vivo*, stereotaxically injecting pre-aggregated $A\beta_{42}$ fibrils into the somatosensory cortex and the hippocampus (CA1) of P301L mice caused a fivefold increase in the numbers of NFT in the amygdala (Gotz *et al.*, 2001b). *In vitro*, using tau overexpressing human SH-SY5Y neuroblastoma cells, treatment with pre-aggregated $A\beta_{42}$ lead to the generation of PHF-like tau-containing filaments and decreased tau solubility (Ferrari *et al.*, 2003). NFT formation in the $A\beta_{42}$-injected P301L mice was tightly correlated with the pathological phosphorylation of tau at the phospho-epitopes pS422 (Ser-422) and AT100 (Thr-212/Ser-214). Congruently, expression of tau mutated at the Ser-422 phospho-epitope in SH-SY5Y cells prevented the $A\beta_{42}$-mediated decrease in solubility and the generation of tau filaments, suggesting a pivotal role of this epitope in fibrillogenesis.

To confirm the previous *in vitro* findings and to further map phospho-epitopes and cleavage sites of tau involved in the β-amyloid-induced decrease in tau solubility and filament formation, I have generated several tau mutant constructs and stably expressed them, as well as the wild-type tau (htau 40) isoform, in SH-SY5Y neuroblastoma cells. Addition of pre-aggregated $A\beta_{42}$ to differentiated wt-tau overexpressing SH-SY5Y cells led to a more than 15-fold increase in $A\beta_{42}$-mediated tau insolubility, whereas mutating the Ser-422 phospho-epitope decreased the level of tau solubility only to baseline levels, comparable to SH-SY5Y control cells. These results also show that endogenous tau is capable of aggregating upon treatment with $A\beta_{42}$. Mutating additional phospho-epitopes of tau (the AT8-epitope of Ser-202/Thr-205 and pT231) prevented the decrease in tau solubility as well. It may even be inhibitory to aggregation of endogenous tau, as shown by a ~ 60 % decrease in tau insolubility compared to baseline levels.

These findings correspond with previous reports, pointing out the importance of these phospho-epitopes in filament formation. The AT8-epitope is widely used in neuro-pathological stagings (Mercken *et al.*, 1992). Phosphorylation at the AT8-epitope distinguishes PHF tau from normal human brain tau (Biernat *et al.*, 1992) and phosphorylation at this site is probably followed and associated with neuronal apoptosis and apoptotic changes in AD brains (Kobayashi *et al.*, 2003).

Antibodies directed against tau phosphorylated at pThr-231 has also been well documented to label filaments in AD brains (Jicha *et al.*, 1997). In addition, this epitope plays an important role as it is the only binding site for Pin1, a prolyl isomerase, which catalyzes a conformational change, restoring tau function and promoting its dephosphorylation (Lu *et al.*, 1999). In

addition, Pin1 expression is inversely correlated with neuronal vulnerability and NFT in post-mortem AD brains. Pin1 knock-out mice show progressive age-dependent neuropathy, tau hyperphosphorylation and tau filament formation (Liou *et al.*, 2003).

Different groups established a hierarchy of tau phosphorylation in AD with varying severity of neuropathological changes using a panel of different tau antibodies. Augustinack and co-workers showed that AT8 intensely stained extraneuronal NFT in advanced cases, whereas pre-NFT were rarely labeled (Augustinack *et al.*, 2002). In the same study, TG3, an antibody directed against the conformational pThr-231-epitope, stained already pre-NFT, indicating an early involvement of this epitope in NFT evolution. However, another study reported contradictionary findings with a prominent labeling of pre-NFT by the AT8 antibody and an exclusive Thr-231 immunoreactivity on extraneuronal NFT (Kimura *et al.*, 1996).

Unfortunately, the data for the AT100 epitope, which was hyperphosphorylated after $A\beta_{42}$-injections in P301L mice (Gotz *et al.*, 2001a) and found to exclusively label AD-filaments (Allen *et al.*, 2002; Zheng-Fischhofer *et al.*, 1998), had finally to be excluded from our analysis due to a loss of the tau transgene as revealed by Western blot analysis of RAB fractions. We encountered a similar problem also with another construct that was stably transfected at the beginning. It seems that one of the limitations of the tissue culture system is that transgenes may be lost, which may be associated with increased passage numbers during culturing. Overall, our results suggest an interplay of different epitopes in tau filament formation.

Interestingly, the Ser-422 epitope is located next to a putative caspase-3 cleavage site at position Asp-421 (Fasulo *et al.*, 2000). That mutagenesis of this epitope prevented tau aggregation could be explained insofar as Ser-422 needs to be phosphorylated such that tau can become a substrate for cleavage by caspase-3. Δ421 tau assembles much faster than wild-type tau *in vitro*, demonstrating an inhibitory effect of the carboxy-terminal tail of the tau molecule on filament formation (Abraha *et al.*, 2000; Berry *et al.*, 2003). In addition, in neurons treated with $A\beta_{42}$, tau is rapidly cleaved at this site (Gamblin *et al.*, 2003). Surprisingly, truncation of the C-terminal region of tau at position 421 prevented the $A\beta_{42}$-mediated decrease in tau solubility in our tissue culture system similar to the phospho-mutants (Fig. 3.21). At first sight, comparing these results with the known characteristics of Δ421 tau is difficult. However, a recent study suggests that C-terminal truncation at the caspase cleavage site Asp-421 occurs only after filament formation from full-length tau in AD-brains (Guillozet-Bongaarts *et al.*, 2005). Taken together, our result would support the view that filaments form first from full-length tau and therefore truncation is likely not an initial step, but rather a subsequent event in tau filament formation. However, obviously additional studies are needed to fully resolve the evolution of tau filament formation.

Wild-type tau transgenic mice develop only a few NFT at very old age, despite high expression levels of the transgene (Gotz *et al.*, 2001a; Ishihara *et al.*, 1999). Obviously, in the mou-

se model, a pathogenic tau mutation is required to catalyze tau aggregation and the formation of PHF-like structures. In the human cell-culture system, however, filament formation also occurs with wild-type tau. This may be related to species differences and points to the possibility that human cells in culture may be more susceptible to the formation of abnormal tau filaments as compared with mouse cells *in vivo*, probably due to differential gene expression. Also, in contrast to humans, mice express only four-repeat tau isoforms (Goedert and Jakes, 1990), whereas SH-SY5Y cells predominantly express fetal tau (the shortest three-repeat tau isoform). Thus, a different 4R/3R ratio could also underlie this discrepancy.

As mentioned above, there are some limitations in the tissue culture system. For instance, the expression levels of tau appear to play a critical role, as other research groups, that is, by using a viral approach, could detect a shift of tau into the FA-fraction even without Aβ treatment (EVOTEC NeuroSciences GmbH, Hamburg, unpublished data), indicating that if enough unbound tau in the cells is available, a self-aggregation process is initialized and tau aggregation starts. A tight regulation of gene expression in a time- and concentration dependant manner would clearly help to gain better insight into the process of tau aggregation and the relationship of Aβ and tau (see below 4.3).

Furthermore, the question remains unanswered whether the 28-kDa band is a truncated tau isoform and / or a second protein. The finding that the band was also detected by an additional antibody recognizing the C-terminal part of tau would favor the “tau-hypothesis”. However, immunoprecipitation experiments failed to detect and isolate this band, as well as mass spectrometry analysis, arguing against a tau origin. Therefore, the 28kDa band was not included in the phospho-epitope mapping experiments.

In search of the true nature of the 28kDa band, another interesting protein, the Rho GDP-dissociation inhibitor (RhoGDI-1), was identified to having a decreased solubility upon Aβ-treatment. RhoGDI is to be an interesting candidate to follow-up in subsequent studies. First, a proteomics analysis of our tissue culture system revealed decreased levels of RhoGDI in RAB fractions obtained with cells treated with $A\beta_{42}$ compared to control cells (David *et al.*, unpublished data), confirming the Western blot results discussed above. Secondly, Rho GDIs negatively regulate Rho-family GTPases, like Rho, Rac and Cdc42 (Fukumoto *et al.*, 1990; Ueda *et al.*, 1990). These proteins appear to play a key role in regulating the assembly and organization of the actin cytoskeleton in response to extracellular stimuli (Johnson and Pringle, 1990; Ridley and Hall, 1992; Ridley *et al.*, 1992). Zhu and colleagues have demonstrated that Cdc42 and Rac are upregulated in selected neuronal populations of AD brains and showed considerable overlap with early cytoskeletal abnormalities (Zhu *et al.*, 2000).

Cdc42 and Rac are also important upstream regulators of the protein kinase cascade that control the SAPK/JNK and p38/Mpk2 activities (Cano and Mahadevan, 1995; Coso *et al.*, 1995; Minden *et al.*, 1995). SAPK/JNK and p38 are involved in the phosphorylation of tau,

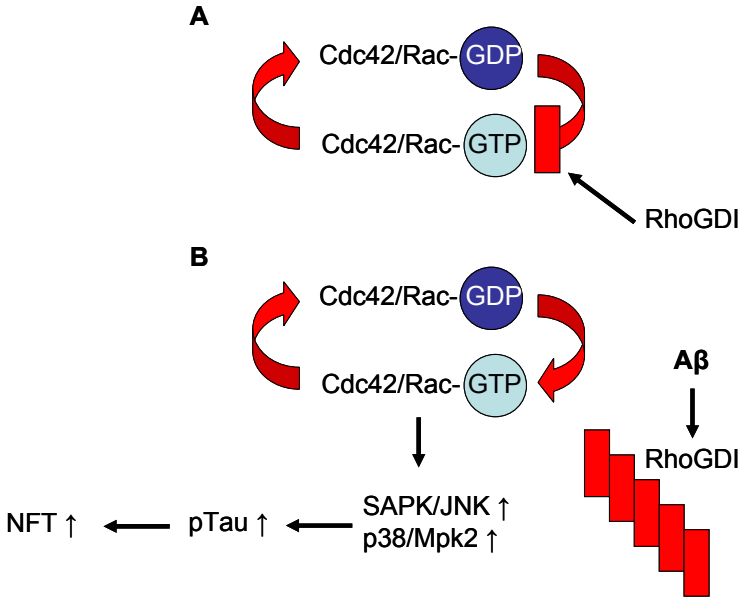

Fig. 4.2 Hypothetical schematic overview of Aβ-mediated effects of RhoGDI-aggregation: (A) GDIs inhibit the GDP to GTP exchange and thus control the activity state of Rho GTPases like Cdc42 and Rac. (B) Upon treatment with Aβ, RhoGDI-proteins aggregate and lose their inhibitory effects. Cdc42 and Rac upregulation can lead to the activation of different protein kinase pathways (SAPK/JNK and p38/Mpk2), which cause tau hyperphosphorylation and finally filament formation.

and activated phospho-JNK was found to be associated with NFT in AD brains (Goedert *et al.*, 1997; Kins *et al.*, 2003; Reynolds *et al.*, 1997; Zhu *et al.*, 2001).

Thus, Aβ-mediated aggregation of RhoGDIs may lead to the inhibition of these proteins and to the activation of Rac and Cdc42 GTPases. Thereby, different protein kinase pathways may be activated, which cause tau phosphorylation and aggregation (Fig. 4.2).

In summary, the human tau-expressing tissue culture system is a suitable tool to address aspects of AD and related disorders. Addition of preaggregated $A\beta_{42}$ to wt-tau expressing SH-SY5Y cells decreases the solubility of tau. Mutagenesis of different phospho-epitopes of tau prevents this decrease in tau solubility, indicating an interplay of different epitopes in tau filament formation. Further adaptation of the SH-SY5Y tissue culture system is likely to provide mechanistic insight into tauopathies and may allow the screening and validation of compounds designed to prevent PHF formation.

4.2.1 Tet-system

Regarding the above mentioned difficulties of the tissue culture system and the apparent discrepancies in the literature concerning the requirements for tau filament formation, it would be beneficial to have a system where expression of the tau gene is tightly regulated in a time- and concentration dependant manner. Different inducible expression systems were generated in the last twenty years that allow genes to be activated or silenced in cells and organisms at will (Lewandoski, 2001). The most widely used binary transcription transactiva-

tion systems are the tetracycline-dependent regulatory systems (Gossen and Bujard, 1992; Gossen *et al.*, 1995). For our study, we have chosen the Tet-on system, where transgene expression is only induced in the presence of an inducer. Furthermore, to be able to determine the effects of intracellular β-amyloid on tau pathophysiology a bi-directional (pBI) Tet vector was used, where both tau and APP are expressed on the same plasmid. For that, we decided to utilize an APP construct containing the Arctic mutation, which leads to enhanced Aβ-protofibril formation (Nilsberth *et al.*, 2001). A further advantage of using an inducible system is that APP can not be stably expressed by many cell lines at high levels because of its toxic effects.

Unfortunately, no reliable expression was achieved in human SH-SY5Y cells, neither with stable nor transient transfection methods. Transient expression in human kidney HEK 293 cells revealed that the regulator and response plasmids are indeed functional. In addition, our findings indicated poor transfection rates of the constructs in the SH-SY5Y cells. A possible reason for this low transfection rate is the relatively large size of the plasmids (e.g. ~ 8400 bp for the wt-tau/APP^{Arc} construct) causing counterselection in neuroblastoma cells.

However, an unregulated basal transcription activity was observed in the transient transfected HEK 293 cells. This is one of the disadvantages of the system, which occurs whenever the transcription units are not integrated into the chromosome or when the two plasmids are integrated in relative proximity to each other (Gossen and Bujard, 1992). The main reasons for this background activity are the absence of chromatin repression and the high copy number of the template in the cells. Several attempts of stable transfections may help to diminish this problem by embedding the templates into chromatin where the minimal CMV-promoter is actively repressed. An additional solution to efficiently repress such background activities can be the use of tetracycline controlled transcriptional silencers (tTS). These are fusions between a transcription factor (rtTA) variant and domains known to function as repressors of transcription (Freundlieb *et al.*, 1999). In the absence of an inducer, tTS binds to the Tet-response element (TRE) and represses the residual activity of the minimal promoter.

Another point to deal with is the poor transcription efficiency of the SH-SY5Y cells. Initially, this neuroblastoma cell line was chosen, because they can be differentiated into neuron-like cells by sequential treatment with RA and BDNF (Encinas *et al.*, 2000). Thus, they mimic more closely the situation in the brain than other non-neuronal cell-types, like the human kidney HEK 293 cells. The use of other transfection methods, such as calcium-phosphate transfection (Graham and van der Eb, 1973) or electroporation (Neumann *et al.*, 1982) may increase the rate of transfection.

In summary, a functional TET-system in which the expression of APP and tau can be regulated in a time- and concentration-dependant manner within the same cell would be very helpful to elucidate the relationship between Aß and tau.

5 REFERENCES

Abraha, A., Ghoshal, N., Gamblin, T.C., Cryns, V., Berry, R.W., Kuret, J., and Binder, L.I. (2000) C-terminal inhibition of tau assembly in vitro and in Alzheimer's disease. *J Cell Sci* **113**: 3737-3745.

Aja, S., Sisouvong, S., Barrett, J.A., and Gietzen, D.W. (2000) Basolateral and central amygdaloid lesions leave aversion to dietary amino acid imbalance intact. *Physiol Behav* **71**: 533-541.

Allen, B., Ingram, E., Takao, M., Smith, M.J., Jakes, R., Virdee, K., Yoshida, H., Holzer, M., Craxton, M., Emson, P.C., Atzori, C., Migheli, A., Crowther, R.A., Ghetti, B., Spillantini, M.G., and Goedert, M. (2002) Abundant tau filaments and nonapoptotic neurodegeneration in transgenic mice expressing human P301S tau protein. *J Neurosci* **22**: 9340-9351.

Alzheimer, A. (1907) About a peculiar disease of the cerebral cortex. *Allgemeine Zeitschrift für Psychiatrie und Psychisch-Gerichtliche Medizin* **64**: 146-148.

Anderton, B.H., Dayanandan, R., Killick, R., and Lovestone, S. (2000) Does dysregulation of the Notch and wingless/Wnt pathways underlie the pathogenesis of Alzheimer's disease? *Mol Med Today* **6**: 54-59.

Arendash, G.W., Lewis, J., Leighty, R.E., McGowan, E., Cracchiolo, J.R., Hutton, M., and Garcia, M.F. (2004) Multi-metric behavioral comparison of APPsw and P301L models for Alzheimer's disease: linkage of poorer cognitive performance to tau pathology in forebrain. *Brain Res* **1012**: 29-41.

Arnold, S.E., Hyman, B.T., Flory, J., Damasio, A.R., and Van Hoesen, G.W. (1991) The topographical and neuroanatomical distribution of neurofibrillary tangles and neuritic plaques in the cerebral cortex of patients with Alzheimer's disease. *Cereb Cortex* **1**: 103-116.

Arriagada, P.V., Growdon, J.H., Hedley-Whyte, E.T., and Hyman, B.T. (1992) Neurofibrillary tangles but not senile plaques parallel duration and severity of Alzheimer's disease. *Neurology* **42**: 631-639.

Ashe, K.H. (2001) Learning and memory in transgenic mice modeling Alzheimer's disease. *Learn Mem* **8**: 301-308.

Augustinack, J.C., Schneider, A., Mandelkow, E.M., and Hyman, B.T. (2002) Specific tau phosphorylation sites correlate with severity of neuronal cytopathology in Alzheimer's disease. *Acta Neuropathol (Berl)* **103**: 26-35.

Bahar, A., Samuel, A., Hazvi, S., and Dudai, Y. (2003) The amygdalar circuit that acquires taste aversion memory differs from the circuit that extinguishes it. *Eur J Neurosci* **17**: 1527-1530.

Balschun, D., Wolfer, D.P., Gass, P., Mantamadiotis, T., Welzl, H., Schutz, G., Frey, J.U., and Lipp, H.P. (2003) Does cAMP response element-binding protein have a pivotal role in hippocampal synaptic plasticity and hippocampus-dependent memory? *J Neurosci* **23**: 6304-6314.

Barghorn, S., Zheng-Fischhofer, Q., Ackmann, M., Biernat, J., von Bergen, M., Mandelkow, E.M., and Mandelkow, E. (2000) Structure, microtubule interactions, and paired helical filament aggregation by tau mutants of frontotemporal dementias. *Biochemistry* **39**: 11714-11721.

Barnham, K.J., Masters, C.L., and Bush, A.I. (2004) Neurodegenerative diseases and oxidative stress. *Nat Rev Drug Discov* **3**: 205-214.

Behl, C., Davis, J.B., Lesley, R., and Schubert, D. (1994) Hydrogen peroxide mediates amyloid beta protein toxicity. *Cell* **77**: 817-827.

Bergeron, C., Pollanen, M.S., Weyer, L., and Lang, A.E. (1997) Cortical degeneration in progressive supranuclear palsy. A comparison with cortical-basal ganglionic degeneration. *J Neuropathol Exp Neurol* **56**: 726-734.

Berry, R.W., Abraha, A., Lagalwar, S., LaPointe, N., Gamblin, T.C., Cryns, V.L., and Binder, L.I. (2003) Inhibition of tau polymerization by its carboxy-terminal caspase cleavage fragment. *Biochemistry* **42**: 8325-8331.

Best, P.J., and Orr, J., Jr. (1973) Effects of hippocampal lesions on passive avoidance and taste aversion conditioning. *Physiol Behav* **10**: 193-196.

Bierer, L.M., Hof, P.R., Purohit, D.P., Carlin, L., Schmeidler, J., Davis, K.L., and Perl, D.P. (1995) Neocortical neurofibrillary tangles correlate with dementia severity in Alzheimer's disease. *Arch Neurol* **52**: 81-88.

Biernat, J., Mandelkow, E.M., Schroter, C., Lichtenberg-Kraag, B., Steiner, B., Berling, B., Meyer, H., Mercken, M., Vandermeeren, A., Goedert, M., and et al. (1992) The switch of tau protein to an Alzheimer-like state includes the phosphorylation of two serine-proline motifs upstream of the microtubule binding region. *Embo J* **11**: 1593-1597.

Billings, L.M., Oddo, S., Green, K.N., McGaugh, J.L., and Laferla, F.M. (2005) Intraneuronal Abeta causes the onset of early Alzheimer's disease-related cognitive deficits in transgenic mice. *Neuron* **45**: 675-688.

Binder, L.I., Guillozet-Bongaarts, A.L., Garcia-Sierra, F., and Berry, R.W. (2005) Tau, tangles, and Alzheimer's disease. *Biochim Biophys Acta* **1739**: 216-223.

Bird, T.D., Nochlin, D., Poorkaj, P., Cherrier, M., Kaye, J., Payami, H., Peskind, E., Lampe, T.H., Nemens, E., Boyer, P.J., and Schellenberg, G.D. (1999) A clinical pathological comparison of three families with frontotemporal dementia and identical mutations in the tau gene (P301L) [published erratum appears in Brain 1999 Jul;122(Pt 7):1398]. *Brain* **122**: 741-756.

Blum, H., Beier, H., and Gross, H.J. (1987) Improved silver staining of plant proteins , RNA and DNA in polyacrylamide gels. *Electrophoresis* **8**: 93-99.

Braak, H., and Braak, E. (1991) Neuropathological stageing of Alzheimer-related changes. *Acta Neuropathol (Berl)* **82**: 239-259.

Braak, H., and Braak, E. (1995) Staging of Alzheimer's disease-related neurofibrillary changes. *Neurobiol Aging* **16**: 271-278; discussion 278-284.

Brion, J.P., Tremp, G., and Octave, J.N. (1999) Transgenic expression of the shortest human tau affects its compartmentalization and its phosphorylation as in the pretangle stage of Alzheimer's disease [see comments]. *Am J Pathol* **154**: 255-270.

Broggio, E., Pluchon, C., Ingrand, P., and Gil, R. (2001) [Taste impairment in Alzheimer's disease]. *Rev Neurol (Paris)* **157**: 409-413.

Buee, L., Bussiere, T., Buee-Scherrer, V., Delacourte, A., and Hof, P.R. (2000) Tau protein isoforms, phosphorylation and role in neurodegenerative disorders. *Brain Res Brain Res Rev* **33**: 95-130.

Bugiani, O., Murrell, J.R., Giaccone, G., Hasegawa, M., Ghigo, G., Tabaton, M., Morbin, M., Primavera, A., Carella, F., Solaro, C., Grisoli, M., Savoiardo, M., Spillantini, M.G., Tagliavini, F., Goedert, M., and Ghetti, B. (1999) Frontotemporal dementia and corticobasal degeneration in a family with a P301S mutation in tau. *J Neuropathol Exp Neurol* **58**: 667-677.

Bures, J., Bermudez-Rattoni, F., and Yamamoto, T. (1998) Conditioned taste aversion - memory of a special kind. *Oxford University Press, Inc., New York*.

Cano, E., and Mahadevan, L.C. (1995) Parallel signal processing among mammalian MAPKs. *Trends Biochem Sci* **20**: 117-122.

Cao, X., and Sudhof, T.C. (2001) A transcriptionally [correction of transcriptively] active complex of APP with Fe65 and histone acetyltransferase Tip60. *Science* **293**: 115-120.

Carmel, G., Mager, E.M., Binder, L.I., and Kuret, J. (1996) The structural basis of monoclonal antibody Alz50's selectivity for Alzheimer's disease pathology. *J Biol Chem* **271**: 32789-32795.

Check, E. (2002) Nerve inflammation halts trial for Alzheimer's drug. *Nature* **415**: 462.

Chen, F., David, D., Ferrari, A., and Gotz, J. (2004a) Posttranslational modifications of tau - Role in human tauopathies and modeling in transgenic animals. *Curr Alz Res* **5**: 503-515.

Chen, G., Chen, K.S., Knox, J., Inglis, J., Bernard, A., Martin, S.J., Justice, A., McConlogue, L., Games, D., Freedman, S.B., and Morris, R.G. (2000) A learning deficit related to age and beta-amyloid plaques in a mouse model of Alzheimer's disease. *Nature* **408**: 975-979.

Chen, Y., Wollmer, M.A., Hoerndli, F., Münch, G., Kuhla, B., Rogaev, E.I., Tsolaki, M., Papassotiropoulos, A., and Gotz, J. (2004b) Role for glyoxalase I in Alzheimer's disease. *Proc Natl Acad Sci U S A* **101**: 7687-7692.

Cherny, R.A., Atwood, C.S., Xilinas, M.E., Gray, D.N., Jones, W.D., McLean, C.A., Barnham, K.J., Volitakis, I., Fraser, F.W., Kim, Y., Huang, X., Goldstein, L.E., Moir, R.D., Lim, J.T., Beyreuther, K., Zheng, H., Tanzi, R.E., Masters, C.L., and Bush, A.I. (2001) Treatment with a copper-zinc chelator markedly and rapidly inhibits beta-amyloid accumulation in Alzheimer's disease transgenic mice. *Neuron* **30**: 665-676.

Chin, S.S., and Goldman, J.E. (1996) Glial inclusions in CNS degenerative diseases. *J Neuropathol Exp Neurol* **55**: 499-508.

Corcoran, K.A., Lu, Y., Turner, R.S., and Maren, S. (2002) Overexpression of hAPPswe impairs rewarded alternation and contextual fear conditioning in a transgenic mouse model of Alzheimer's disease. *Learn Mem* **9**: 243-252.

Coso, O.A., Chiariello, M., Yu, J.C., Teramoto, H., Crespo, P., Xu, N., Miki, T., and Gutkind, J.S. (1995) The small GTP-binding proteins Rac1 and Cdc42 regulate the activity of the JNK/SAPK signaling pathway. *Cell* **81**: 1137-1146.

Crowther, R.A., and Wischik, C.M. (1985) Image reconstruction of the Alzheimer paired helical filament. *Embo J* **4**: 3661-3665.

Crystal, H., Dickson, D., Fuld, P., Masur, D., Scott, R., Mehler, M., Masdeu, J., Kawas, C., Aronson, M., and Wolfson, L. (1988) Clinico-pathologic studies in dementia: nondemented subjects with pathologically confirmed Alzheimer's disease. *Neurology* **38**: 1682-1687.

Cummings, J.L. (2004) Alzheimer's disease. *N Engl J Med* **351**: 56-67.

David, D.C., Hauptmann, S., Scherping, I., Schuessel, K., Keil, U., Rizzu, P., Ravid, R., Drose, S., Brandt, U., Muller, W.E., Eckert, A., and Gotz, J. (2005) Proteomic and functional analysis reveal a mitochondrial dysfunction in P301L tau transgenic mice. *J Biol Chem* **in press**.

De, F., Gv, and Inestrosa, N.C. (2000) Wnt signaling function in Alzheimer's disease [In Process Citation]. *Brain Res Brain Res Rev* **33**: 1-12.

Delacourte, A., Sergeant, N., Wattez, A., Gauvreau, D., and Robitaille, Y. (1998) Vulnerable neuronal subsets in Alzheimer's and Pick's disease are distinguished by their tau isoform distribution and phosphorylation. *Ann Neurol* **43**: 193-204.

Delacourte, A., David, J.P., Sergeant, N., Buee, L., Wattez, A., Vermersch, P., Ghozali, F., Fallet-Bianco, C., Pasquier, F., Lebert, F., Petit, H., and Di Menza, C. (1999) The biochemical pathway of neurofibrillary degeneration in aging and Alzheimer's disease [see comments]. *Neurology* **52**: 1158-1165.

Delacourte, A., Sergeant, N., Champain, D., Wattez, A., Maurage, C.A., Lebert, F., Pasquier, F., and David, J.P. (2002) Nonoverlapping but synergetic tau and APP pathologies in sporadic Alzheimer's disease. *Neurology* **59**: 398-407.

Delobel, P., Flament, S., Hamdane, M., Mailliot, C., Sambo, A.V., Begard, S., Sergeant, N., Delacourte, A., Vilain, J.P., and Buee, L. (2002) Abnormal Tau phosphorylation of the Alzheimer-type also occurs during mitosis. *J Neurochem* **83**: 412-420.

D'Souza, I., Poorkaj, P., Hong, M., Nochlin, D., Lee, V.M., Bird, T.D., and Schellenberg, G.D. (1999) Missense and silent tau gene mutations cause frontotemporal dementia with parkinsonism-chromosome 17 type, by affecting multiple alternative RNA splicing regulatory elements. *Proc Natl Acad Sci U S A* **96**: 5598-5603.

Dunn, L.T., and Everitt, B.J. (1988) Double dissociations of the effects of amygdala and insular cortex lesions on conditioned taste aversion, passive avoidance, and neophobia in the rat using the excitotoxin ibotenic acid. *Behav Neurosci* **102**: 3-23.

Ebneth, A., Godemann, R., Stamer, K., Illenberger, S., Trinczek, B., and Mandelkow, E. (1998) Overexpression of tau protein inhibits kinesin-dependent trafficking of vesicles, mitochondria, and endoplasmic reticulum: implications for Alzheimer's disease. *J Cell Biol* **143**: 777-794.

Edbauer, D., Winkler, E., Regula, J.T., Pesold, B., Steiner, H., and Haass, C. (2003) Reconstitution of gamma-secretase activity. *Nat Cell Biol* **5**: 486-488.

Encinas, M., Iglesias, M., Liu, Y., Wang, H., Muhaisen, A., Cena, V., Gallego, C., and Comella, J.X. (2000) Sequential treatment of SH-SY5Y cells with retinoic acid and brain-derived neurotrophic factor gives rise to fully differentiated, neurotrophic factor-dependent, human neuron-like cells. *J Neurochem* **75**: 991-1003.

Esch, F.S., Keim, P.S., Beattie, E.C., Blacher, R.W., Culwell, A.R., Oltersdorf, T., McClure, D., and Ward, P.J. (1990) Cleavage of amyloid beta peptide during constitutive processing of its precursor. *Science* **248**: 1122-1124.

Escobar, M.L., and Bermudez-Rattoni, F. (2000) Long-term potentiation in the insular cortex enhances conditioned taste aversion retention. *Brain Res* **852**: 208-212.

Fasulo, L., Ugolini, G., Visintin, M., Bradbury, A., Brancolini, C., Verzillo, V., Novak, M., and Cattaneo, A. (2000) The neuronal microtubule-associated protein tau is a substrate for caspase-3 and an effector of apoptosis. *J Neurochem* **75**: 624-633.

Ferrari, A., Hoerndli, F., Baechi, T., Nitsch, R.M., and Gotz, J. (2003) Beta-amyloid induces PHF-like tau filaments in tissue culture. *J Biol Chem* **278**: 40162-40168.

Ferrer, I., Boada Rovira, M., Sanchez Guerra, M.L., Rey, M.J., and Costa-Jussa, F. (2004) Neuropathology and pathogenesis of encephalitis following amyloid-beta immunization in Alzheimer's disease. *Brain Pathol* **14**: 11-20.

Flanagan, L.A., Cunningham, C.C., Chen, J., Prestwich, G.D., Kosik, K.S., and Janmey, P.A. (1997) The structure of divalent cation-induced aggregates of PIP2 and their alteration by gelsolin and tau. *Biophys J* **73**: 1440-1447.

Forman, M.S., Lal, D., Zhang, B., Dabir, D.V., Swanson, E., Lee, V.M., and Trojanowski, J.Q. (2005) Transgenic mouse model of tau pathology in astrocytes leading to nervous system degeneration. *J Neurosci* **25**: 3539-3550.

Freundlieb, S., Schirra-Muller, C., and Bujard, H. (1999) A tetracycline controlled activation/repression system with increased potential for gene transfer into mammalian cells. *J Gene Med* **1**: 4-12.

Fukumoto, Y., Kaibuchi, K., Hori, Y., Fujioka, H., Araki, S., Ueda, T., Kikuchi, A., and Takai, Y. (1990) Molecular cloning and characterization of a novel type of regulatory protein (GDI) for the rho proteins, ras p21-like small GTP-binding proteins. *Oncogene* **5**: 1321-1328.

Gamblin, T.C., Chen, F., Zambrano, A., Abraha, A., Lagalwar, S., Guillozet, A.L., Lu, M., Fu, Y., Garcia-Sierra, F., LaPointe, N., Miller, R., Berry, R.W., Binder, L.I., and Cryns, V.L. (2003) Caspase cleavage of tau: linking amyloid and neurofibrillary tangles in Alzheimer's disease. *Proc Natl Acad Sci U S A* **100**: 10032-10037.

Geschwind, D.H., Robidoux, J., Alarcon, M., Miller, B.L., Wilhelmsen, K.C., Cummings, J.L., and Nasreddine, Z.S. (2001) Dementia and neurodevelopmental predisposition: cognitive dysfunction in presymptomatic subjects precedes dementia by decades in frontotemporal dementia. *Ann Neurol* **50**: 741-746.

Giannakopoulos, P., Herrmann, F.R., Bussiere, T., Bouras, C., Kovari, E., Perl, D.P., Morrison, J.H., Gold, G., and Hof, P.R. (2003) Tangle and neuron numbers, but not amyloid load, predict cognitive status in Alzheimer's disease. *Neurology* **60**: 1495-1500.

Glenner, G.G., and Wong, C.W. (1984) Alzheimer's disease: initial report of the purification and characterization of a novel cerebrovascular amyloid protein. *Biochem Biophys Res Commun* **120**: 885-890.

Goate, A., Chartier-Harlin, M.C., Mullan, M., Brown, J., Crawford, F., Fidani, L., Giuffra, L., Haynes, A., Irving, N., James, L., and et al. (1991) Segregation of a missense mutation in the amyloid precursor protein gene with familial Alzheimer's disease. *Nature* **349**: 704-706.

Goedert, M., Wischik, C.M., Crowther, R.A., Walker, J.E., and Klug, A. (1988) Cloning and sequencing of the cDNA encoding a core protein of the paired helical filament of Alzheimer disease: identification as the microtubule-associated protein tau. *Proc Natl Acad Sci U S A* **85**: 4051-4055.

Goedert, M., Spillantini, M.G., Jakes, R., Rutherford, D., and Crowther, R.A. (1989) Multiple isoforms of human microtubule-associated protein tau: sequences and localization in neurofibrillary tangles of Alzheimer's disease. *Neuron* **3**: 519-526.

Goedert, M., and Jakes, R. (1990) Expression of separate isoforms of human tau protein: correlation with the tau pattern in brain and effects on tubulin polymerization. *Embo J* **9**: 4225-4230.

Goedert, M., Spillantini, M.G., Cairns, N.J., and Crowther, R.A. (1992) Tau proteins of Alzheimer paired helical filaments: abnormal phosphorylation of all six brain isoforms. *Neuron* **8**: 159-168.

Goedert, M., Spillantini, M.G., Jakes, R., Crowther, R.A., Vanmechelen, E., Probst, A., Gotz, J., Burki, K., and Cohen, P. (1995) Molecular dissection of the paired helical filament. *Neurobiol Aging* **16**: 325-334.

Goedert, M., Hasegawa, M., Jakes, R., Lawler, S., Cuenda, A., and Cohen, P. (1997) Phosphorylation of microtubule-associated protein tau by stress-activated protein kinases. *FEBS Lett* **409**: 57-62.

Goedert, M., Jakes, R., and Crowther, R.A. (1999a) Effects of frontotemporal dementia FTDP-17 mutations on heparin-induced assembly of tau filaments. *FEBS Lett* **450**: 306-311.

Goedert, M., Spillantini, M.G., Crowther, R.A., Chen, S.G., Parchi, P., Tabaton, M., Lanska, D.J., Markesbery, W.R., Wilhelmsen, K.C., Dickson, D.W., Petersen, R.B., and Gambetti, P. (1999b) Tau gene mutation in familial progressive subcortical gliosis. *Nat Med* **5**: 454-457.

Goosens, K.A., and Maren, S. (2001) Contextual and auditory fear conditioning are mediated by the lateral, basal, and central amygdaloid nuclei in rats. *Learn Mem* **8**: 148-155.

Gossen, M., and Bujard, H. (1992) Tight control of gene expression in mammalian cells by tetracycline-responsive promoters. *Proc Natl Acad Sci U S A* **89**: 5547-5551.

Gossen, M., Freundlieb, S., Bender, G., Muller, G., Hillen, W., and Bujard, H. (1995) Transcriptional activation by tetracyclines in mammalian cells. *Science* **268**: 1766-1769.

Gotz, J., Probst, A., Spillantini, M.G., Schafer, T., Jakes, R., Burki, K., and Goedert, M. (1995) Somatodendritic localization and hyperphosphorylation of tau protein in transgenic mice expressing the longest human brain tau isoform. *Embo J* **14**: 1304-1313.

Gotz, J. (2001) Tau and transgenic animal models. *Brain Res Brain Res Rev* **35**: 266-286.

Gotz, J., Chen, F., Barmettler, R., and Nitsch, R.M. (2001a) Tau Filament Formation in Transgenic Mice Expressing P301L Tau. *J Biol Chem* **276**: 529-534.

Gotz, J., Chen, F., van Dorpe, J., and Nitsch, R.M. (2001b) Formation of neurofibrillary tangles in P301L tau transgenic mice induced by Abeta 42 fibrils. *Science* **293**: 1491-1495.

Gotz, J., and Nitsch, R.M. (2001) Compartmentalized tau hyperphosphorylation and increased levels of kinases in transgenic mice. *Neuroreport* **12**: 2007-2016.

Gotz, J., Tolnay, M., Barmettler, R., Chen, F., Probst, A., and Nitsch, R.M. (2001c) Oligodendroglial tau filament formation in transgenic mice expressing G272V tau. *Eur J Neurosci* **13**: 2131-2140.

Gotz, J., Schild, A., Hoerndli, F., and Pennanen, L. (2004a) Amyloid-induced neurofibrillary tangle formation in Alzheimer's disease: insight from transgenic mouse and tissue-culture models. *Int J Dev Neurosci* **22**: 453-465.

Gotz, J., Streffer, J.R., David, D., Schild, A., Hoerndli, F., Pennanen, L., Kurosinski, P., and Chen, F. (2004b) Transgenic animal models of Alzheimer's disease and related disorders: Histopathology, behavior and therapy. *Mol Psychiatry* **9**: 664-683.

Graham, F.L., and van der Eb, A.J. (1973) A new technique for the assay of infectivity of human adenovirus 5 DNA. *Virology* **52**: 456-467.

Grover, A., Houlden, H., Baker, M., Adamson, J., Lewis, J., Prihar, G., Pickering-Brown, S., Duff, K., and Hutton, M. (1999) 5' splice site mutations in tau associated with the inherited dementia FTDP-17 affect a stem-loop structure that regulates alternative splicing of exon 10. *J Biol Chem* **274**: 15134-15143.

Guillozet-Bongaarts, A.L., Garcia-Sierra, F., Reynolds, M.R., Horowitz, P.M., Fu, Y., Wang, T., Cahill, M.E., Bigio, E.H., Berry, R.W., and Binder, L.I. (2005) Tau truncation during neurofibrillary tangle evolution in Alzheimer's disease. *Neurobiol Aging* **26**: 1015-1022.

Hall, G.F., Lee, V.M., Lee, G., and Yao, J. (2001) Staging of neurofibrillary degeneration caused by human tau overexpression in a unique cellular model of human tauopathy. *Am J Pathol* **158**: 235-246.

Hall, G.F., Lee, S., and Yao, J. (2002) Neurofibrillary degeneration can be arrested in an in vivo cellular model of human tauopathy by application of a compound which inhibits tau filament formation in vitro. *J Mol Neurosci* **19**: 253-260.

Hamann, S., Monarch, E.S., and Goldstein, F.C. (2002) Impaired fear conditioning in Alzheimer's disease. *Neuropsychologia* **40**: 1187-1195.

Hanger, D.P., Brion, J.P., Gallo, J.M., Cairns, N.J., Luthert, P.J., and Anderton, B.H. (1991) Tau in Alzheimer's disease and Down's syndrome is insoluble and abnormally phosphorylated. *Biochem J* **275 (Pt 1)**: 99-104.

Hardy, J.A., and Higgins, G.A. (1992) Alzheimer's disease: the amyloid cascade hypothesis. *Science* **256**: 184-185.

Hartley, D.M., Walsh, D.M., Ye, C.P., Diehl, T., Vasquez, S., Vassilev, P.M., Teplow, D.B., and Selkoe, D.J. (1999) Protofibrillar intermediates of amyloid beta-protein induce acute electrophysiological changes and progressive neurotoxicity in cortical neurons. *J Neurosci* **19**: 8876-8884.

Hasegawa, M., Smith, M.J., and Goedert, M. (1998) Tau proteins with FTDP-17 mutations have a reduced ability to promote microtubule assembly. *FEBS Lett* **437**: 207-210.

Hausheer-Zarmakupi, Z., Wolfer, D.P., Leisinger-Trigona, M.C., and Lipp, H.P. (1996) Selective breeding for extremes in open-field activity of mice entails a differentiation of hippocampal mossy fibers. *Behav Genet* **26**: 167-176.

Hebert, L.E., Scherr, P.A., Bienias, J.L., Bennett, D.A., and Evans, D.A. (2003) Alzheimer disease in the US population: prevalence estimates using the 2000 census. *Arch Neurol* **60**: 1119-1122.

Higuchi, M., Ishihara, T., Zhang, B., Hong, M., Andreadis, A., Trojanowski, J., and Lee, V.M. (2002) Transgenic mouse model of tauopathies with glial pathology and nervous system degeneration. *Neuron* **35**: 433-446.

Hock, C., Konietzko, U., Papassotiropoulos, A., Wollmer, A., Streffer, J., von Rotz, R.C., Davey, G., Moritz, E., and Nitsch, R.M. (2002) Generation of antibodies specific for beta-amyloid by vaccination of patients with Alzheimer disease. *Nat Med* **8**: 1270-1275.

Hock, C., Konietzko, U., Streffer, J.R., Tracy, J., Signorell, A., Muller-Tillmanns, B., Lemke, U., Henke, K., Moritz, E., Garcia, E., Wollmer, M.A., Umbricht, D., de Quervain, D.J., Hofmann, M., Maddalena, A., Papassotiropoulos, A., and Nitsch, R.M. (2003) Antibodies against beta-Amyloid Slow Cognitive Decline in Alzheimer's Disease. *Neuron* **38**: 547-554.

Hoerndli, F.J., Toigo, M., Schild, A., Gotz, J., and Day, P.J. (2004) Reference genes identified in SH-SY5Y cells using custom-made gene arrays with validation by quantitative polymerase chain reaction. *Anal Biochem* **335**: 30-41.

Hof, P.R., Bouras, C., Perl, D.P., and Morrison, J.H. (1994) Quantitative neuropathologic analysis of Pick's disease cases: cortical distribution of Pick bodies and coexistence with Alzheimer's disease. *Acta Neuropathol* **87**: 115-124.

Hutton, M., Lendon, C.L., Rizzu, P., Baker, M., Froelich, S., Houlden, H., Pickering-Brown, S., Chakraverty, S., Isaacs, A., Grover, A., Hackett, J., Adamson, J., Lincoln, S., Dickson, D., Davies, P., Petersen, R.C., Stevens, M., de Graaff, E., Wauters, E., van Baren, J., Hillebrand, M., Joosse, M., Kwon, J.M., Nowotny, P., Heutink, P., and et al. (1998) Association of missense and 5'-splice-site mutations in tau with the inherited dementia FTDP-17. *Nature* **393**: 702-705.

Ishihara, T., Hong, M., Zhang, B., Nakagawa, Y., Lee, M.K., Trojanowski, J.Q., and Lee, V.M. (1999) Age-dependent emergence and progression of a tauopathy in transgenic mice overexpressing the shortest human tau isoform. *Neuron* **24**: 751-762.

Ishihara, T., Zhang, B., Higuchi, M., Yoshiyama, Y., Trojanowski, J.Q., and Lee, V.M. (2001) Age-Dependent Induction of Congophilic Neurofibrillary Tau Inclusions in Tau Transgenic Mice. *Am J Pathol* **158**: 555-562.

Jackson, G.R., Wiedau-Pazos, M., Sang, T.-K., Wagle, N., Brown, C.A., Massachi, S., and Geschwind, D.H. (2002) Human wild-type tau interacts with wingless pathway components and produces neurofibrillary pathology in Drosophila. *Neuron* **34**: 509-519.

Janus, C., Welzl, H., Hanna, A., Lovasic, L., Lane, N., St George-Hyslop, P., and Westaway, D. (2004) Impaired conditioned taste aversion learning in APP transgenic mice. *Neurobiol Aging* **25**: 1213-1219.

Jenkins, S.M., and Johnson, G.V. (1998) Tau complexes with phospholipase C-gamma in situ. *Neuroreport* **9**: 67-71.

Jicha, G.A., Lane, E., Vincent, I., Otvos, L., Jr., Hoffmann, R., and Davies, P. (1997) A conformation- and phosphorylation-dependent antibody recognizing the paired helical filaments of Alzheimer's disease. *J Neurochem* **69**: 2087-2095.

Johnson, D.I., and Pringle, J.R. (1990) Molecular characterization of CDC42, a Saccharomyces cerevisiae gene involved in the development of cell polarity. *J Cell Biol* **111**: 143-152.

Kelley, A.E., Cador, M., and Stinus, L. (1989) Exploration and its measurement - A psychopharmacological perspective. *Neuromethods; Volume 13 (Psychopharmacology) Boulton, A. A., Baker, G. B. & Greenshaw, A. J. (Eds.), The Humana Press, Inc. Clifton, NJ* **13**.

Kerr, M.L., and Small, D.H. (2005) Cytoplasmic domain of the beta-amyloid protein precursor of Alzheimer's disease: Function, regulation of proteolysis, and implications for drug development. *J Neurosci Res* **80**: 151-159.

Kimble, D.P., Bremiller, R., Schroeder, L., and Smotherman, W.P. (1979) Hippocampal lesions slow extinction of a conditioned taste aversion in rats. *Physiol Behav* **23**: 217-222.

Kimura, T., Ono, T., Takamatsu, J., Yamamoto, H., Ikegami, K., Kondo, A., Hasegawa, M., Ihara, Y., Miyamoto, E., and Miyakawa, T. (1996) Sequential changes of tau-site-specific phosphorylation during development of paired helical filaments. *Dementia* **7**: 177-181.

Kishi, T., and Elmquist, J.K. (2005) Body weight is regulated by the brain: a link between feeding and emotion. *Mol Psychiatry* **10**: 132-146.

Kins, S., Kurosinski, P., Nitsch, R.M., and Gotz, J. (2003) Activation of the ERK and JNK signaling pathways caused by neuron specific inhibition of PP2A in transgenic mice. *Am J Pathol* **163**: 833-843.

Kobayashi, K., Nakano, H., Hayashi, M., Shimazaki, M., Fukutani, Y., Sasaki, K., Sugimori, K., and Koshino, Y. (2003) Association of phosphorylation site of tau protein with neuronal apoptosis in Alzheimer's disease. *J Neurol Sci* **208**: 17-24.

Komori, T. (1999) Tau-positive glial inclusions in progressive supranuclear palsy, corticobasal degeneration and Pick's disease. *Brain Pathol* **9**: 663-679.

Kraemer, B.C., Zhang, B., Leverenz, J.B., Thomas, J.H., Trojanowski, J.Q., and Schellenberg, G.D. (2003) Neurodegeneration and defective neurotransmission in a Caenorhabditis elegans model of tauopathy. *Proc Natl Acad Sci U S A* **100**: 9980-9985.

Kramer, J.H., Jurik, J., Sha, S.J., Rankin, K.P., Rosen, H.J., Johnson, J.K., and Miller, B.L. (2003) Distinctive neuropsychological patterns in frontotemporal dementia, semantic dementia, and Alzheimer disease. *Cogn Behav Neurol* **16**: 211-218.

Ksiezak-Reding, H., Binder, L.I., and Yen, S.H. (1990) Alzheimer disease proteins (A68) share epitopes with tau but show distinct biochemical properties. *J Neurosci Res* **25**: 420-430.

Laghmouch, A., Bertholet, J.Y., and Crusio, W.E. (1997) Hippocampal morphology and open-field behavior in Mus musculus domesticus and Mus spretus inbred mice. *Behav Genet* **27**: 67-73.

Lahiri, D.K., Farlow, M.R., Sambamurti, K., Greig, N.H., Giacobini, E., and Schneider, L.S. (2003) A critical analysis of new molecular targets and strategies for drug developments in Alzheimer's disease. *Curr Drug Targets* **4**: 97-112.

Lamprecht, R., Hazvi, S., and Dudai, Y. (1997) cAMP response element-binding protein in the amygdala is required for long- but not short-term conditioned taste aversion memory. *J Neurosci* **17**: 8443-8450.

LeDoux, J.E. (2000) Emotion circuits in the brain. *Annu Rev Neurosci* **23**: 155-184.

Lee, G., and Rook, S.L. (1992) Expression of tau protein in non-neuronal cells: microtubule binding and stabilization. *J Cell Sci* **102**: 227-237.

Lee, V.M., Goedert, M., and Trojanowski, J.Q. (2001) Neurodegenerative tauopathies. *Annu Rev Neurosci* **24**: 1121-1159.

Lee, V.M., Kenyon, T.K., and Trojanowski, J.Q. (2005) Transgenic animal models of tauopathies. *Biochim Biophys Acta* **1739**: 251-259.

Lewandoski, M. (2001) Conditional control of gene expression in the mouse. *Nat Rev Genet* **2**: 743-755.

Lewis, J., McGowan, E., Rockwood, J., Melrose, H., Nacharaju, P., Van Slegtenhorst, M., Gwinn-Hardy, K., Murphy, P.M., Baker, M., Yu, X., Duff, K., Hardy, J., Corral, A., Lin, W.L., Yen, S.H., Dickson, D.W., Davies, P., and Hutton, M. (2000) Neurofibrillary tangles, amyotrophy and progressive motor disturbance in mice expressing mutant (P301L) tau protein. *Nat Genet* **25**: 402-405.

Lewis, J., Dickson, D.W., Lin, W.-L., Chisholm, L., Corral, A., Jones, G., Yen, S.-H., Sahara, N., Skipper, L., Yager, D., Eckman, C., Hardy, J., Hutton, M., and McGowan, E. (2001) Enhanced neurofibrillary degeneration in transgenic mice expressing mutant Tau and APP. *Science* **293**: 1487-1491.

Lichtenberg, B., Mandelkow, E.M., Hagestedt, T., and Mandelkow, E. (1988) Structure and elasticity of microtubule-associated protein tau. *Nature* **334**: 359-362.

Liou, Y.C., Sun, A., Ryo, A., Zhou, X.Z., Yu, Z.X., Huang, H.K., Uchida, T., Bronson, R., Bing, G., Li, X., Hunter, T., and Lu, K.P. (2003) Role of the prolyl isomerase Pin1 in protecting against age-dependent neurodegeneration. *Nature* **424**: 556-561.

Loo, D.T., Copani, A., Pike, C.J., Whittemore, E.R., Walencewicz, A.J., and Cotman, C.W. (1993) Apoptosis is induced by beta-amyloid in cultured central nervous system neurons. *Proc Natl Acad Sci U S A* **90**: 7951-7955.

Lu, P.J., Wulf, G., Zhou, X.Z., Davies, P., and Lu, K.P. (1999) The prolyl isomerase Pin1 restores the function of Alzheimer-associated phosphorylated tau protein. *Nature* **399**: 784-788.

Maas, T., Eidenmuller, J., and Brandt, R. (2000) Interaction of tau with the neural membrane cortex is regulated by phosphorylation at sites that are modified in paired helical filaments. *J Biol Chem* **275**: 15733-15740.

Mandelkow, E.M., Schweers, O., Drewes, G., Biernat, J., Gustke, N., Trinczek, B., and Mandelkow, E. (1996) Structure, microtubule interactions, and phosphorylation of tau protein. *Ann N Y Acad Sci* **777**: 96-106.

Masliah, E., Hansen, L., Adame, A., Crews, L., Bard, F., Lee, C., Seubert, P., Games, D., Kirby, L., and Schenk, D. (2005) Abeta vaccination effects on plaque pathology in the absence of encephalitis in Alzheimer disease. *Neurology* **64**: 129-131.

Masters, C.L., Simms, G., Weinman, N.A., Multhaup, G., McDonald, B.L., and Beyreuther, K. (1985) Amyloid plaque core protein in Alzheimer disease and Down syndrome. *Proc Natl Acad Sci U S A* **82**: 4245-4249.

Mattson, M.P., Cheng, B., Davis, D., Bryant, K., Lieberburg, I., and Rydel, R.E. (1992) beta-Amyloid peptides destabilize calcium homeostasis and render human cortical neurons vulnerable to excitotoxicity. *J Neurosci* **12**: 376-389.

McDaniel, W.F., Compton, D.M., and Smith, S.R. (1994) Spatial learning following posterior parietal or hippocampal lesions. *Neuroreport* **5**: 1713-1717.

McGaugh, J.L., McIntyre, C.K., and Power, A.E. (2002) Amygdala modulation of memory consolidation: interaction with other brain systems. *Neurobiol Learn Mem* **78**: 539-552.

Mercken, M., Vandermeeren, M., Lubke, U., Six, J., Boons, J., Van de Voorde, A., Martin, J.J., and Gheuens, J. (1992) Monoclonal antibodies with selective specificity for Alzheimer Tau are directed against phosphatase-sensitive epitopes. *Acta Neuropathol (Berl)* **84**: 265-272.

Minden, A., Lin, A., Claret, F.X., Abo, A., and Karin, M. (1995) Selective activation of the JNK signaling cascade and c-Jun transcriptional activity by the small GTPases Rac and Cdc42Hs. *Cell* **81**: 1147-1157.

Mirra, S.S., Murrell, J.R., Gearing, M., Spillantini, M.G., Goedert, M., Crowther, R.A., Levey, A.I., Jones, R., Green, J., Shoffner, J.M., Wainer, B.H., Schmidt, M.L., Trojanowski, J.Q., and Ghetti, B. (1999) Tau pathology in a family with dementia and a P301L mutation in tau. *J Neuropathol Exp Neurol* **58**: 335-345.

Morgan, D., Diamond, D.M., Gottschall, P.E., Ugen, K.E., Dickey, C., Hardy, J., Duff, K., Jantzen, P., DiCarlo, G., Wilcock, D., Connor, K., Hatcher, J., Hope, C., Gordon, M., and Arendash, G.W. (2000) A beta peptide vaccination prevents memory loss in an animal model of Alzheimer's disease. *Nature* **408**: 982-985.

Morishima-Kawashima, M., and Kosik, K.S. (1996) The pool of map kinase associated with microtubules is small but constitutively active. *Mol Biol Cell* **7**: 893-905.

Morris, R.G., Garrud, P., Rawlins, J.N., and O'Keefe, J. (1982) Place navigation impaired in rats with hippocampal lesions. *Nature* **297**: 681-683.

Mullan, M., Crawford, F., Axelman, K., Houlden, H., Lilius, L., Winblad, B., and Lannfelt, L. (1992) A pathogenic mutation for probable Alzheimer's disease in the APP gene at the N-terminus of beta-amyloid. *Nat Genet* **1**: 345-347.

Mullis, K.B. (1990) Target amplification for DNA analysis by the polymerase chain reaction. *Ann Biol Clin (Paris)* **48**: 579-582.

Nacharaju, P., Lewis, J., Easson, C., Yen, S., Hackett, J., Hutton, M., and Yen, S.H. (1999) Accelerated filament formation from tau protein with specific FTDP-17 missense mutations. *FEBS Lett* **447**: 195-199.

Nagy, Z., Jobst, K.A., Esiri, M.M., Morris, J.H., King, E.M., MacDonald, B., Litchfield, S., Barnetson, L., and Smith, A.D. (1996) Hippocampal pathology reflects memory deficit and brain imaging measurements in Alzheimer's disease: clinicopathologic correlations using three sets of pathologic diagnostic criteria. *Dementia* **7**: 76-81.

Nakagawa, T., Zhu, H., Morishima, N., Li, E., Xu, J., Yankner, B.A., and Yuan, J. (2000) Caspase-12 mediates endoplasmic-reticulum-specific apoptosis and cytotoxicity by amyloid-beta. *Nature* **403**: 98-103.

Neary, D., Snowden, J.S., Gustafson, L., Passant, U., Stuss, D., Black, S., Freedman, M., Kertesz, A., Robert, P.H., Albert, M., Boone, K., Miller, B.L., Cummings, J., and Benson, D.F. (1998) Frontotemporal lobar degeneration: a consensus on clinical diagnostic criteria [see comments]. *Neurology* **51**: 1546-1554.

Neumann, E., Schaefer-Ridder, M., Wang, Y., and Hofschneider, P.H. (1982) Gene transfer into mouse lyoma cells by electroporation in high electric fields. *Embo J* **1**: 841-845.

Nicoll, J.A., Wilkinson, D., Holmes, C., Steart, P., Markham, H., and Weller, R.O. (2003) Neuropathology of human Alzheimer disease after immunization with amyloid-beta peptide: a case report. *Nat Med* **9**: 448-452.

Nilsberth, C., Westlind-Danielsson, A., Eckman, C.B., Condron, M.M., Axelman, K., Forsell, C., Stenh, C., Luthman, J., Teplow, D.B., Younkin, S.G., Naslund, J., and Lannfelt, L. (2001) The 'Arctic' APP mutation (E693G) causes Alzheimer's disease by enhanced Abeta protofibril formation. *Nat Neurosci* **4**: 887-893.

Oddo, S., Caccamo, A., Shepherd, J.D., Murphy, M.P., Golde, T.E., Kayed, R., Metherate, R., Mattson, M.P., Akbari, Y., and LaFerla, F.M. (2003) Triple-transgenic model of Alzheimer's disease with plaques and tangles. Intracellular abeta and synaptic dysfunction. *Neuron* **39**: 409-421.

Paxinos, K.B.J.F.a.G. (1997) *The mouse brain in stereotaxic coordinates.* San Diego: Academic Press Inc.

Pennanen, L., Welzl, H., D'Adamo, P., Nitsch, R.M., and Gotz, J. (2004) Accelerated extinction of conditioned taste aversion in P301L tau transgenic mice. *Neurobiol Dis* **15**: 500-509.

Pennanen, L., Wolfer, D., Nitsch, R.M., and Gotz, J. (2005) Impaired spatial reference memory in P301L tau transgenic mice. *Genes Brain Behav* **in revision**.

Petrovich, G.D., Canteras, N.S., and Swanson, L.W. (2001) Combinatorial amygdalar inputs to hippocampal domains and hypothalamic behavior systems. *Brain Res Brain Res Rev* **38**: 247-289.

Poorkaj, P., Bird, T.D., Wijsman, E., Nemens, E., Garruto, R.M., Anderson, L., Andreadis, A., Wiederholt, W.C., Raskind, M., and Schellenberg, G.D. (1998) Tau is a candidate gene for chromosome 17 frontotemporal dementia. *Ann Neurol* **43**: 815-825.

Probst, A., Gotz, J., Wiederhold, K.H., Tolnay, M., Mistl, C., Jaton, A.L., Hong, M., Ishihara, T., Lee, V.M., Trojanowski, J.Q., Jakes, R., Crowther, R.A., Spillantini, M.G., Burki, K., and Goedert, M. (2000) Axonopathy and amyotrophy in mice transgenic for human four-repeat tau protein. *Acta Neuropathol (Berl)* **99**: 469-481.

Puglielli, L., Tanzi, R.E., and Kovacs, D.M. (2003) Alzheimer's disease: the cholesterol connection. *Nat Neurosci* **6**: 345-351.

Reed, L.A., Grabowski, T.J., Schmidt, M.L., Morris, J.C., Goate, A., Solodkin, A., Van Hoesen, G.W., Schelper, R.L., Talbot, C.J., Wragg, M.A., and Trojanowski, J.Q. (1997) Autosomal dominant dementia with widespread neurofibrillary tangles [see comments]. *Ann Neurol* **42**: 564-572.

Reszka, A.A., Seger, R., Diltz, C.D., Krebs, E.G., and Fischer, E.H. (1995) Association of mitogen-activated protein kinase with the microtubule cytoskeleton. *Proc Natl Acad Sci U S A* **92**: 8881-8885.

Reynolds, C.H., Utton, M.A., Gibb, G.M., Yates, A., and Anderton, B.H. (1997) Stress-activated protein kinase/c-jun N-terminal kinase phosphorylates tau protein. *J Neurochem* **68**: 1736-1744.

Ridley, A.J., and Hall, A. (1992) The small GTP-binding protein rho regulates the assembly of focal adhesions and actin stress fibers in response to growth factors. *Cell* **70**: 389-399.

Ridley, A.J., Paterson, H.F., Johnston, C.L., Diekmann, D., and Hall, A. (1992) The small GTP-binding protein rac regulates growth factor-induced membrane ruffling. *Cell* **70**: 401-410.

Rocchi, A., Pellegrini, S., Siciliano, G., and Murri, L. (2003) Causative and susceptibility genes for Alzheimer's disease: a review. *Brain Res Bull* **61**: 1-24.

Roher, A.E., Chaney, M.O., Kuo, Y.M., Webster, S.D., Stine, W.B., Haverkamp, L.J., Woods, A.S., Cotter, R.J., Tuohy, J.M., Krafft, G.A., Bonnell, B.S., and Emmerling, M.R. (1996) Morphology and toxicity of Abeta-(1-42) dimer derived from neuritic and vascular amyloid deposits of Alzheimer's disease. *J Biol Chem* **271**: 20631-20635.

Rollins, B.L., Stines, S.G., McGuire, H.B., and King, B.M. (2001) Effects of amygdala lesions on body weight, conditioned taste aversion, and neophobia. *Physiol Behav* **72**: 735-742.

Roozendaal, B., Phillips, R.G., Power, A.E., Brooke, S.M., Sapolsky, R.M., and McGaugh, J.L. (2001) Memory retrieval impairment induced by hippocampal CA3 lesions is blocked by adrenocortical suppression. *Nat Neurosci* **4**: 1169-1171.

Roozendaal, B., Griffith, Q.K., Buranday, J., De Quervain, D.J., and McGaugh, J.L. (2003) The hippocampus mediates glucocorticoid-induced impairment of spatial memory retrieval: dependence on the basolateral amygdala. *Proc Natl Acad Sci U S A* **100**: 1328-1333.

Sanger, F., Nicklen, S., and Coulson, A.R. (1977) DNA sequencing with chain-terminating inhibitors. *Proc Natl Acad Sci U S A* **74**: 5463-5467.

Schenk, D., Barbour, R., Dunn, W., Gordon, G., Grajeda, H., Guido, T., Hu, K., Huang, J., Johnson-Wood, K., Khan, K., Kholodenko, D., Lee, M., Liao, Z., Lieberburg, I., Motter, R., Mutter, L., Soriano, F., Shopp, G., Vasquez, N., Vandevert, C., Walker, S., Wogulis, M., Yednock, T., Games, D., and Seubert, P. (1999) Immunization with amyloid-beta attenuates Alzheimer-disease-like pathology in the PDAPP mouse. *Nature* **400**: 173-177.

Schenk, D. (2002) Amyloid-beta immunotherapy for Alzheimer's disease: the end of the beginning. *Nat Rev Neurosci* **3**: 824-828.

Schiffman, S.S., Clark, C.M., and Warwick, Z.S. (1990) Gustatory and olfactory dysfunction in dementia: not specific to Alzheimer's disease. *Neurobiol Aging* **11**: 597-600.

Schweers, O., Schonbrunn-Hanebeck, E., Marx, A., and Mandelkow, E. (1994) Structural studies of tau protein and Alzheimer paired helical filaments show no evidence for beta-structure. *J Biol Chem* **269**: 24290-24297.

Senior, K. (2002) Dosing in phase II trial of Alzheimer's vaccine suspended. *Lancet Neurol* **1**: 3.

Sherrington, R., Rogaev, E.I., Liang, Y., Rogaeva, E.A., Levesque, G., Ikeda, M., Chi, H., Lin, C., Li, G., Holman, K., and et al. (1995) Cloning of a gene bearing missense mutations in early-onset familial Alzheimer's disease. *Nature* **375**: 754-760.

Shulman, J.M., and Feany, M.B. (2003) Genetic modifiers of tauopathy in Drosophila. *Genetics* **165**: 1233-1242.

Sinha, S., and Lieberburg, I. (1999) Cellular mechanisms of beta-amyloid production and secretion. *Proc Natl Acad Sci U S A* **96**: 11049-11053.

Sisodia, S.S., and St George-Hyslop, P.H. (2002) gamma-Secretase, Notch, Abeta and Alzheimer's disease: where do the presenilins fit in? *Nat Rev Neurosci* **3**: 281-290.

Sobrido, M.J., Miller, B.L., Havlioglu, N., Zhukareva, V., Jiang, Z., Nasreddine, Z.S., Lee, V.M., Chow, T.W., Wilhelmsen, K.C., Cummings, J.L., Wu, J.Y., and Geschwind, D.H. (2003) Novel tau polymorphisms, tau haplotypes, and splicing in familial and sporadic frontotemporal dementia. *Arch Neurol* **60**: 698-702.

Sontag, E., Nunbhakdi-Craig, V., Lee, G., Brandt, R., Kamibayashi, C., Kuret, J., White, C.L., 3rd, Mumby, M.C., and Bloom, G.S. (1999) Molecular interactions among protein phosphatase 2A, tau, and microtubules. Implications for the regulation of tau phosphorylation and the development of tauopathies. *J Biol Chem* **274**: 25490-25498.

Soto, C., Sigurdsson, E.M., Morelli, L., Kumar, R.A., Castano, E.M., and Frangione, B. (1998) Beta-sheet breaker peptides inhibit fibrillogenesis in a rat brain model of amyloidosis: implications for Alzheimer's therapy. *Nat Med* **4**: 822-826.

Spillantini, M.G., Murrell, J.R., Goedert, M., Farlow, M.R., Klug, A., and Ghetti, B. (1998) Mutation in the tau gene in familial multiple system tauopathy with presenile dementia. *Proc Natl Acad Sci U S A* **95**: 7737-7741.

Spittaels, K., Van den Haute, C., Van Dorpe, J., Bruynseels, K., Vandezande, K., Laenen, I., Geerts, H., Mercken, M., Sciot, R., Van Lommel, A., Loos, R., and Van Leuven, F. (1999) Prominent axonopathy in the brain and spinal cord of transgenic mice overexpressing four-repeat human tau protein. *Am J Pathol* **155**: 2153-2165.

Sumi, S.M., Bird, T.D., Nochlin, D., and Raskind, M.A. (1992) Familial presenile dementia with psychosis associated with cortical neurofibrillary tangles and degeneration of the amygdala. *Neurology* **42**: 120-127.

Tanemura, K., Akagi, T., Murayama, M., Kikuchi, N., Murayama, O., Hashikawa, T., Yoshiike, Y., Park, J.M., Matsuda, K., Nakao, S., Sun, X., Sato, S., Yamaguchi, H., and Takashima, A. (2001) Formation of filamentous tau aggregations in transgenic mice expressing V337M human tau. *Neurobiol Dis* **8**: 1036-1045.

Tanemura, K., Murayama, M., Akagi, T., Hashikawa, T., Tominaga, T., Ichikawa, M., Yamaguchi, H., and Takashima, A. (2002) Neurodegeneration with tau accumulation in a transgenic mouse expressing V337M human tau. *J Neurosci* **22**: 133-141.

Tatebayashi, Y., Miyasaka, T., Chui, D.H., Akagi, T., Mishima, K., Iwasaki, K., Fujiwara, M., Tanemura, K., Murayama, M., Ishiguro, K., Planel, E., Sato, S., Hashikawa, T., and Takashima, A. (2002) Tau filament formation and associative memory deficit in aged mice expressing mutant (R406W) human tau. *Proc Natl Acad Sci U S A* **99**: 13896-13901.

Thal, D.R., Rub, U., Orantes, M., and Braak, H. (2002) Phases of A beta-deposition in the human brain and its relevance for the development of AD. *Neurology* **58**: 1791-1800.

Treit, D., and Menard, J. (1997) Dissociations among the anxiolytic effects of septal, hippocampal, and amygdaloid lesions. *Behav Neurosci* **111**: 653-658.

Ueda, T., Kikuchi, A., Ohga, N., Yamamoto, J., and Takai, Y. (1990) Purification and characterization from bovine brain cytosol of a novel regulatory protein inhibiting the dissociation of GDP from and the subsequent binding of GTP to rhoB p20, a ras p21-like GTP-binding protein. *J Biol Chem* **265**: 9373-9380.

Upchurch, M., and Wehner, J.M. (1988) Differences between inbred strains of mice in Morris water maze performance. *Behav Genet* **18**: 55-68.

Upchurch, M., and Wehner, J.M. (1989) Inheritance of spatial learning ability in inbred mice: a classical genetic analysis. *Behav Neurosci* **103**: 1251-1258.

Van Broeckhoven, C., Backhovens, H., Cruts, M., De Winter, G., Bruyland, M., Cras, P., and Martin, J.J. (1992) Mapping of a gene predisposing to early-onset Alzheimer's disease to chromosome 14q24.3. *Nat Genet* **2**: 335-339.

van Swieten, J.C., Stevens, M., Rosso, S.M., Rizzu, P., Joosse, M., de Koning, I., Kamphorst, W., Ravid, R., Spillantini, M.G., Niermeijer, M.F., and Heutink, P. (1999) Phenotypic variation in hereditary frontotemporal dementia with tau mutations. *Ann Neurol* **46**: 617-626.

Varani, L., Hasegawa, M., Spillantini, M.G., Smith, M.J., Murrell, J.R., Ghetti, B., Klug, A., Goedert, M., and Varani, G. (1999) Structure of tau exon 10 splicing regulatory element RNA and destabilization by mutations of frontotemporal dementia and parkinsonism linked to chromosome 17. *Proc Natl Acad Sci U S A* **96**: 8229-8234.

Vassar, R., Bennett, B.D., Babu-Khan, S., Kahn, S., Mendiaz, E.A., Denis, P., Teplow, D.B., Ross, S., Amarante, P., Loeloff, R., Luo, Y., Fisher, S., Fuller, J., Edenson, S., Lile, J., Jarosinski, M.A., Biere, A.L., Curran, E., Burgess, T., Louis, J.C., Collins, F., Treanor, J., Rogers, G., and Citron, M. (1999) Beta-secretase cleavage of Alzheimer's amyloid precursor protein by the transmembrane aspartic protease BACE. *Science* **286**: 735-741.

Welzl, H., D'Adamo, P., and Lipp, H.P. (2001) Conditioned taste aversion as a learning and memory paradigm. *Behav Brain Res* **125**: 205-213.

Wischik, C.M., Crowther, R.A., Stewart, M., and Roth, M. (1985) Subunit structure of paired helical filaments in Alzheimer's disease. *J Cell Biol* **100**: 1905-1912.

Wittmann, C.W., Wszolek, M.F., Shulman, J.M., Salvaterra, P.M., Lewis, J., Hutton, M., and Feany, M.B. (2001) Tauopathy in Drosophila: neurodegeneration without neurofibrillary tangles. *Science* **293**: 711-714.

Wolfer, D.P., Muller, U., Stagliar, M., and Lipp, H.P. (1997) Assessing the effects of the 129/Sv genetic background on swimming navigation learning in transgenic mutants: a study using mice with a modified beta-amyloid precursor protein gene. *Brain Res* **771**: 1-13.

Wolfer, D.P., and Lipp, H.P. (2000) Dissecting the behaviour of transgenic mice: is it the mutation, the genetic background, or the environment? *Exp Physiol* **85**: 627-634.

Wolfer, D.P., Madani, R., Valenti, P., and Lipp, H.P. (2001) Extended analysis of path data from mutant mice using the public domain software Wintrack. *Physiol Behav* **73**: 745-753.

Wright, J.W., Murphy, E.S., Elijah, I.E., Holtfreter, K.L., Davis, C.J., Olson, M.L., Muhunthan, K., and Harding, J.W. (2004) Influence of hippocampectomy on habituation, exploratory behavior, and spatial memory in rats. *Brain Res* **1023**: 1-14.

Yamamoto, T., Fujimoto, Y., Shimura, T., and Sakai, N. (1995) Conditioned taste aversion in rats with excitotoxic brain lesions. *Neurosci Res* **22**: 31-49.

Yasuda, M., Kawamata, T., Komure, O., Kuno, S., D'Souza, I., Poorkaj, P., Kawai, J., Tanimukai, S., Yamamoto, Y., Hasegawa, H., Sasahara, M., Hazama, F., Schellenberg, G.D., and Tanaka, C. (1999) A mutation in the microtubule-associated protein tau in pallido-nigro-luysian degeneration. *Neurology* **53**: 864-868.

Zheng-Fischhofer, Q., Biernat, J., Mandelkow, E.M., Illenberger, S., Godemann, R., and Mandelkow, E. (1998) Sequential phosphorylation of Tau by glycogen synthase kinase-3beta and protein kinase A at Thr212 and Ser214 generates the Alzheimer-specific epitope of antibody AT100 and requires a paired-helical-filament-like conformation. *Eur J Biochem* **252**: 542-552.

Zhong, J., Iqbal, K., and Grundke-Iqbal, I. (1999) Hyperphosphorylated tau in SY5Y cells: similarities and dissimilarities to abnormally hyperphosphorylated tau from Alzheimer disease brain. *FEBS Lett* **453**: 224-228.

Zhu, X., Raina, A.K., Boux, H., Simmons, Z.L., Takeda, A., and Smith, M.A. (2000) Activation of oncogenic pathways in degenerating neurons in Alzheimer disease. *Int J Dev Neurosci* **18**: 433-437.

Zhu, X., Raina, A.K., Rottkamp, C.A., Aliev, G., Perry, G., Boux, H., and Smith, M.A. (2001) Activation and redistribution of c-Jun N-terminal kinase/stress activated protein kinase in degenerating neurons in Alzheimer's disease. *J Neurochem* **76**: 435-441.

ABBREVIATIONS

aa	Amino acids
ACo	Anterior cortical amygdaloid nucleus
AD	Alzheimer's disease
AIP	Agranular insular cortex
Amb	Ambiguus nucleus
ANOVA	One-way analysis of variance
AP	Anteroposterior
ApoE	Apolipoprotein E
APP	Amyloid precursor protein
APPα	Soluble extracellular fragment of APP generated by α-cleavage
APPβ	Soluble extracellular fragment of APP generated by β-cleavage
Aβ	β-amyloid
BACE	β-site APP cleaving enzyme
BDNF	Brain-derived neurotrophic factor
BLA	Basolateral nucleus of the amygdala
BM	Basomedial nucleus of the amygdala
bp	Base pair
BSA	Bovine serum albumin
C83	C-terminal fragment of APP generated by a α-secretase
C99	C-terminal fragment of APP generated by a β-secretase
CBD	Corticobasal degeneration
CE	Central nucleus of the amygdala
CNS	Central nervous system
CS	Conditioned stimulus
CTA	Conditioned taste aversion
ddH_2O	Double deionised water
DEn	Dorsal endopiriform nucleus
DMEM	Dulbecco’s modified Eagle medium
DMSO	Dimethylsulfoxid
DNA	Deoxyribonucleic acid
dNTP	Deoxynucleoside triphosphate
Dox	Doxycycline
DTT	DiThioThreitol
E. coli	*Escherichia coli*
ECIC	External cortex of the inferior colliculus

EDTA	Ethylenediamine tetraacetic acid
FA	Formic acid
FAD	Familial Alzheimer's disease
FCS	Fetal calf serum
FTDP-17	Frontotemporal dementia with Parkinsonism linked to chromosome 17
GFAP	glial fibrillary acidic protein
HEK 293	Human embryonal kidney cells
HS	Horse serum
IC	Insular cortex
IO	Inferior olive
IP	Immunoprecipitation
i.p.	Intraperitoneal
L/D	Light-dark test
LA	Lateral nucleus of the amygdala
LB-medium	Luria-Bertani medium
LiCl	Lithium chlorid
MALDI-TOF	Matrix-assisted laser desorption/ionization tandem time-of-flight mass spectrometry
MWM	Morris water maze
NFT	Neurofibrillary tangles
ORF	Open reading frame
PBS	Phosphate buffered saline
PCR	Polymerase chain reaction
PFA	Paraformaldehyde
PHF	Paired helical filaments
PiD	Pick’s disease
PMCo	Posteromedial cortical amygdaloid nucleus
PMSF	Phenyl-methyl-sulfonyl-fluoride
PnO	Oral pontine reticular nucleus
PS 1+2	Presenilin 1+2
PSP	Progressive supranuclear palsy
RA	Retinoic acid
RAB	High-salt reassembly buffer
RIPA	Radioimmunoprecipitation buffer
RNA	Ribonucleic acid
RPC	Red nucleus (parvocellular part)
rpm	Rotations per minute

RPO	Rostral periolivary region
rtTA	Transactivator
RtTG	Reticulotegmental nucleus pons
SAD	Sporadic Alzheimer’s disease
SDS	Sodium dodecyl sulfate
SDS-PAGE	Sodium dodecyl sulfate polyacrylamid gel electrophoresis
SEM	Standard error of the mean
SF	Straight filaments
SH-SY5Y	Human neuroblastoma cell line
TET	Tetracycline
Tg	Transgenic
TRE	Tet-response element
Tris	Tris(hydroxymethyl)-amino-methane
US	Unconditioned stimulus
VTA	Ventral tegmental area
WB	Western blot
wt	Wild-type

ACKNOWLEDGEMENTS

I would especially like to thank Jürgen Götz, who supervised this work, for having been so helpful and for his kind support in every way. His experience and professional competence in the Alzheimer / tau field has helped me a lot.

My thanks go to Prof. Roger M. Nitsch for the opportunity to do my PhD work in his department, to Prof. Peter Sonderegger for his kindness to accept me as an external PhD student and to Prof. Hanns Möhler for refereeing my thesis.

I would also like to thank PD Dr. Hans Welzl and PD Dr. David Wolfer from the Institute of Anatomy, University of Zurich, for their assist in the behavioral part of my thesis.

Special thanks to Della David for her help and friendship.

I also thank Alex Ferrari, Fred Hörndli and Ruth von Rotz for their help with the cell culture, Eva Moritz and Daniel Schuppli for being a help in histology and cloning procedures, as well as all the other members of the lab.

I would thank the Swiss National Foundation for supporting my thesis.

Finally, I am grateful to my family, whose support made this work possible.

CURRICULUM VITAE

Personal:

Name (Last):	Pennanen
Name (First/Middle):	Luis Javier Carlos
Birth Date:	24th February, 1976
Home Town:	Dottikon / Aargau
Nationality:	Swiss

Education:

1996-2001:	Study of Biology at the MNF-faculty, University of Zurich, Switzerland
1998:	"Vordiplom" (BSc) in Biology
2000 – 2001:	Diploma work at the Behavioral Neurobiology Laboratory, Swiss Federal Institute of Technology (ETH) Zurich Topic: **Analysis of cognitive functions of the marmoset monkey (*Callithrix jacchus*) in the laboratory: Relevance for biomedical and behavior-ecological questions** (*in German*), Advisors: Dr. Christopher R. Pryce and Prof. Dr. Barbara König.
2001:	Diploma (Masters) in Zoology (with specialization in Behavioral Biology, Neurobiology and Ecology) and in Molecular Biology
2002 - 2005:	Ph.D. study at the Division of Psychiatry Research, University of Zurich, Advisor: PD Dr. Jürgen Götz. Topic: **Analysis of tau pathology in transgenic mouse and tissue culture models of Alzheimer's disease and related disorders** Participated in the ZNZ Ph.D. program (Neuroscience Centre Zurich)

Congresses and symposia:

6th EMRG (European marmoset research group) workshop: Inter-disciplinary Forum for discussion and training in primate biological and biomedical research: Paris, 2000.

ZNZ Symposium 2000 - Neuroscience Center Zurich.

6th International Conference AD/PD, Seville, 2003.

ZNZ Symposium 2003 - Neuroscience Center Zurich.

Society of Neuroscience, 33th Annual Meeting New Orleans, October, 2003.

ZNZ Symposium 2004 - Neuroscience Center Zurich.

Society of Neuroscience, 34th Annual Meeting San Diego, October, 2004.

Jobs:

1999 – 2000:	Technical assistant at the Natural History Museum Zürich, Department of Ecology.
2000:	Technical assistant at the Department of Materials, ETH Zurich.
2000 - 2002:	„Touch-Table“ staff member, Zoo Zürich (2000 - 2002).
2002 - 2005:	Official tour guide, Zoo Zürich (guided tours for groups in German and English)

PUBLICATIONS

Chen, F., Ferrari, A., Schild, A., Kurosinski, P., David, D., Hoerndli, F., **Pennanen, L.**, Kins, S., van Dorpe, J., Nitsch, R.M., and Gotz, J. (2003) Amyloid-induced neurofibrillary tangle formation. In *Alzheimer's disease and related disorders: Research advances*. Iqbal, K. and Winblad, B. (eds): Ana Aslan International Foundation.

Spinelli, S., **Pennanen, L.**, Dettling, A.C., Feldon, J., Higgins, G.A., and Pryce, C.R. (2004) Performance of the marmoset monkey on computerized tasks of attention and working memory. *Brain Res Cogn Brain Res* **19**: 123-137.

Gotz, J., Schild, A., Hoerndli, F., and **Pennanen, L.** (2004) Amyloid-induced neurofibrillary tangle formation in Alzheimer's disease: insight from transgenic mouse and tissue-culture models. *Int J Dev Neurosci* **22**: 453-465.

Gotz, J., Streffer, J.R., David, D., Schild, A., Hoerndli, F., **Pennanen, L.**, Kurosinski, P., and Chen, F. (2004) Transgenic animal models of Alzheimer's disease and related disorders: Histopathology, behavior and therapy. *Mol Psychiatry* **9**: 664-683.

Pennanen, L., Welzl, H., D'Adamo, P., Nitsch, R.M., and Gotz, J. (2004) Accelerated extinction of conditioned taste aversion in P301L tau transgenic mice. *Neurobiol Dis* **15**: 500-509.

Pennanen, L., Wolfer, D., Nitsch, R.M., and Gotz, J. (2005) Impaired spatial reference memory and increased exploratory behavior in P301L tau transgenic mice. *Genes Brain Behav*, **In Revision**.

POSTERS

Pryce C.R., **Pennanen L.**, Dettling A., Konig B., Feldon J., and Higgins G. Computer-based behavioral testing in the marmoset monkey: Validation & applications. ZNZ Symposium 2000 - Neuroscience Center Zurich.

Chen F., Schild A., Kurosinski P., **Pennanen L.**, Hoerndli F., David D., Ferrari A., Nitsch R.M. and Gotz J. (S.03.01) In vivo and in vitro models of AD demonstrate a role of distinct phosphorylation sites of tau in neurofibrillary tangle formation. European Neuropsychopharmacology, Volume **13**, Supplement 4, October 2003, Pages S99-S100.

Chen F., David D.C., **Pennanen L.**, Hoerndli F., Ferrari A., Schild A., Kurosinski P., Nitsch R.M. and Gotz J. Characterization of the transgenic mice expressing P301L tau. 6th International Conference AD/PD, 2003, Seville.

Pennanen L., Welzl H., D'Adamo P., Nitsch R.M. and Gotz J. Accelerated extinction of conditioned taste aversion in P301L tau transgenic mice. Program No. 628.3. 2003 Abstract Viewer/Itinerary Planner. Washington, DC: Society for Neuroscience, 2003. Online.

Pennanen L., David D., Hoerndli F., Kurosinski P., Chen F., Schild A., Ferrari A., Nitsch R.M. and Gotz J. (P2-110) Amyloid-induced neurofibrillary tangle formation addressed in vivo and in vitro. Neurobiology of Aging, Volume 25, Supplement 2, July 2004, Page S255.

Pennanen L., Hoerndli F., Ferrari A., Nitsch R.M. and Gotz. J. Characterization of tau expressing human SH-SY5Y neuroblastoma cells. Program No. 218.7. *2004 Abstract Viewer/Itinerary Planner.* Washington, DC: Society for Neuroscience, 2004. Online.

ELSEVIER

Neurobiology of Disease

www.elsevier.com/locate/ynbdi
Neurobiology of Disease 15 (2004) 500–509

Accelerated extinction of conditioned taste aversion in P301L tau transgenic mice

Luis Pennanen,[a] Hans Welzl,[b] Patrizia D'Adamo,[b] Roger M. Nitsch,[a] and Jürgen Götz[a,*]

[a] *Division of Psychiatry Research, University of Zürich, 8008 Zürich, Switzerland*
[b] *Institute of Anatomy, University of Zürich, 8057 Zürich, Switzerland*

Received 1 July 2003; revised 29 September 2003; accepted 18 November 2003

Neurofibrillary tangles, insoluble protein deposits composed of filamentous tau aggregates, are neuropathological hallmarks of Alzheimer's disease and familial frontotemporal dementia (FTDP-17). Transgenic mice expressing the FTDP-17 mutation P301L of tau recapitulate key features of the human pathology, that is, tau proteins aggregate and neurofibrillary tangles begin to appear in the amygdala at 6 months of age. To detect early signs of tau aggregate-associated changes, we investigated behavioral alterations and cognitive deficits in such mice using an amygdala-specific test battery for anxiety-related and cognitive behavior. P301L mice had anxiety levels not different from wild-types, but their exploratory behavior was significantly increased. Acquisition of a fear response to tone and context as well as taste aversion was comparable to wild-types. However, extinction of a conditioned taste aversion was significantly accelerated. We conclude that already aggregation of tau proteins not yet accompanied by massive formation of neurofibrillary tangles causes selective behavioral deficits.

Keywords: Alzheimer's disease; Frontotemporal dementia; Tau; Transgenic mice; Conditioned taste aversion; Amygdala; Neurofibrillary tangles; Extinction

Introduction

Alzheimer's disease (AD) and frontotemporal dementia with Parkinsonism linked to chromosome 17 (FTDP-17) are common forms of age-related dementing diseases. Whereas AD is characterized by extracellular β-amyloid-containing plaques and intracellular neurofibrillary tangles (NFT), in neurodegenerative diseases such as FTDP-17, NFT form in the absence of amyloid plaques (Gotz, 2001; Lee et al., 2001). In cells affected in these tauopathies, the microtubule-associated protein tau is abnormally phosphorylated and relocalized from axonal to somatodendritic compartments where it accumulates in pretangle, filamentous aggregates that eventually assemble into NFT (Buee et al., 2000; Goedert et al., 1995). The discovery of mutations in the tau gene in FTDP-17 established that dysfunction of tau alone can cause neurodegeneration and lead to dementia (Hutton et al., 1998; Poorkaj et al., 1998; Spillantini et al., 1998).

Expression of FTDP-17 mutant tau in transgenic mice caused NFT formation both in neurons (Allen et al., 2002; Gotz et al., 2001a; Lewis et al., 2000; Tanemura et al., 2001; Tatebayashi et al., 2002) and in glial cells (Gotz et al., 2001b; Higuchi et al., 2002; Lin et al., 2003). Whereas extensive behavioral studies have been performed in β-amyloid-forming APP transgenic mice (Chapman et al., 1999; Chen et al., 2000; Dodart et al., 1999; Hsiao et al., 1996; Janus et al., 2000; Morgan et al., 2000; Routtenberg et al., 1997), less information is available for tau mutant mice (Tanemura et al., 2002; Tatebayashi et al., 2002). We investigated our P301L (FTDP-17) mutant mice in several amygdala-dependent tasks because tau aggregates mainly formed in the amygdala (Gotz et al., 2001c). This brain area is involved in mediating effects of emotion and stress on learning and memory as determined in fear conditioning and conditioned taste aversion (CTA) tests (LeDoux, 2000; Welzl et al., 2001). It plays a role in modulating consolidation processes which involve other brain areas (McGaugh et al., 2002). To correlate behavior with tau expression, we determined the distribution of P301L tau in more detail with special emphasis on brain areas shown to be involved in CTA.

We found that the P301L mice showed increased exploratory behavior but normal anxiety levels and no impairment in fear conditioning. CTA is a well-established learning and memory paradigm in which subjects learn to associate a novel taste with nausea and, as a consequence, avoid consumption of this specific taste at the next presentation. Acquisition and consolidation of CTA memory were not significantly affected by the transgene. However, transgenic mice extinguished the CTA more rapidly than wild-type mice. Together, our data show that tau aggregation, as found in particular in the basolateral and basomedial nucleus of the amygdala, has functional consequences for specific forms of learning and memory.

Materials and Methods

Animals

The transgenic mice used in this study express the human pathogenic mutation P301L of tau together with the longest

* Corresponding author. Division of Psychiatry Research, University of Zürich, August Forel Str. 1, 8008, Zürich, Switzerland. Fax: +41-1-634-8874.
E-mail address: goetz@bli.unizh.ch (J. Götz).
Available online on ScienceDirect (www.sciencedirect.com.)

0969-9961/$ - see front matter © 2004 Elsevier Inc. All rights reserved.
doi:10.1016/j.nbd.2003.11.020

human brain tau isoform (htau40) under control of the neuron-specific mThy1.2 promoter. Pronuclear injections were done into C57Bl/6 × DBA/2 F2 oocytes to obtain founder animals that were back-crossed with C57Bl/6 mice to establish transgenic lines (Gotz et al., 2001a). Line pR5-183 expressed mutant human tau in many brain areas; however, NFT formation was mainly confined to the amygdala (Gotz et al., 2001c). Here, male wild-type (wt) and P301L mice were sequentially analyzed in two sets, which were balanced for the genotype and subjected to behavioral tests at the age of 6 months when NFT began to form. Data were pooled, as no statistically significant differences were found between sets. Group-housed mice were transferred to individual cages at 6 months of age when testing began. They were kept under an inverted 12 h light/dark cycle with a room temperature of 22°C. Food pellets and water were available ad libitum unless otherwise noted. Thirty minutes before each test session, the mice were transferred to the behavioral room.

Histology

Coronal 4-μm paraffin brain sections were immunohistologically stained as previously described (Gotz and Nitsch, 2001; Gotz et al., 2001a) and brain areas were mapped based on the mouse atlas by Paxinos (1997). Sections were dehydrated in an ascending series of ethanol, stained and flat-embedded between glass slides and coverslips in Eukitt (Kindler, Germany). For signal enhancement, sections were microwave-treated in citrate-buffer pH 5.8 at 70°C for 15 min. They were stained with the human tau-specific antibody HT7 (Innogenetics Inc, diluted 1:200) and the phosphorylation-dependant anti-tau antibody CP13 (Dr. Peter Davies, diluted 1:200) directed against phosphorylated S202/T205. For the peroxidase/DAB stainings, secondary antibodies were obtained from Vector Laboratories (Vectastain ABC kits PK-6101 and PK-6102).

Motor coordination on the Rotarod

The body weight was determined at 6 and again at 8 months of age, when the CTA test was performed. To test locomotor coordination, the accelerating Rotarod (Udo Basile, Milano, Italy) was used which consists of a rotating drum with a diameter of 3 cm covered with knurled Perspex to provide an adequate grip. The mice were first placed on the rod at the lowest speed of 4 rpm for 2 min. Only then the rod was switched to acceleration mode and the time on the rod was recorded for up to 5 min when the speed reached the maximum of 40 rpm. Mice were assessed daily in two trials on three consecutive days, with an intertrial interval of at least 3 h.

Open-field test

The open-field test analyzes spontaneous locomotor activity, exploratory behavior, and anomalies of locomotion patterns. Mice were placed at the border of a dimly lit (50 lx) circular arena (diameter of 150 cm) for 10 min followed by a second session on the following day. The arena was divided into an outer zone (within 7 cm of the wall), an inner zone (inner circle with a diameter of 110 cm), and an intermediate zone. Paths were tracked with an electronic imaging system (EthoVision 1.96, Noldus Information Technology, Wageningen, The Netherlands) at a frequency of 4.2 Hz and a spatial resolution of 256 × 256 pixels. Raw data were analyzed with the Wintrack 2.3 software (Wolfer et al., 2001). Locomotor activity was assessed by measuring the total distance traveled and the total number of zone transitions. Thigmotaxis, that is, moving along the wall, was quantified by measuring the time spent in the outer zone. To determine measures of anxiety and exploratory behavior, the following parameters were assessed: number of visits to the inner zone, average distance to inner zone, and the number of activity state changes. Three activity states were distinguished: progression (periods with a locomotion speed above the progression threshold of 0.085 m/s and a minimal distance moved exceeding 0.05 m), resting (periods lasting at least 2 s with a speed below 0.025 m/s) and scanning (periods meeting neither resting nor progression criteria).

Light–dark (L–D) test

Unconditioned anxiety-like behavior was tested in the light–dark (L–D) test. The mice were placed into the 30 × 20 cm area of a Perspex L–D box that was illuminated with an average of 700 lx. A dark compartment of 15 × 20 cm was attached opposite to the releasing site with an opening facing the center of the illuminated part. Movements were tracked in the illuminated part over a 5-min trial as described above. Anxiety was measured by the latency to enter the dark compartment and the time spent in it. Exploration was defined by the number of rearings in the illuminated part, and the percentage of visited tiles/total of 36 tiles (5 × 3.3 cm) entered with all four paws, defined as exploration index.

Fear conditioning test

The conditioning chamber consisted of a gray opaque box (16.5 × 25 cm) with a grid floor through which shocks could be delivered (0.15 mA) as the unconditioned stimulus (US). The chamber was placed into a dimly lit sound-attenuating box with a speaker on top delivering a 92 dB/2000 Hz tone as the conditioned stimulus (CS). Two measures were used to quantify freezing as the conditioned reaction: a grid of photobeams (1 × 1 cm) detected the inactivity of the mice, which was defined as no photobeam breaks for at least 2 s. Freezing was also detected manually while observing the animal and was defined as no movement except for respiration (as defined and applied by the experimenter). The two measures correlated well with each other. However, we finally used the manually detected measurement due to technical problems with the photobeams during cue testing: sawdust was used in the new environment and unfortunately, from time to time, the photobeams were concealed, which caused a higher, inappropriate measurement of inactivity. During the conditioning session, a 1-min adaptation period in the box was followed by three identical conditioning trials, each trial consisting of 30-s CS presentation, with the US being applied during the last 2 s of the CS, separated by an intertrial interval of 30 s.

Retrieval tests for context conditioning and, 2 h later, for conditioning to tone were carried out 24 h and 15 days after the conditioning session by recording freezing as mentioned above. To evaluate context conditioning, mice were placed for 2 min in the conditioning chamber. To evaluate conditioning to tone, the physical characteristics of the chamber were changed (shape, light, smell, and bedding material). Each mouse was then placed for 2 min into this new chamber, and the CS was presented throughout the second minute.

Conditioned taste aversion test (CTA)

For the first 4 days of the experiment, water-deprived mice were adapted to obtain water only during two daily drinking sessions, a morning session lasting 20 min and an afternoon session lasting 10 min, with a 4-h intertrial interval. Water was presented in two 15-ml bottles that were weighed before and after the test to measure fluid intake. During the morning session on the conditioning day, mice were only allowed to drink a 0.5% saccharin solution (CS) (saccharin sodium salt hydrate, Fluka Chemie, Buchs, Switzerland) from one bottle. 40 min later, the mice were injected intraperitoneally with a 0.14 M LiCl solution (at 2% of body weight) as the nausea-inducing agent (US). Two days after conditioning, during the 20-min morning session, all mice could drink either tap water from one bottle or a 0.5% saccharin solution from another bottle (two-bottle choice test). The percentage of saccharin consumption per total fluid intake was calculated. Extinction was determined by repeating the choice tests 3 days after conditioning and on 3 consecutive days, beginning 1 week after conditioning. The mice of the second set were analyzed in three additional choice tests starting 5 weeks following conditioning.

To determine whether P301L mice were able to discriminate basic taste qualities, a separate group of water-deprived naive mice was adapted to the drinking schedule as described above. Then, they were tested for their natural preference for a 0.5% saccharin solution in a choice test with the second bottle filled with tap water. Finally, to determine the natural aversion towards a bitter taste, a choice test between a 0.02% quinine solution (quinine hydrochloride dihydrate, Fluka, Buchs, Switzerland) and water was carried out.

Data analysis

For statistical analysis, the SPSS software was used. Between-group comparisons were analyzed using a one-way analysis of variance (ANOVA) or a two-way ANOVA with repeated measures. Significant effects were analyzed post hoc using Fisher's PLSD (protected least significant difference) for pairwise comparison. All data are represented as mean ± SEM with a statistical significance given at $P < 0.05$.

Results

Expression pattern of P301L tau

To determine the expression pattern of human P301L tau in more detail, with special emphasis on brain areas involved in the CTA task, we analyzed frontal sections of four P301L tau expressing mice by immunohistochemistry using the human tau-specific antibody HT7 and the phosphorylation-dependant anti-tau antibody CP13 (Fig. 1). We found expression of human tau in the motor, somatosensory and insular cortex (IC) and in the claustrum at position AP +1.1 mm. At AP −0.82, tau was present in cortical motor and somatosensory neurons, and to a variable degree in the posterior part of the agranular insular cortex (AIP), in the anterior cortical amygdaloid nucleus (ACo) and different regions of the thalamus. At position AP −1.34, expression was found in the cortex, in the basolateral (BLA) and the basomedial nucleus of the amygdala (BM), in the dorsal endopiriform nucleus (DEn) and in

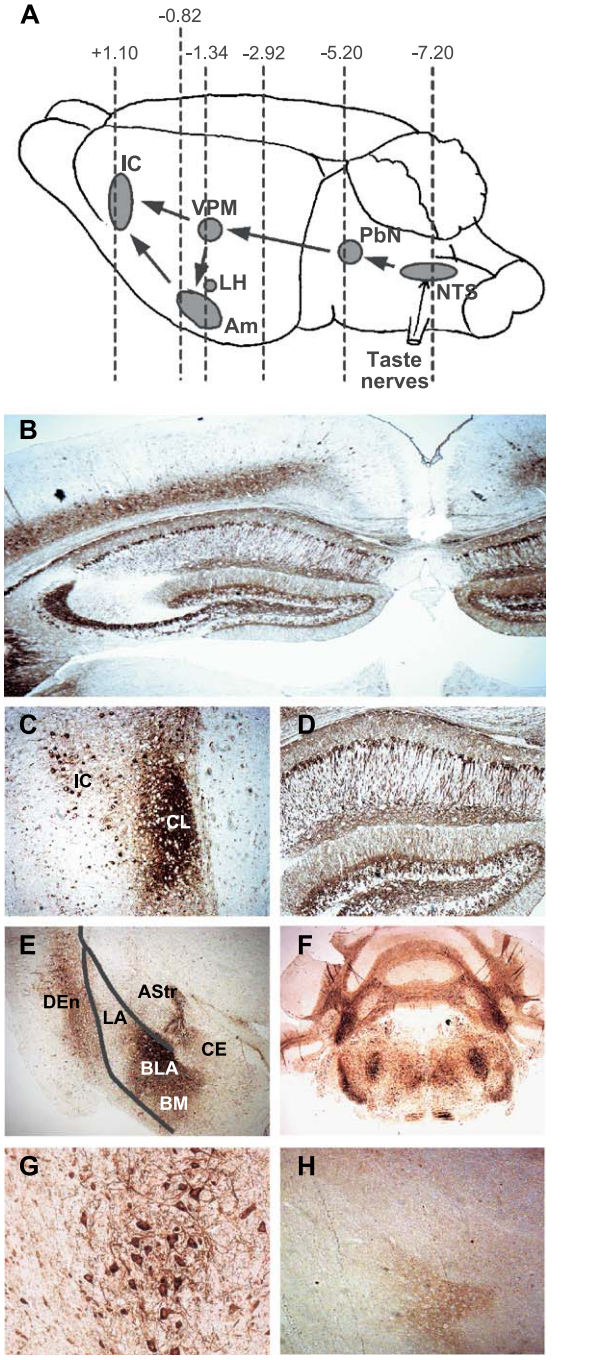

Fig. 1. Expression pattern of tau in P301L tau transgenic mice. (A) Areas involved in CTA are shown in gray: IC, insular cortex; VPM, ventral posteromedial nucleus of the thalamus; LH, lateral hypothalamus; Am, amygdala; PbN, parabrachial nucleus and NTS, nucleus of the solitary tract. (B) Tau was expressed in the cortex, hippocampus and adjacent brain areas. (C) Higher magnification of tau expression in the IC and CL (claustrum), (D) the hippocampus, (E) the DEn (dorsal endopiriform nucleus), the BLA (basolateral nucleus), and BM (basomedial nucleus) of the amygdala, the Astr (amygdalostriatal transition area), but not in the lateral nucleus (LA) and the central nucleus of the amygdala (CE). (F) Tau was expressed in the brain stem. (G) Higher magnification of (F) shows high tau expression in motor neurons of the brain stem. (H) The amygdala of a wild-type mouse is shown as a negative control. The sections were stained with the human tau-specific antibody HT7 (B, D, F, G, H) and the phospho-tau specific antibody CP13 (C, E).

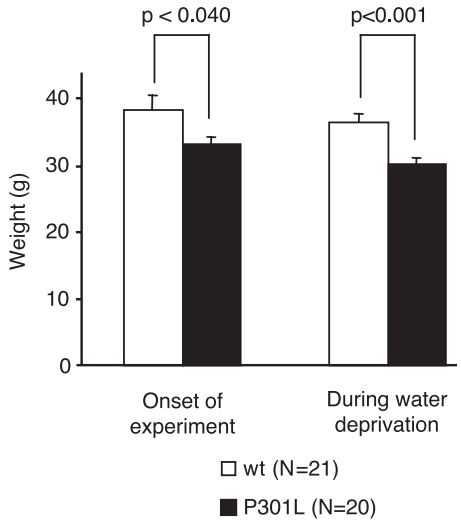

Fig. 2. Weight reduction of P301L mice. The weight of the P301L mice was significantly reduced at the onset of the experiment ($P < 0.04$) and, more pronounced, during the CTA task ($P < 0.001$). The values represent the mean ± SEM.

the ACo. No tau expression was found in the lateral nucleus (LA) and the central nucleus of the amygdala (CE). HT7 staining revealed also a strong expression of human tau in the hippocampus (CA1, CA3, and dentate gyrus), whereas staining of these brain areas with the CP13 antibody was very weak. However, both antibodies strongly stained the posterior part of these hippocampal regions at position AP −2.92 (where human tau was also expressed in cortical neurons), the posterior part of the basolateral amygdala, and to a variable degree, neurons in the red nucleus (parvocellular part, RPC), the ventral tegmental area (VTA) and the posteromedial cortical amygdaloid nucleus (PMCo). At AP −4.60, tau was present in cortical neurons, especially in the lateral entorhinal cortex and the external cortex of the inferior colliculus (ECIC) and to a variable degree in the oral pontine reticular nucleus (PnO), the rostral periolivary region (RPO) and the reticulotegmental nucleus pons (RtTG). Particularly high levels of expression were found in the brain stem (AP −7.20), predominantly in the inferior olive (IO), the ambiguus nucleus (Amb), and in various parts of the reticular formation and medulla. In contrast to the tau expression in the BLA, IC, and some thalamic nuclei, no expression was found in CTA-relevant areas such as the ventral posteromedial nucleus of the thalamus (VPM), the parabrachial nucleus (PBN), and the nucleus of the solitary tract (NTS).

Weight reduction and motor coordination of P301L tau transgenic mice

At the beginning of experiments, body weights of wild-types (38.2 ± 2.2 g) were significantly higher than that of P301L tau transgenic mice (33.0 ± 1.2 g; $P < 0.04$) (wt: $N = 21$; P301L: $N = 20$). This difference was even more pronounced during the CTA task (wt: 36.4 ± 1.2 g; P301L: 30.2 ± 0.8 g; $P < 0.001$) (Fig. 2). To test whether expression of the transgene affected locomotor coordination, the accelerating Rotarod test was performed ($N = 11$/group). P301L mice stayed significantly longer on the Rotarod than wt mice (wt: 124.3 ± 14.2 s; P301L: 178.2 ± 17.5 s; $F(1,20) = 5.316$, $P < 0.032$) and therefore reached a significantly higher average speed (wt: 18.7 ± 2.0 rpm; P301L: 25.3 ± 2.3 rpm; $F(1,20) = 4.647$, $P < 0.043$) before slipping off the rod. However, when the data were normalized for weight (by calculating a weight coefficient), the differences between the two groups disappeared ($F(1,20) = 0.364$, $P > 0.553$), demonstrating a correlation between weight and performance on the Rotarod.

Slightly increased exploration of P301L mice in the open-field and light–dark test

Levels of spontaneous locomotor activity, anxiety-like behavior and exploration were assessed in the open-field and light–dark (L–D) tests. In the open-field test ($N = 21$/group), no genotype

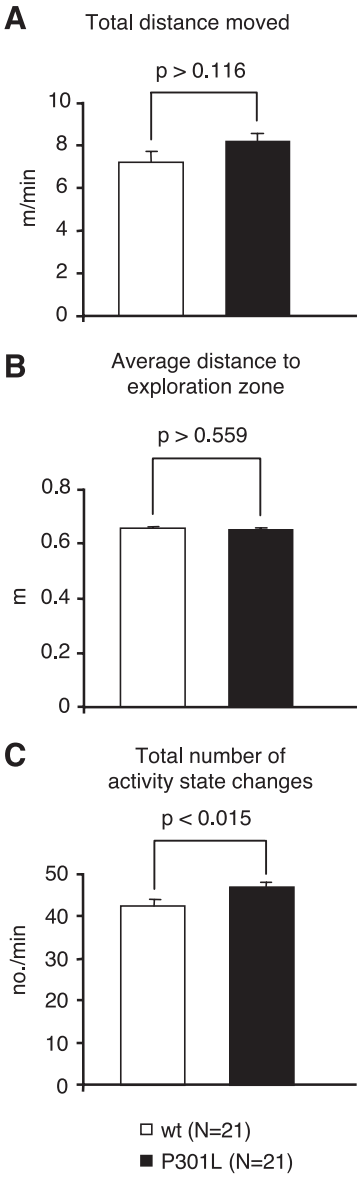

Fig. 3. No altered activity levels of P301L mice in the open-field test but slightly increased exploratory behavior. (A) Total distance moved; (B) average distance to exploration zone; and (C) total number of activity state changes. Values represent the mean ± SEM.

effect was found for measures of locomotor activity [total distance traveled: $F(1,40) = 2.587$, $P > 0.116$; total number of zone transitions: $F(1,40) = 0.003$, $P > 0.956$]. Similarly, no differences were found for measures of anxiety such as thigmotaxis ($F(1,40) = 0.119$, $P > 0.732$), the time spent in the inner zone ($F(1,40) = 0.473$, $P > 0.496$), and the average distance to the inner zone ($F(1,40) = 0.347$, $P > 0.559$). Only for the total number of activity state changes a significant genotype effect was detected ($F(1,40) = 6.469$, $P < 0.015$) (Fig. 3).

No significant differences were found in the L–D test (wt: $N = 20$; P301L: $N = 21$) for measures of anxiety such as the latency to enter the dark compartment ($F(1,39) = 0.082$, $P > 0.776$) and the time spent in the dark compartment ($F(1,39) = 0.040$, $P > 0.843$). In contrast, additional parameters for exploration such as the number of rearings ($F(1,39) = 4.624$, $P < 0.038$), and the exploration index ($F(1,39) = 4.078$, $P < 0.050$) were significantly increased in P301L tau transgenic mice (Fig. 4).

No altered fear conditioning in P301L mice

To test the ability of P301L mice to acquire a conditioned fear response, freezing was recorded during the conditioning session as well as the retrieval sessions for conditioning to context or tone. During conditioning, freezing increased significantly in both groups after the first US has been delivered ($F(7,273) = 38.022$, $P < 0.001$; wt: $N = 21$; P301L: $N = 20$; Fig 5A). Neither genotype nor genotype × interval significantly affected freezing during conditioning (genotype: $F(1,39) = 2.857$, $P > 0.099$; genotype × interval: $F(7,273) = 1.436$, $P > 0.191$), although freezing levels of transgenic mice consistently were below that of wild-type mice (Fig. 5A).

During the retrieval test for context conditioning, no significant differences between transgenic and wild-type mice could be found 24 h ($F(1,39) = 0.344$, $P > 0.561$) (wt: $N = 21$; P301L: $N = 20$) as well as 15 days ($F(1,19) = 0.242$, $P > 0.629$) (wt: $N = 11$; P301L: $N = 10$) post-conditioning (Fig. 5B). No significant genotype

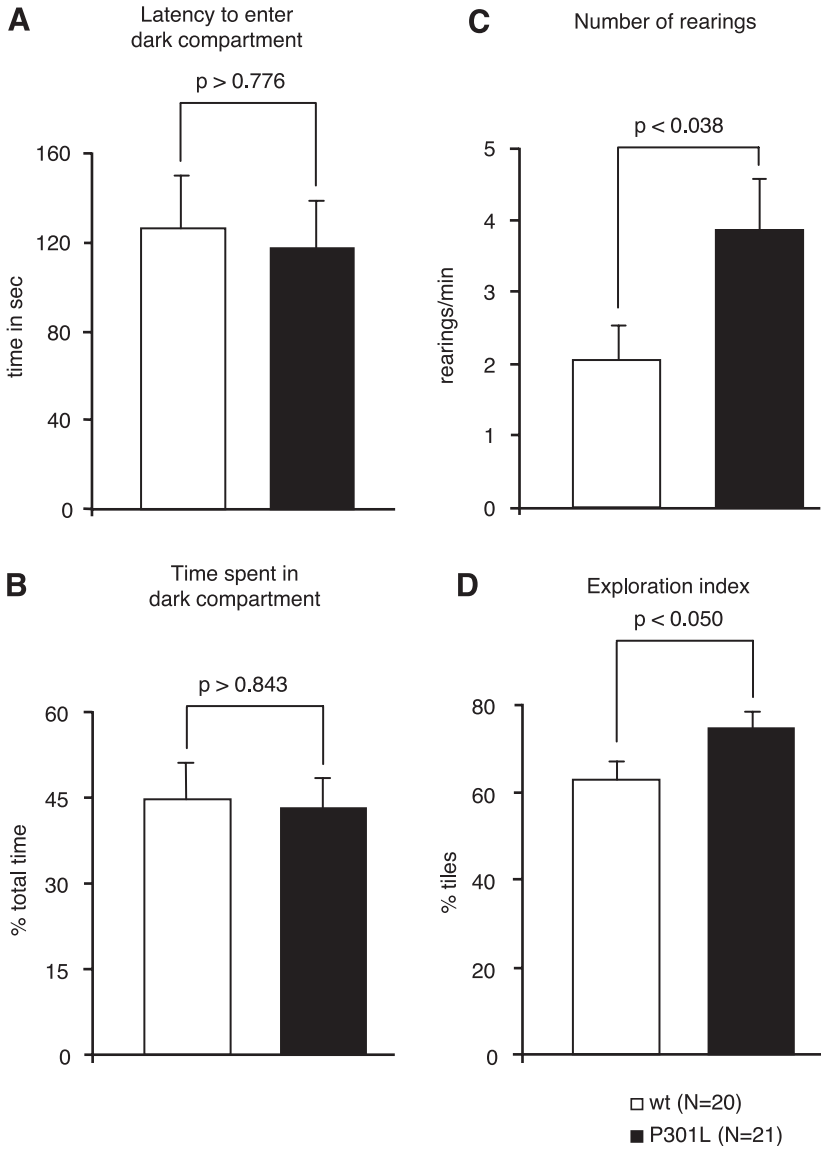

Fig. 4. No altered anxiety levels of P301L mice in the light–dark test but slightly increased exploratory behavior. (A) Latency to enter the dark compartment; (B) time spent in the dark compartment; (C) number of rearings; and (D) exploration index. Values represent the mean ± SEM.

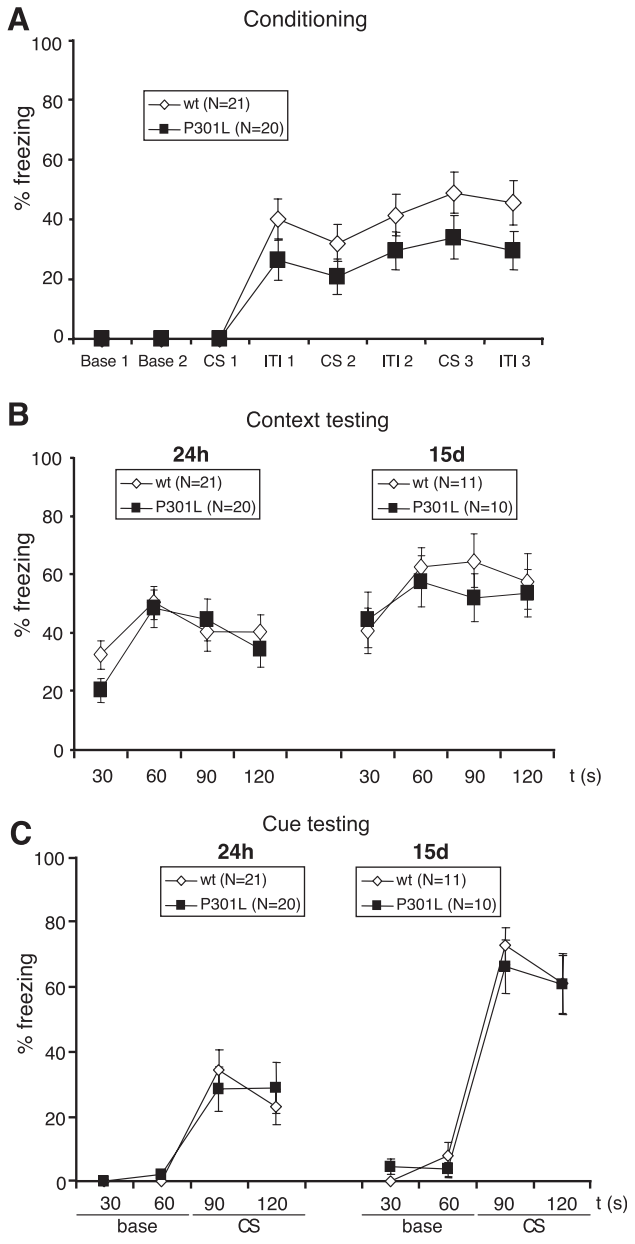

Fig. 5. No altered fear conditioning in P301L mice. (A) Genotype did not significantly affect freezing during conditioning ($P > 0.099$). Base, baseline activity; CS, tone presentation; ITI, inter-trial interval. (B) In the context test, no significant differences between genotypes were detected, neither at 24 h ($P > 0.561$) nor at 15 days ($P > 0.629$) post-conditioning. (C) Conditioning to tone also revealed no significant differences between genotypes, neither at 24 h ($P > 0.911$) nor at 15 days ($P > 0.798$) post-conditioning. The values represent the mean ± SEM.

effect was observed in freezing during the retrieval test for conditioning to tone, neither at 24 h ($F(1,39) = 0.013$, $P > 0.911$) nor at 15 days ($F(1,19) = 0.068$, $P > 0.798$) post-conditioning. Freezing significantly increased in response to tone presentation (second minute of the test) in both groups (24 h: $F(3,117) = 34.287$, $P < 0.001$, 15 days: $F(3,57) = 112.458$, $P < 0.001$) demonstrating that wild-type as well as P301L mice learned to associate the tone with the US. Tone presentation elicited a similar increase of freezing in both groups (genotype × interval interaction: 24 h: $F(3,117) = 0.776$, $P > 0.510$, 15 days: $F(3,57) = 0.512$, $P > 0.676$) (Fig. 5C).

Enhanced extinction of CTA in P301L mice

To test the ability to develop a taste aversion, P301L mice and wild-type littermate controls ($N = 19$/group) were exposed to the novel taste saccharin (CS) followed by a single injection of LiCl (US). A two-way ANOVA with repeated measures over the choice tests conducted 48, 72 h and 1 week after conditioning showed a significant main effect of genotype ($F(1,36) = 8.167$, $P < 0.007$), choice test ($F(4,144) = 8.352$, $P < 0.001$), and genotype × choice test interaction ($F(4,144) = 3.266$, $P < 0.013$) (Fig. 6A). Post hoc

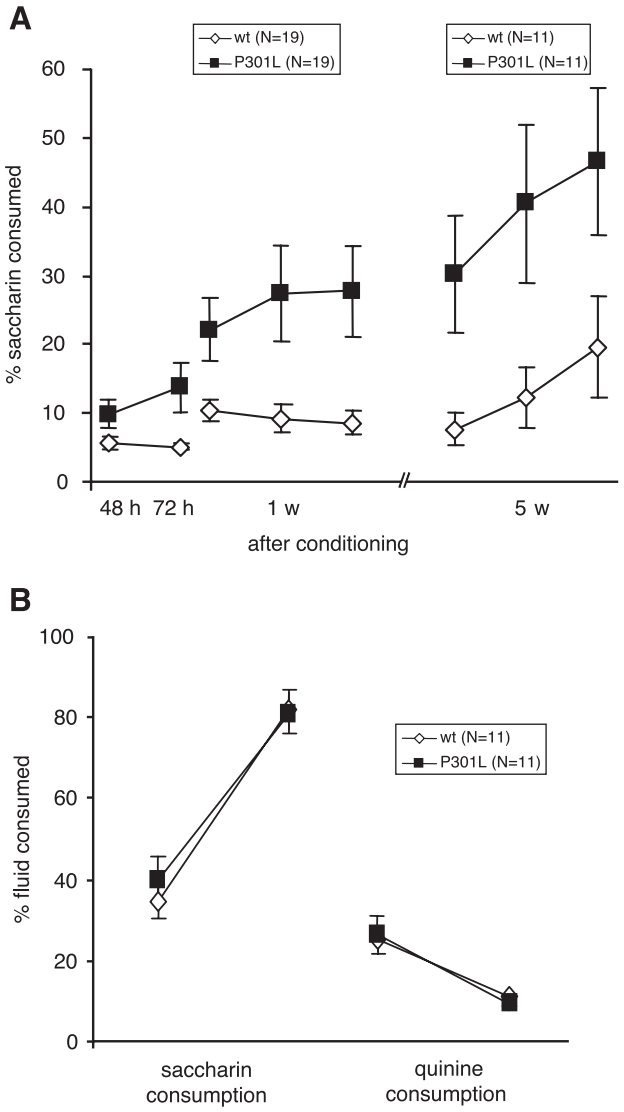

Fig. 6. Accelerated extinction of CTA in P301L mice. (A) During the first choice test 48 h after conditioning no significant genotype effect was observed ($P > 0.094$). However, during all subsequent choice tests, 72 h and 1 week after conditioning, P301L mice consumed significantly more saccharin ($N = 19$/group). Additionally, a subset of mice ($N = 11$/group) was again tested 5 weeks after conditioning. P301L mice continued to show a significantly accelerated extinction. (B) Basic taste qualities in naive mice were not impaired by the tau pathology. Values represent the mean ± SEM.

pairwise comparisons revealed that during the first choice test 48 h after conditioning both groups developed a strong taste aversion for saccharin (percentage of saccharin consumed: wt: 5.6 ± 1.0%; P301L: 9.8 ± 2.1%; $P > 0.094$), indicating that acquisition and consolidation of a taste aversion was not significantly impaired by the tau pathology. However, during the second choice test, P301L mice began to consume significantly more saccharin than wild-types ($P < 0.017$), demonstrating a faster extinction of the taste aversion. Repetition of these choice tests on 3 consecutive days starting 1 week after conditioning showed that CTA memory in wild-type mice extinguished slowly, whereas extinction was significantly faster in transgenic mice. A subset of mice ($N = 11$/group) was again exposed 5 weeks after conditioning to three such choice tests. P301L mice still continued to show a significantly accelerated extinction (main effect of genotype: $F(1,20) = 5.404$, $P < 0.031$) (Fig. 6A). Neither the amount of water intake during the last adaptation day before conditioning (wt: 1.34 ± 0.07 g; P301L: 1.41 ± 0.05 g; $F(1,36) = 0.592$, $P > 0.447$), nor the amount of saccharin consumed on the conditioning day itself (wt: 1.27 ± 0.11 g; P301L: 1.35 ± 0.06 g; $F(1,36) = 0.339$, $P > 0.564$) revealed a significant effect of the transgene. In addition, total liquid intake (water plus saccharin) of P301L mice did not differ significantly from wild-type controls at any time point during the choice tests ($F(1,36) = 0.094$, $P > 0.761$).

Basic taste qualities were assessed in water-deprived naive mice ($N = 11$/group) by presenting saccharin and quinine solutions. This did not reveal any significant differences between transgenic and control mice (for saccharin: $F(1,20) = 0.147$, $P > 0.706$; and for quinine: $F(1,20) = 0.002$, $P > 0.968$), indicating that P301L mice possess a normal taste sensitivity (Fig. 6B).

Discussion

Our immunohistochemical and behavioral analysis of P301L tau transgenic mice revealed a widespread aggregation of tau in the forebrain that is accompanied by selective changes in behavior. Behavioral changes include a small increase in exploratory behavior and an accelerated extinction of an aversion against a taste that has been previously paired with nausea. No changes, with respect to wild-types, were found in locomotor activity, fear conditioning, taste neophobia, and unconditioned natural taste preference for a sweet solution and natural taste aversion against a bitter solution. Extending previously published data, we found tau aggregation in the forebrain in nuclei of the amygdalar complex, the hippocampus and all areas of the neocortex investigated (sensory, motor, and associative areas). Aggregates were also present in several brain stem areas including the red nucleus, ventral tegmental area, and parts of the reticular formation, inferior olive, and ambiguus nucleus. At 6 months of age, NFT began to form in a subset of amygdaloid neurons, possibly reflecting high relative levels of tau expression and/or a selective vulnerability of distinct amygdaloid nuclei (Gotz and Nitsch, 2001; Gotz et al., 2001c).

Our study also revealed that body weights of P301L mice were slightly lower than that of wild-types already at the beginning of behavioral testing. This weight difference was even larger during the final (CTA) task of the test battery. Such a weight loss could be due to disturbances in several different brain sites. In light of the widespread appearance of tau aggregates in the brain, it would be difficult to pinpoint the structure(s) responsible for the weight loss. However, a defect that very unlikely contributes to the observed weight loss is diminished amygdalar function since damage to amygdaloid nuclei has been reported to cause either no change or just the opposite, that is, weight gain in rats (Rollins et al., 2001).

In the open-field, P301L and wild-type mice moved equal distances, but P301L mice changed their activity state somewhat more often from progression to resting to scanning. Furthermore, in the light–dark box they were more active and clearly increased the frequency of rearing, all of which are signs for greater exploratory behavior. In both the open-field and light–dark test, measures of anxiety were unchanged. Several brain structures have been found to be involved in exploratory behavior including the hippocampus and amygdala. That the amygdala might be affected in our transgenic mice is suggested by the observation that amygdala lesions increase exploratory behavior (Kelley et al., 1989). Dysfunction of the amygdala, however, would not affect unconditioned anxiety as measured with an anxiety test (elevated plus-maze) in rats (Treit and Menard, 1997).

Expression of the transgene and formation of tau aggregates in the forebrain did not impair fear conditioning to tone or context. When tested 15 days after conditioning, wild-types as well as P301L mice also showed no signs of extinction and froze even more in response to the conditioned stimuli (context, auditory cue). The non-significant tendency of reduced freezing of P301L mice only during conditioning remains puzzling, and to our knowledge, no treatment with a similar selective effect has been described. Anyhow, it is difficult to imagine how emotional or cognitive changes could affect freezing during conditioning but not during retrieval.

That P301L mice had no deficits in fear conditioning to a tone is in agreement with the expression pattern of tau aggregates in their brains. Conditioning to an auditory CS is dependent on functionally intact lateral and central nuclei of the amygdala (LeDoux, 2000), sites that were free of tau aggregates in our transgenic mice. The involvement of the basolateral amygdala (BLA), a site with tau aggregates in P301L mice, is less well established (but see also Goosens and Maren, 2001). In contrast to fear conditioning to a tone, successful context fear conditioning depends on an intact hippocampus which projects to the BLA (LeDoux, 2000). However, despite a prominent expression of P301L tau in the hippocampus and the BLA of P301L mice, no deficits were found in context fear conditioning compared with control mice. This may be due to the design of the fear conditioning task that was probably not sensitive enough to reveal differences between the two groups. Similar to our P301L mice, aged APP^{Swe} mutant mice also showed no deficits in fear conditioning to a tone or a context when compared to corresponding wild-types (Corcoran et al., 2002). These APP^{Swe} mice had β-amyloid plaques in the hippocampus as well as the amygdala and a reduction in function might have been expected. Only when the salience of the context CS was reduced, an indication of impairment in APP^{Swe} mice appeared. The general lack of massive neurodegeneration in animal models of AD may explain the largely normal performance of both P301L and APP^{Swe} mice in fear conditioning, which is in contrast to the reported impaired fear conditioning in AD patients (Hamann et al., 2002). This demonstrates the importance to design highly sensitive protocols for the measurement of different behavioral tasks.

P301L mice acquired a taste aversion indistinguishable from that of wild-types; that is, when given a choice to drink either a saccharin solution or water 2 days after pairing saccharin drinking with nausea, both genotypes greatly preferred water and avoided

the saccharin solution. However, repeated exposure to such a choice situation attenuated the aversion, and this extinction was drastically accelerated in P301L mice compared to wild-types. The possibility has to be considered that a stronger conditioning in wild-type mice might not have shown due to a flooring effect, that is, wild-type mice performed already close to an optimum with no further capacity of improvement.

The CTA deficits in P301L mice cannot be explained by a reduced neophobia, an increased sweet preference or a reduced aversion for unpleasantly tasting solutions. With respect to these three traits, no genotype differences could be found. P301L, as well as wild-type mice reduced their fluid intake, when first exposed to the saccharin solution (neophobia) developed a strong preference for the sweet solution when drinking was not followed by nausea, and avoided a bitter-tasting quinine solution to the same degree. Further, despite their slightly reduced body weight, P301L mice did not consume less saccharin solution on the conditioning day, that is, exposure to the conditioned stimulus was comparable in both groups.

It has been suggested that lesions of the BLA have a general effect on the response to novel stimuli (such as food) by decreasing neophobia (Dunn and Everitt, 1988). However, in our study, no attenuation of a taste neophobia was found. Thus, the observed formation of tau aggregates in the amygdala in P301L mice very unlikely caused a severe functional impairment of this structure.

Tau was expressed in brain areas which have been shown to be involved in CTA including the BLA, the insular cortex, and some thalamic nuclei (Welzl et al., 2001). No expression was found in other CTA-relevant areas such as the ventral posteromedial nucleus of the thalamus (VPM), the parabrachial nucleus (PBN), and the nucleus of the solitary tract (NTS).

Little is known about what might accelerate extinction of CTA. Several studies implicated hormonal systems, neurotransmitter systems, or specific brain structures in CTA extinction (for review, see Bures et al., 1998); but in general, these studies described retarded, but not accelerated, extinction upon treatments. For example, whereas hippocampal lesions affected acquisition of CTA only mildly or not at all (Best and Orr, 1973; Yamamoto et al., 1995), they slowed extinction of an already conditioned aversion (Kimble et al., 1979). In one study, excitotoxic lesions of the VPM had little effect on the acquisition of CTA but markedly accelerated its extinction similar to what we observed in our transgenic mice (Yamamoto et al., 1995). However, tau is not expressed in the VPM of P301L mice.

Numerous studies support a critical involvement of the amygdala in CTA (Aja et al., 2000; Lamprecht et al., 1997; Yamamoto et al., 1995). Similar to its effect on other aversive memories, the amygdala could modulate consolidation processes (e.g., of CTA) in other brain areas via its projections to these areas (McGaugh et al., 2002). Such a modulation could be achieved by pathways from the amygdala to the insular cortex, a structure critical for storage of a CTA. Stimulation in the BLA induced LTP in the insular cortex which enhanced retention of CTA memory in subsequent extinction trials (Escobar and Bermudez-Rattoni, 2000). Overexpression of P301L tau in the BLA could impair this modulatory effect resulting in accelerated extinction, either directly or by weakening the strength of the memory trace.

Interestingly, a recent study showed that the BLA is essential for extinction of CTA memory whereas acquisition is dependent on an intact central nucleus (Bahar et al., 2003). The differential effect of tau aggregates on fear conditioning and CTA fits well with their distribution pattern in the amygdala. We observed the aggregates in the basolateral but not the lateral and central nucleus. In contrast to CTA, fear conditioning to a tone is not dependent on an intact BLA, but an intact lateral and central nucleus (for review, see Bures et al., 1998; LeDoux, 2000). It also seems noteworthy to mention that, again, APP^{Swe} mice resemble to some degree P301L mice. APP^{Swe} mice expressed amyloid plaques in the amygdala and were drastically impaired in the acquisition of a CTA and, therefore, also in the extinction of this task (Janus et al., 2002).

AD patients exhibit an impairment at all levels of gustatory information processing, in line with the notion of a dissociation between preservation of olfactory and gustatory thresholds and an alteration in odor identification in patients with mild stage AD, suggesting that the alteration is central rather than peripheral (Broggio et al., 2001). Significant losses in the ability to detect the taste of glutamic acid and to recognize odorants were found in demented AD and non-AD patients when compared with age-matched controls (Schiffman et al., 1990). These findings are consistent with our transgenic model as the P301L mice share features of AD and FTD.

A range of behavioral tasks that did not include a test for CTA have been performed with other transgenic mouse strains expressing a mutated form of tau. PrP promoter-driven P301L tau transgenic mice strongly overexpress mutant tau in the brain and in motor neurons of the spinal cord. They develop a progressive motor phenotype commonly not observed in AD (Lewis et al., 2000). V337M tau mutant mice, on the other hand, express mutant tau only in the hippocampus, which is in contrast to our mice that develop a more widespread tau pathology similar to the human tau pathology. V337M mice show an increased locomotor activity and memory deficits in the elevated plus maze, increased spontaneous locomotion in the open-field, but no significant impairments in the Morris water maze (Tanemura et al., 2002). R406W tau mutant mice express tau at highest levels in the hippocampus and to a lesser extent in other cortical and subcortical brain areas. However, in the amygdala, only few cells strongly expressed mutant tau, even in 16- to 23-month-old animals (Tatebayashi et al., 2002). Not unexpectedly, the form of mutant tau and the type of promotor controlling its expression in transgenic mice determines the expression pattern of tau pathology and, as a consequence, results in very different behavioral phenotypes. The distribution of mutant tau in P301L mice investigated in the present study is widespread and comes close to the pattern of tau pathology observed in patients. These mice also lack the motor disturbances observed in other tau mutants, disturbances that are not characteristic of AD. P301L mice share, however, some characteristics with behavioral disturbances observed in APP mutant mice. Furthermore, disturbances can be detected already when mice are 6 months old. Thus, we think that P301L mice are a good model to investigate the contribution of tau pathology, as observed in AD and FTDP-17, to behavioral disturbances.

In summary, although this investigation raised several questions that have to be addressed in future studies, several conclusions on the early effects of tau aggregation in transgenic P301L mutant tau mice can be drawn. Firstly, in the open-field and light–dark box, subtle signs for increased exploratory behavior were manifest in P301L mice. Other behaviors indicative of general activity or anxiety, however, were unaffected by the transgene. Secondly, fear conditioning to tone or to context remained unaffected, probably due to the specific distribution of tau aggregates in the amygdala, and/or the design for this task that was probably not sensitive

enough to detect differences. Thirdly, a selective alteration in the extinction of a taste aversion could be seen in P301L mice. This, again, resembles data collected in APP^{Swe} mice submitted to a similar paradigm. Thus, CTA suggests itself as a sensitive measure of altered brain function in response to the formation of tau aggregates. One possible common factor for all these results could be a dysfunction of specific nuclei of the amygdala.

Acknowledgments

The authors thank Eva Moritz for help with immunohistochemistry, Dr. David Wolfer for data analysis, and Dr. Peter Davies for antibody CP13. This research was supported in parts by grants from the SNF, the ZNZ (Neuroscience Center Zurich), the Hartmann Müller Fund, the Olga Mayenfisch Foundation and by the NCCR "Neuronal plasticity and repair".

References

Aja, S., Sisouvong, S., Barrett, J.A., Gietzen, D.W., 2000. Basolateral and central amygdaloid lesions leave aversion to dietary amino acid imbalance intact. Physiol. Behav. 71, 533–541.

Allen, B., Ingram, E., Takao, M., Smith, M.J., Jakes, R., Virdee, K., Yoshida, H., Holzer, M., Craxton, M., Emson, P.C., Atzori, C., Migheli, A., Crowther, R.A., Ghetti, B., Spillantini, M.G., Goedert, M., 2002. Abundant tau filaments and nonapoptotic neurodegeneration in transgenic mice expressing human P301S tau protein. J. Neurosci. 22, 9340–9351.

Bahar, A., Samuel, A., Hazvi, S., Dudai, Y., 2003. The amygdalar circuit that acquires taste aversion memory differs from the circuit that extinguishes it. Eur. J. Neurosci. 17, 1527–1530.

Best, P.J., Orr Jr., J., 1973. Effects of hippocampal lesions on passive avoidance and taste aversion conditioning. Physiol. Behav. 10, 193–196.

Broggio, E., Pluchon, C., Ingrand, P., Gil, R., 2001. Taste impairment in Alzheimer's disease. Rev. Neurol. (Paris) 157, 409–413.

Buee, L., Bussiere, T., Buee-Scherrer, V., Delacourte, A., Hof, P.R., 2000. Tau protein isoforms, phosphorylation and role in neurodegenerative disorders. Brain Res. Brain Res. Rev. 33, 95–130.

Bures, J., Bermudez-Rattoni, F., Yamamoto, T., 1998. Conditioned Taste Aversion—Memory of a Special Kind. Oxford Univ. Press, New York.

Chapman, P.F., White, G.L., Jones, M.W., Cooper-Blacketer, D., Marshall, V.J., Irizarry, M., Younkin, L., Good, M.A., Bliss, T.V., Hyman, B.T., Younkin, S.G., Hsiao, K.K., 1999. Impaired synaptic plasticity and learning in aged amyloid precursor protein transgenic mice. Nat. Neurosci. 2, 271–276.

Chen, G., Chen, K.S., Knox, J., Inglis, J., Bernard, A., Martin, S.J., Justice, A., McConlogue, L., Games, D., Freedman, S.B., Morris, R.G., 2000. A learning deficit related to age and beta-amyloid plaques in a mouse model of Alzheimer's disease. Nature 408, 975–979.

Corcoran, K.A., Lu, Y., Turner, R.S., Maren, S., 2002. Overexpression of hAPPswe impairs rewarded alternation and contextual fear conditioning in a transgenic mouse model of Alzheimer's disease. Learn. Mem. 9, 243–252.

Dodart, J.C., Meziane, H., Mathis, C., Bales, K.R., Paul, S.M., Ungerer, A., 1999. Behavioral disturbances in transgenic mice overexpressing the V717F beta-amyloid precursor protein. Behav. Neurosci. 113, 982–990.

Dunn, L.T., Everitt, B.J., 1988. Double dissociations of the effects of amygdala and insular cortex lesions on conditioned taste aversion, passive avoidance, and neophobia in the rat using the excitotoxin ibotenic acid. Behav. Neurosci. 102, 3–23.

Escobar, M.L., Bermudez-Rattoni, F., 2000. Long-term potentiation in the insular cortex enhances conditioned taste aversion retention. Brain Res. 852, 208–212.

Goedert, M., Spillantini, M.G., Jakes, R., Crowther, R.A., Vanmechelen, E., Probst, A., Gotz, J., Burki, K., Cohen, P., 1995. Molecular dissection of the paired helical filament. Neurobiol. Aging 16, 325–334.

Goosens, K.A., Maren, S., 2001. Contextual and auditory fear conditioning are mediated by the lateral, basal, and central amygdaloid nuclei in rats. Learn Mem. 8, 148–155.

Gotz, J., 2001. Tau and transgenic animal models. Brain Res. Brain Res. Rev. 35, 266–286.

Gotz, J., Nitsch, R.M., 2001. Compartmentalized tau hyperphosphorylation and increased levels of kinases in transgenic mice. NeuroReport 12, 2007–2016.

Gotz, J., Chen, F., Barmettler, R., Nitsch, R.M., 2001a. Tau filament formation in transgenic mice expressing P301L tau. J. Biol. Chem. 276, 529–534.

Gotz, J., Tolnay, M., Barmettler, R., Chen, F., Probst, A., Nitsch, R.M., 2001b. Oligodendroglial tau filament formation in transgenic mice expressing G272V tau. Eur. J. Neurosci. 13, 2131–2140.

Gotz, J., Chen, F., van Dorpe, J., Nitsch, R.M., 2001c. Formation of neurofibrillary tangles in P301L tau transgenic mice induced by Abeta 42 fibrils. Science 293, 1491–1495.

Hamann, S., Monarch, E.S., Goldstein, F.C., 2002. Impaired fear conditioning in Alzheimer's disease. Neuropsychologia 40, 1187–1195.

Higuchi, M., Ishihara, T., Zhang, B., Hong, M., Andreadis, A., Trojanowski, J., Lee, V.M., 2002. Transgenic mouse model of tauopathies with glial pathology and nervous system degeneration. Neuron 35, 433–446.

Hsiao, K., Chapman, P., Nilsen, S., Eckman, C., Harigaya, Y., Younkin, S., Yang, F., Cole, G., 1996. Correlative memory deficits, Abeta elevation, and amyloid plaques in transgenic mice. Science 274, 99–102.

Hutton, M., Lendon, C.L., Rizzu, P., Baker, M., Froelich, S., Houlden, H., Pickering-Brown, S., Chakraverty, S., Isaacs, A., Grover, A., Hackett, J., Adamson, J., Lincoln, S., Dickson, D., Davies, P., Petersen, R.C., Stevens, M., de Graaff, E., Wauters, E., van Baren, J., Hillebrand, M., Joosse, M., Kwon, J.M., Nowotny, P., Heutink, P., et al., 1998. Association of missense and 5′-splice-site mutations in tau with the inherited dementia FTDP-17. Nature 393, 702–705.

Janus, C., Pearson, J., McLaurin, J., Mathews, P.M., Jiang, Y., Schmidt, S.D., Chishti, M.A., Horne, P., Heslin, D., French, J., Mount, H.T., Nixon, R.A., Mercken, M., Bergeron, C., Fraser, P.E., St George-Hyslop, P., Westaway, D., 2000. A beta peptide immunization reduces behavioural impairment and plaques in a model of Alzheimer's disease. Nature 408, 979–982.

Janus, C., Lovasic, L., Johnson, S.-H., Welzl, H., 2002. Learning and Memory of Transgenic App-Expressing Mice in Conditioned Taste Aversion Paradigm. Program No. 778.2. 2002 Abstract Viewer and Itinerary Planner. Society for Neuroscience, Washington, DC. Online.

Kelley, A.E., Cador, M., Stinus, L., 1989. Exploration and its measurement—A psychopharmacological perspective. In: Boulton, A.A., Baker, G.B., Greenshaw, A.J. (Eds.), Neuromethods. The Humana Press, New Jersey, pp. 95–144.

Kimble, D.P., Bremiller, R., Schroeder, L., Smotherman, W.P., 1979. Hippocampal lesions slow extinction of a conditioned taste aversion in rats. Physiol. Behav. 23, 217–222.

Lamprecht, R., Hazvi, S., Dudai, Y., 1997. cAMP response element-binding protein in the amygdala is required for long- but not short-term conditioned taste aversion memory. J. Neurosci. 17, 8443–8450.

LeDoux, J.E., 2000. Emotion circuits in the brain. Annu. Rev. Neurosci. 23, 155–184.

Lee, V.M., Goedert, M., Trojanowski, J.Q, 2001. Neurodegenerative tauopathies. Annu. Rev. Neurosci. 24, 1121–1159.

Lewis, J., McGowan, E., Rockwood, J., Melrose, H., Nacharaju, P., Van Slegtenhorst, M., Gwinn-Hardy, K., Paul Murphy, M., Baker, M., Yu, X., Duff, K., Hardy, J., Corral, A., Lin, W.L., Yen, S.H., Dickson, D.W., Davies, P., Hutton, M., 2000. Neurofibrillary tangles, amyotrophy and progressive motor disturbance in mice expressing mutant (P301L) tau protein. Nat. Genet. 25, 402–405.

Lin, W.L., Lewis, J., Yen, S.H., Hutton, M., Dickson, D.W., 2003. Filamentous tau in oligodendrocytes and astrocytes of transgenic mice

expressing the human tau isoform with the P301L mutation. Am. J. Pathol. 162, 213–218.

McGaugh, J.L., McIntyre, C.K., Power, A.E., 2002. Amygdala modulation of memory consolidation: interaction with other brain systems. Neurobiol. Learn. Mem. 78, 539–552.

Morgan, D., Diamond, D.M., Gottschall, P.E., Ugen, K.E., Dickey, C., Hardy, J., Duff, K., Jantzen, P., DiCarlo, G., Wilcock, D., Connor, K., Hatcher, J., Hope, C., Gordon, M., Arendash, G.W., 2000. A beta peptide vaccination prevents memory loss in an animal model of Alzheimer's disease. Nature 408, 982–985.

Paxinos, K.B.J.F.a.G., 1997. The Mouse Brain in Stereotaxic Coordinates. Academic Press, San Diego.

Poorkaj, P., Bird, T.D., Wijsman, E., Nemens, E., Garruto, R.M., Anderson, L., Andreadis, A., Wiederholt, W.C., Raskind, M., Schellenberg, G.D., 1998. Tau is a candidate gene for chromosome 17 frontotemporal dementia. Ann. Neurol. 43, 815–825.

Rollins, B.L., Stines, S.G., McGuire, H.B., King, B.M., 2001. Effects of amygdala lesions on body weight, conditioned taste aversion, and neophobia. Physiol. Behav. 72, 735–742.

Routtenberg, A., Hsiao, K., Chapman, P., Nilsen, S., Eckman, C., Harigaya, Y., Younkin, S., Yang, F., Cole, G., 1997. Measuring memory in a mouse model of Alzheimer's disease. Science 277, 839–841.

Schiffman, S.S., Clark, C.M., Warwick, Z.S., 1990. Gustatory and olfactory dysfunction in dementia: not specific to Alzheimer's disease. Neurobiol. Aging 11, 597–600.

Spillantini, M.G., Murrell, J.R., Goedert, M., Farlow, M.R., Klug, A., Ghetti, B., 1998. Mutation in the tau gene in familial multiple system tauopathy with presenile dementia. Proc. Natl. Acad. Sci. U. S. A. 95, 7737–7741.

Tanemura, K., Akagi, T., Murayama, M., Kikuchi, N., Murayama, O., Hashikawa, T., Yoshiike, Y., Park, J.M., Matsuda, K., Nakao, S., Sun, X., Sato, S., Yamaguchi, H., Takashima, A., 2001. Formation of filamentous tau aggregations in transgenic mice expressing V337M human tau. Neurobiol. Dis. 8, 1036–1045.

Tanemura, K., Murayama, M., Akagi, T., Hashikawa, T., Tominaga, T., Ichikawa, M., Yamaguchi, H., Takashima, A., 2002. Neurodegeneration with tau accumulation in a transgenic mouse expressing V337M human tau. J. Neurosci. 22, 133–141.

Tatebayashi, Y., Miyasaka, T., Chui, D.H., Akagi, T., Mishima, K., Iwasaki, K., Fujiwara, M., Tanemura, K., Murayama, M., Ishiguro, K., Planel, E., Sato, S., Hashikawa, T., Takashima, A., 2002. Tau filament formation and associative memory deficit in aged mice expressing mutant (R406W) human tau. Proc. Natl. Acad. Sci. U. S. A. 99, 13896–13901.

Treit, D., Menard, J., 1997. Dissociations among the anxiolytic effects of septal, hippocampal, and amygdaloid lesions. Behav. Neurosci. 111, 653–658.

Welzl, H., D'Adamo, P., Lipp, H.P., 2001. Conditioned taste aversion as a learning and memory paradigm. Behav. Brain Res. 125, 205–213.

Wolfer, D.P., Madani, R., Valenti, P., Lipp, H.P., 2001. Extended analysis of path data from mutant mice using the public domain software Wintrack. Physiol. Behav. 73, 745–753.

Yamamoto, T., Fujimoto, Y., Shimura, T., Sakai, N., 1995. Conditioned taste aversion in rats with excitotoxic brain lesions. Neurosci. Res. 22, 31–49.